The Effects of Manganese-Reducing Bacteria on Desorption of Manganese from $MnO_{x(s)}$ Coated Media

Lindsay Ellen Swain

Thesis submitted to the faculty of the Virginia Polytechnic Institute and State University in partial fulfillment of the requirements for the degree of

Master of Science

In

Civil Engineering

William R. Knocke

Joseph O. Falkinham, III

Amy J. Pruden

May 4, 2016

Blacksburg, Virginia

Keywords:

manganese, manganese-reducing bacteria, desorption, in vitro reduction

The Effects of Manganese-Reducing Bacteria on Desorption of Manganese from $MnO_{x(s)}$ Coated Media

Lindsay Ellen Swain

ABSTRACT

In the past, water treatment plants have stopped the application of pre-filter oxidants to create a bioactive filtration process to remove soluble Mn. After the cessation of pre-filter oxidants, a Mn desorption phenomenon was seen where effluent Mn exceeds influent Mn concentrations. The reason for the sudden increase in effluent Mn was not known, but it was hypothesized that Mn-reducing bacteria on the filter media play a substantial role in this phenomenon. The primary goal of this research was to assess the role of Mn-reducing microorganisms in the desorption of $MnO_{x(s)}$ from coated filters once pre-filtration chlorine ceased. A secondary objective included the development of a molecular detection method for Mn-reducing microorganisms in laboratory and environmental samples. Bench-scale filter column studies were completed to investigate the impacts of Mn-reducing microbial populations on desorption of Mn from $MnO_{x(s)}$ coatings. Secondarily, the effects of influent carbon loading and $MnO_{x(s)}$ age on Mn desorption were investigated. *In situ* vial assays were created to gain insight into the impacts of $MnO_{x(s)}$ age on Mn reducing microorganism bioavailability. Lastly, a qPCR detection method was developed that targeted the *mtrB* gene. Results determined that microbially mediated Mn desorption was possible when sufficient numbers of Mn-reducing microorganisms were present on the $MnO_{x(s)}$ surface and that those organisms contributed to the Mn desorption phenomenon. qPCR detection methods were able to show a greater number of Mn-reducing microorganisms in studies where Mn desorption was observed. Lastly, $MnO_{x(s)}$ age was shown to play an important, but unexplained, role in bioavailability.

The Effects of Manganese-Reducing Bacteria on Desorption of Manganese from $MnO_{x(s)}$ Coated Media

Lindsay Ellen Swain

GENERAL AUDIENCE ABSTRACT

Previously, drinking water plants have stopped adding chemical oxidants before the filtration process in order to grow a population of microorganisms to remove Mn from the water. After the chemical oxidants were removed, a phenomenon was observed in certain water plants where the amount of Mn exiting was greater than the amount of Mn entering the plant. The reason for this phenomenon was not known, but it is thought that bacteria that are able to biologically reduce Mn play an important role. The main purpose of this research was to investigate the role of Mn-reducing bacteria in the observed increase of Mn released into the effluent. A second purpose for this research was to develop a method to detect the DNA of Mn-reducing bacteria in environmental and laboratory samples on a molecular level. Laboratory filtration columns were completed to research the effects of Mn-reducing bacteria, carbon content and filter media age on the release of Mn from the filtration media. Results showed that when a sufficient population of Mn-reducing bacteria was present, Mn released from the filter increased. Detection of Mn-reducing bacterial DNA was able to confirm these observations. The age of the filtration media was also shown to have an important but not well-understood effect on the amount of Mn released from the filter. This research is applicable to water treatment professionals that no longer desire to use chemical oxidants for drinking water treatment but need to maintain Mn removal capacity.

Dedicated to my daughter, Madison Swain.

You are my strength, my constant inspiration and my world.

ACKNOWLEDGEMENTS

As Helen Keller once stated, “Alone we can do so little; together we can do so much.” Research is best done in collaboration with others and I most certainly could not have completed this research project single-handedly. Consequently, there are numerous people I would like to thank for their expertise, time and effort. I would like to express sincere gratitude to my chair adviser Dr. Knocke whose knowledge, patience and guidance along the often winding and branched path of research was truly invaluable. I would like to thank Dr. Falkinham for letting me talk through my experimental ideas and providing me a laboratory workspace, which was always kept at California comfortable temperatures. Thank you to Dr. Pruden who provided a truly enjoyable graduate teaching experience and offered valuable insights into the complicated world of biotechnology.

I would also like to thank the following people and organizations: Dr. Parks who was so accommodating when it came to use of the ICP-MS and for taking column samples for me when I could not be on campus; Dr. Nealson for the cultures of *S. oneidensis*, Dr. Melville who was gracious enough to let me use his anaerobic chamber and his graduate students who took the time to train me on how to use it; Julie Petruska for many laughs and help in all things laboratory; Jody Smiley for her help in troubleshooting the ICP when I would break it and help with TOC analysis; Myra Williams for help and guidance around the microbiology lab; Anurag Marantha for shake flask sampling when I was out of state interviewing for jobs; Dr. D’Imperio for his assistance and expertise in completing the *mtrB* gene alignment and qPCR primer design; Dr. Walke for letting me constantly borrow DNA extraction equipment that saved me an enormous amount of time; Dr. Hochella for his direction on manganese aging and bioavailability; Randy Hawkins and the Harwood Mills WTP for providing several rounds of media samples and Excel sheets full of WTP plant data and lastly Beth Lucas for all of her administrative help.

Last but not least, I want to say thank you to all of my friends and family who have supported me through my graduate school journey. To everyone who has provided words of encouragement or watched my daughter so that I could study, maintain my columns or write my thesis, I could never have finished this journey with out your help. Finally, to my husband and daughter, your love and support have made it all worthwhile.

TABLE OF CONTENTS

TABLE OF FIGURES

TABLE OF TABLES

LIST OF ABBREVIATIONS

BDOC	Biodegradable Dissolved Organic Carbon
C	Carbon
CFU	Colony Forming Unit
Cq	Quantification Cycle
DOC	Dissolved Organic Carbon
EPA	Environmental Protection Agency
gpm	Gallons Per Minute
HAS	Hydroxylamine Sulfate
ICP-MS	Inductively Coupled Plasma Mass Spectroscopy
ID	Inner Diameter
MCL	Maximum Contaminant Level
Mn	Manganese
NOM	Natural Organic Matter
PCR	Polymerase Chain Reaction
POC	Particulate Organic Carbon
ppm	Parts Per Million
qPCR	Quantitative Polymerase Chain Reaction
WTP	Water Treatment Plant

1.0 INTRODUCTION

Excess manganese (Mn) exposure in drinking water has been linked to a variety of health problems including impaired neurological development and neural tube defects in fetuses (Haynes 2015). Therefore, adequate removal of Mn to a concentration of 0.05 mg/L (EPA 1979) is often accomplished through conventional oxidation and filtration methods during the water treatment process. Often, water treatment plants (WTP) will desire to make their filtration process biologically active as to allow Mn oxidation from active site adsorption and naturally occurring microbial population of manganese oxidizing bacteria that live on the $MnO_{x(s)}$ surface (Hoyland 2014). Microbially mediated and surface catalyzed Mn oxidation becomes the primary method for Mn removal when the application of a pre-filter oxidant such as chlorine is stopped. The decline in chlorine usage results in a cost savings as well as a decrease in generated disinfection by-products (Womba 2000).

For various WTPs, when pre-filter free chlorine is removed, Mn will actually desorb from the $MnO_{x(s)}$ surface so that effluent Mn will exceed influent Mn concentrations for a certain period of time (Gabelich 2006). After that time, effluent Mn levels typically decrease below influent levels and reach a steady state for Mn release. The increase in effluent Mn is of concern to WTP due to the aesthetic and health effects of Mn detailed above. The Mn desorption phenomenon has not been widely observed, documented or studied. Mechanisms thought to cause or contribute to the Mn desorption phenomenon are biologically mediated reduction (Islam 2010), reduction catalyzed by contact with organic matter (Lovley 1988) or an unknown chemical mechanism (Gabelich 2006).

The goal of this research was to assess the role of Mn reducing microorganisms in desorption of $MnO_{x(s)}$ coated filters after free-filter chlorination had ceased. The main objectives of this research were:

1. Attempt to quantify what proportion of Mn desorption from the laboratory filter columns is attributed to Mn-reducing microorganism activity
2. Develop a molecular probe for the detection and quantification of Mn-reducing microorganisms

3. Determine a method to eliminate or greatly reduce Mn desorption from $MnO_{x(s)}$ coated media by inhibiting or inactivating Mn-reducing microorganisms present on bench-scale filters
4. Extrapolate the method for eliminating or decreasing Mn desorption to find operational modifications that are applicable and practical for full scale treatment plants

2.0 LITERATURE REVIEW

2.1 Manganese Background

Manganese (Mn) is a transition metal that is used in countless biological systems and industrial applications. Mn is a required trace metal in biological organisms that helps in processes such as the production of enzyme cofactors that aid in detoxification of superoxide free radicals and in photosynthesis for plant species (Costa 2015). In natural systems, Mn is a large component of sediments and soils and is found primarily in three oxidation states: Mn(II), Mn(III) and Mn(IV). Insoluble Mn(IV) can be reduced into the soluble form, Mn(II), either chemically (abiotic) or by microbially mediated (biotic) reduction (Burdige 1993).

2.2 Health and Aesthetic Concerns Associated with Manganese

Health and aesthetic concerns are the two main reasons why Mn removal during the water treatment process is important. It is well known that Mn is critical to many essential biological processes necessary for life such as growth, development, oxidative defense and enzymatic activity (Costa 2015). Paradoxically, exposure of too much Mn can lead to a variety of health problems and neurological diseases. Excessive acute or long-term Mn exposure has been linked to impaired neurological development, the early onset of puberty in females and neural tube defects in fetuses (Haynes 2015). The EPA has established a Secondary Maximum Contaminant Level (SMCL) of 0.05 mg/L Mn (EPA 1979).

The inclusion of excess reduced Mn in water traveling through the distribution system into a consumer's home can also cause aesthetic concerns. Mn is oxidized through the addition of an oxidizing agent such as chlorine bleach and during water transmission to the consumer's home (Cerrato 2006). Upon entering the consumer's home, water that contains oxidized Mn would have a black-brown color, which often leads to water discoloration complaints (Sly 1990). Excess Mn in consumer's drinking water can also cause an undesirable metallic taste (Sain 2014).

2.3 Biogeochemical Cycling

Mn reduction in sediments, defined as the conversion of Mn(IV) to Mn(II), has been shown to be both chemically and microbially mediated in natural systems. Mn oxides found in sediments are most often referred to as $MnO_{x(s)}$ as to generalize the average oxidation state,

between Mn(II) and Mn(IV), in which it is usually found (Burdige 1993). Mn oxides in sediments are considered to be mostly amorphous in nature and are found in close proximity to iron oxides. Many times these compounds are complexed with other cations and have formed crystalline lattices. Mn(III) is generally assumed to be present, but is thermodynamically unstable and is, therefore, a temporary intermediate in the Mn reduction pathway (Lin 2012).

Mn reduction reactions lead to water gradients across the redox boundary where the reduced form is found. This leads to an upward diffusion of reduced Mn where it is ultimately re-oxidized (Madison 2012). The newly formed Mn oxides settle and contribute to the cycle of burial and reduction in the redox cycle. In steady-state conditions and under low turbulence, this leads to a well-defined fixed zone of solid Mn just above the redox boundary (Burdige 1993).

For a compound, such as $MnO_{x(s)}$, to be able to be utilized through a redox reaction, the electron acceptor must have an appropriate redox potential (Johnson 2006). The electron potential must be low enough to not be toxic but high enough to be energetically favorable. The redox potential of Mn (IV), characterized as the change in Gibbs free energy, is just below the reaction for denitrification (NO_2^- to N_2) and above sulfate reduction (HSO_3^- to HS^-). In bodies of water that contain stratified reduction zones, the order of preferential redox reactions is maintained. Denitrification occurred above Mn reduction zones, where sulfate reduction occurred below (Burnes 2000).

2.4 Mn Reduction Genetics and Physiology

Microbial metal reduction is a crucial part of the geochemical cycling in redox-stratified waters for iron, Mn and carbon (Johnson 2006). Yet, little is known about the molecular mechanisms by which the Mn reduction process takes place. When Mn reduction is microbially mediated, the process is referred to as dissimilatory (heterotrophic) Mn-reduction (Burdige 1993). Where metal reducing microorganisms are found, Mn (IV) and Fe (III) oxides are often the principal electron acceptors found in anoxic and anaerobic zones of freshwater and marine sediments. Metal-reducing bacteria are also critical to the oxidation and remineralization of organic carbon (Szeinbaum 2014).

At neutral pH conditions, Mn oxides are highly insoluble and can be crystalline in nature (Yang 2013). In order for reduction to occur, microorganisms are required to transfer electrons to external Mn oxides since contact with a localized inner membrane electron transport chain is not

possible (Lovley 2004). There have been three novel respiratory mechanisms identified in metal reducing bacteria to which electrons are transferred to Mn oxides. Those mechanisms have been identified as direct enzymatic reduction via metal reducing c-type cytochromes on the cell surface, reductive oxide solubilization with electron transfer from metal-organic ligands and a two-step indirect enzymatic reduction by endogenous or exogenous electron shuttles (Szeinbaum 2014). It is generally accepted that Mn(IV) reduction occurs directly at the outer membrane via single two-electron successive transfers, resulting in Mn(II) as the final product (Thamdrup 2000). The first electron transfer forms soluble Mn(III) as a temporary intermediate before a final electron transfer and reduction to Mn(II). The first electron transfer step increases the bioavailability of Mn by reductive solubilization while the second step is coupled to the production of inorganic carbon (Lin 2012).

In a majority of the peer-reviewed published studies regarding microbially mediated Mn reduction, *Shewanella* species have been used as the model organism. This is because *Shewanella* is easily grown and studied under laboratory conditions (Szeinbaum 2014). *Shewanella* is able to use a wide variety of electron acceptors, including the capacity to transfer electrons to many solid metal oxide compounds (Osterman 2008).

The electron transport chain of *S. oneidensis,* shown in Figure 1, is made up of many different types of interacting proteins and allows the utilization of extracellular electron acceptors for Mn reduction (Szeinbaum 2014). The main outer membrane protein complex is MtrCBA, which is an electron channel that allows the passage of electrons to extracellular metal hydroxide complexes (Burnes 2000). MtrCBA is mainly associated with the reduction of Mn(IV) but not Mn(III). Inside the cell, dehydrogenases oxidize electron donors, pump protons to the periplasmic space and then transfer electrons to the menaquinone. The reduced menaquinone then transfers electrons to a c-type cytochrome CymA. CymA transfers electrons to the periplasmic c-type cytochrome MtrA. An outer membrane β-barrel protein, MtrB, allows interaction and electron transfer between MtrA and MtrC. The type II protein secretion system produces MtrC and c-type cytochrome OmcA, which is associated with the reduction of Mn(III) (Szeinbaum 2014). Type II secretion systems are responsible for the translocation of proteins to the outer membrane which is essential for microorganisms that reduce insoluble metal complexes (Ross 2009). It has been shown that MtrB and GspD, an outer membrane porin, as well as the terminal reductase MtrC and OmcA are required for Mn(IV) and Mn(III) reduction (Lin 2012).

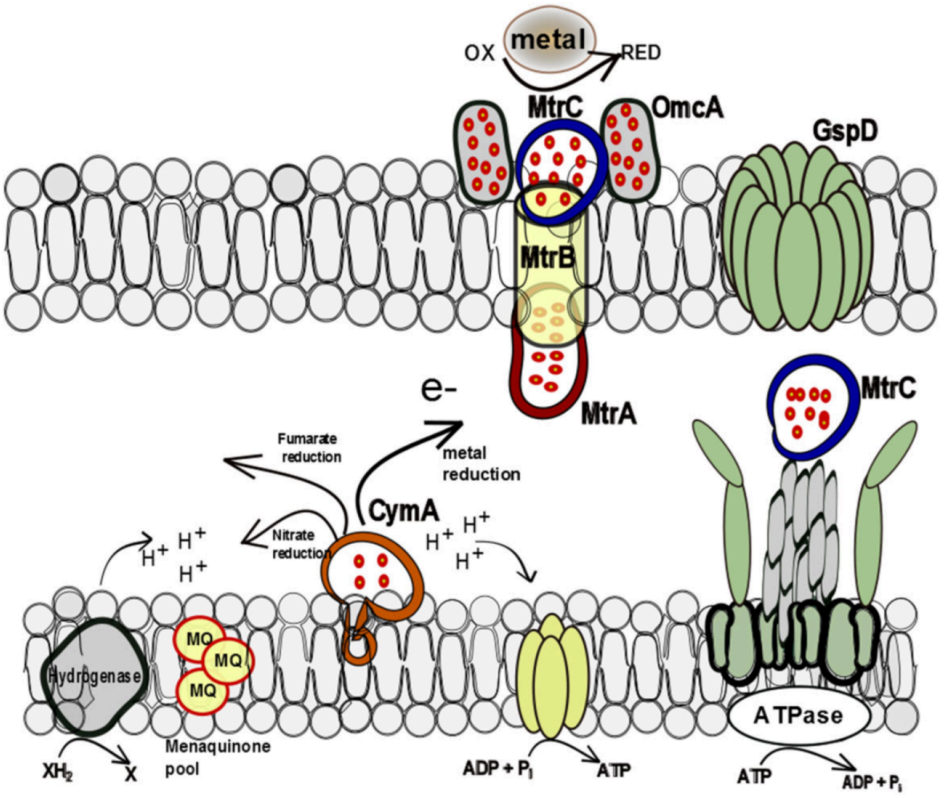

Figure 1. Proteins and mechanisms necessary in the *S. oneidensis* MR-1 electron transport chain for Mn Reduction (Szeinbaum 2014)

2.5 Mn Removal Through Filtration

One of the more common methods of dissolved Mn removal in water treatment facilities is through chemical oxidation and active site adsorption onto filtration media (Tobiason 2008). Oxidants such as free chlorine or potassium permanganate are added prior to filtration, which drives the oxidation of soluble Mn (II) into an insoluble amorphous $MnO_{x(s)}$ form (Carlson 1999). Through the chemical oxidation process, the filtration media physically removes insoluble Mn. Once an $MnO_{x(s)}$ coating begins to form on the filtration media from chemical oxidation, Mn adsorption onto active sites is able to occur. $MnO_{x(s)}$ strongly absorbs to Mn(II) so that reduced Mn from the filtration influent adsorbs to the oxidant formed Mn oxide coating (Knocke 1991, Carlson 1999). This process has been referred to as the natural greensand effect and is a self-regenerating process that removes additional Mn (Bierlein 2012).

2.6 Mn Desorption Phenomenon

In some water treatment plants where adsorption of soluble Mn to oxide coated filtration media is the main method utilized for Mn removal, Mn desorption phenomenons have been observed when pre-filter free chlorination is stopped (Islam 2010). In these cases, the effluent Mn can exceed influent concentrations for extended periods of time after chlorine application ceases (Gabelich 2006). This desorption phenomenon has been documented at the Aquarion Water Company (AWC) Stamford WTP (Stamford, CT) (Tobiason 2008) and at the Henry J. Mills WTP (Riverside, CA) (Gabelich 2006). The Stamford WTP ceased pre-filter chlorination in an attempt to create a biologically active filtration process. Figure 2 demonstrates effluent Mn levels exceeding influent concentrations at the Stamford WTP for several months until chlorine was reapplied to the filters. The desorption phenomenon was also observed in a laboratory setting using filtration media from the AWC Lantern Hill WTP (Stonington, CT). Investigations into the origin of additional released Mn seen in filter effluent waters indicated Mn release was due to desorption primarily from anthracite filtration media (Islam 2010).

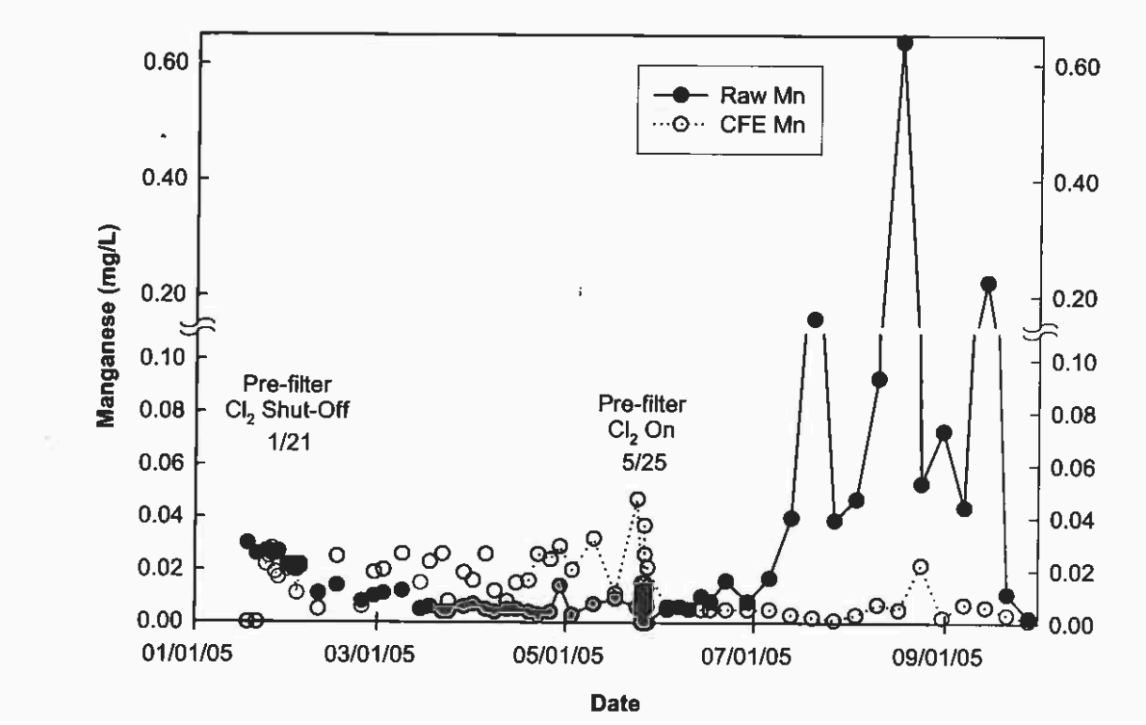

Figure 2. Raw and filter effluent Mn concentrations at the AWC Stamford plant before and after the cessation of pre-filter free chlorine (Tobiason 2008)

Mn desorption has been documented in relatively few water treatment facilities and, therefore, minimal research to investigate the cause for this phenomenon has been completed. In general, there are three main hypotheses as to the cause of Mn desorption. These hypotheses included: (1) biologically mediated reduction (Islam 2010), (2) reduction through contact with organic matter (Lovley 1988) and (3) other undefined chemical reduction mechanisms (Gabelich 2006). In a study using media from the Henry J. Mills WTP, biologically mediated Mn desorption was discounted as a likely reason for elevated concentrations of effluent Mn (Gabelich 2006).

Islam et, al. completed a study with Lantern Hill WTP anthracite filtration media, using 16s rRNA to evaluate the types and abundance of microorganisms present on greensand media. On the Lantern Hill media, approximately 45% of the total microbial population had the ability to utilize $MnO_{2(s)}$ as their terminal electron acceptor. Mn-reducing microbes were also found in the Lantern Hill WTP source ground water based off of 16s DNA analysis, but at less than half of the numbers seen on the greensand media. From this study, results indicated that Mn-reducing microbes accumulated on the oxide coating of the filtration media and remained present, even during the application of pre-filtration free chlorine. Researchers from this study hypothesized that Mn-reducing populations increased in activity and number in the absence of free chlorine. To further support this hypothesis, results from these experiments demonstrated that the population of Mn reducing microbes decreased on the Lantern Hill WTP greensand media by 40% when pre-filtration chlorine resumed. This study concluded that biological activity was a likely contributor for Mn desorption seen at the Lantern Hill WTP and in laboratory studies (Islam 2010).

3.0 EXPERIMENTAL METHODS AND MATERIALS

In the context of ion exchange systems, breakthrough is typically defined as the amount of a substance that passes through a system when media exhaustion has occurred. Breakthrough occurs in Mn-coated media when active sites have adsorbed as much soluble Mn as possible. In the context of this research, Mn release will be defined as actual desorption off of the $MnO_{x(s)}$ surface, which is then passed through the system. Because the $MnO_{x(s)}$ surface, in many of the column studies completed for this research will be experiencing both breakthrough and release simultaneously, the term breakthrough will be mostly used through this document to describe both processes during the explanation and discussion of results.

3.1 Bench-Scale Filter Column Experiments

Bench-scale filter columns were set up to produce Mn breakthrough curves as well as replicate manganese removal and desorption trends intermittently seen in full-scale water treatment plants (Figure 3).

3.1.1 General Filter Column Setup

Two glass columns of $^{7}/_{16}$ inch ID were used for this experiment. Preceding the experiment, columns were cleaned with a mixture containing 10 g/L of a strong reducing agent, hydroxylamine sulfate (HAS), to remove any accumulations of $MnO_{x(s)}$. Columns were then triple rinsed with deionized water prior to use. Using a burette clamp, the columns were secured onto a metal rod stand. A ½ x ¼ inch plastic coupling was inserted into a ½ inch ID piece of plastic tubing approximately 2 inches in length, followed by a small piece of glass wool to keep the media in the column. To direct the effluent flow, ¼ inch ID plastic tubing was attached to the other side of the coupling and directed into a funnel. The effluent tubing was attached to a separate metal rod at a height above the media depth to maintain a positive hydraulic head. Effluent flow from the funnel was discharged into a sink.

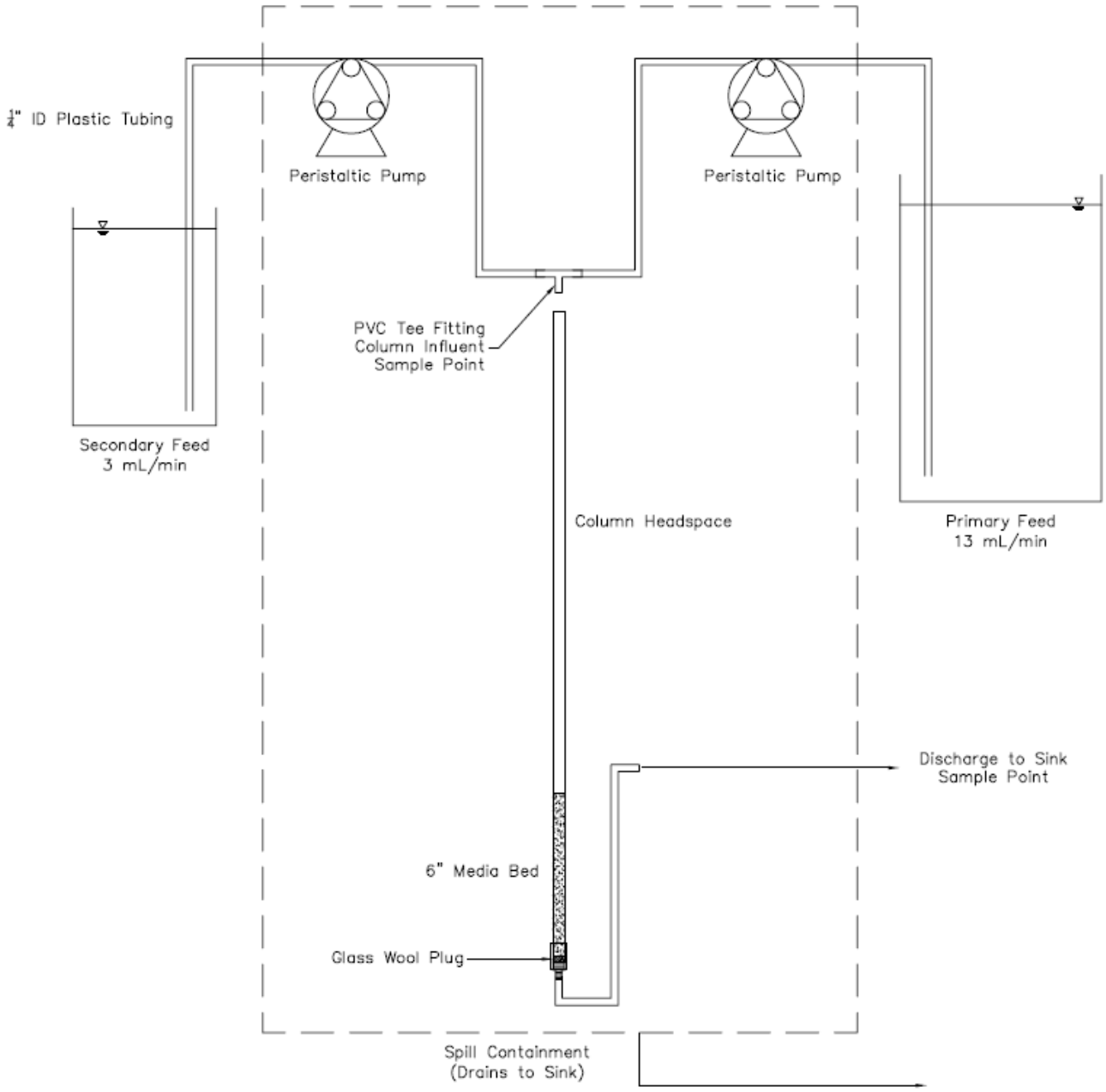

Figure 3. Schematic of Bench-Scale Column Experimental Layout without the sodium acetate feed (Hinds 2015)

Two peristaltic pumps were used to supply the main influent components to the columns. The hydraulic loading rate (HLR) for each of the columns was 4 gpm/ft^2. The total flow (16 mL/min) for each column was split between two influent feed solutions to equal the desired HLR. The main influent feed solution containing soluble Mn, aluminum, and alkalinity was

pumped into the column at a rate of 13 mL/min. The second influent solution contained either alkalinity and chlorine, or alkalinity only (when chlorine application ceased) and was fed at a rate of 3 mL/min. If needed, according to experimental setup, a third pump calibrated to a flow of 1 mL/min was used for the addition of sodium acetate when the columns were inoculated with Mn-reducing microorganisms. The pumps were calibrated to the desired flow before the start of each experiment. All columns and peristaltic pumps were placed inside a plastic tub for security against accidental overflow.

Influent flow solutions were drawn from the plastic reservoirs and delivered to the column through ¼ inch ID plastic tubing. The flows were then combined using a plastic tee that was placed in the top of the columns. This allowed the influent feed solutions to combine at the desired flow rates, 13 and 3 mL/min, and drip down to the filter sand media for a combined flow of 16 mL/min.

3.1.2 Column Influent Solution Preparation

Influent feed solutions were prepared with deionized water in five-gallon increments and stored in larger plastic reservoirs (Table 1). A 100x stock solution of soluble Mn was prepared weekly by dissolving 0.16 g of manganese chloride tetrahydrate ($MnCl_2*4H_2O$) into 100 mL of deionized water. A 100x Al stock solution was also prepared weekly by dissolving 1.09 g of aluminum sulfate octadecahydrate ($Al_2(SO_4)_3*18H_2O$) into 100 mL of deionized water. A volume of 2.5 or 10 mL of the 100x solutions (Mn^{2+} and Al^{3+}) along with 1.52 g of sodium bicarbonate ($NaHCO_3$) were combined with five gallons of deionized water as the working feedstock.

During times when protocol dictated that free chlorine was to be fed to the column at 2.0 mg/L, 0.47 mL of concentrated household chlorine bleach (Clorox, 8.25% available free chlorine) was added to 5 gallons of deionized water. This chlorine concentration provided an effluent concentration of approximately 1.0 mg/L. Chlorine demand across the column at a 0.2 mg/L soluble influent Mn concentration was 1.0 mg/L. When free chlorine was being fed to the column at 1.1 mg/L, which resulted in an effluent concentration of 0.1 mg/L, 0.24 mL of concentrated household chlorine bleach was added to 5 gallons of deionized water. Alkalinity was also added at a mass of 1.52 g $NaHCO_3$ for an additional 1 meq of alkalinity. Total combined influent feed characteristics can be viewed in Table 1.

A mass of 0.8 or 20 g/L of sodium acetate was dissolved in nanopure water to prepare the sodium acetate feed. A five-gallon volume was prepared every other day. Spare feed lines, of the same length, were made in order to allow for bleaching of tubing as needed. Using a syringe, a 50:50 Clorox bleach (8.25%) solution was pushed through the tubing to decrease biofilm growth and carbon consumption before column entry.

Table 1. Combined Feed Characteristic Ranges for Column Influent

Influent Characteristic	Value
Alkalinity (meq/L)	2.0
Free Chlorine (mg/L as Cl_2)	0.5-2.0
Manganese (μg/L)	50 - 200
Aluminum (μg/L)	50 - 200
pH	6.3 – 7.3
TOC as C* (mg/L)	0.5 or 12

* Required in inoculated anthracite column desorption study

3.1.3 pH Control

The pH of the influent feed solutions was monitored and adjusted with concentrated hydrochloric acid (HCl) as needed. The feed solutions were buffered with 2 meq/L of alkalinity added as bicarbonate. As the feed solutions would age, an upward drift in pH would naturally occur due to the loss of carbon dioxide (CO_2) to the atmosphere. Also, an increase in pH was seen when the influent feed solutions combined. Because of this upward pH drift over time, the pH of the stock solutions was generally made to be a little lower than the goal pH to compensate for this trend. The pH meter (HACH HQ40d) that was utilized for this experiment was calibrated daily before use.

3.1.4 Chlorine Discontinuation

For all conducted experiments, $MnO_{x(s)}$ coating developed by the reaction of soluble Mn^{2+} with free chlorine. During the time period when the media was being coated, free chlorine, at a targeted effluent concentration range of 0.1 to 1.0 mg/L, was applied to the filter depending on the experimental setup. After a predetermined number of days, the free chlorine and 2 meq

alkalinity stock was removed from the filters and was replaced by deionized water that still contained 2 meq of alkalinity.

3.1.5 Column Backwashing Procedure

Over the time the column is operated, particulate Mn and Al form together and are captured by the filter media. After a period of accumulation of this particulate matter, head loss begins to occur in the columns, reducing filter capacity, and backwashing is necessary. The columns used were six inches in height, which resulted in 18 inches of free board water due to headloss. Once head loss began to accumulate and water in the column was close to 18 inches in height over the media bed, flow to the column was temporarily stopped and an upflow backwash procedure was performed. The filter columns were backwashed approximately every 24 hours of operation. The effluent tubing from the column was attached to a peristaltic pump. Deionized water was pumped through the bottom of the column at a rate of 100 mL/min (25 gpm/ft^2). This allowed for approximately 30% bed expansion of the media. An additional piece of ½ inch ID tubing with a ½ x ¼ inch ID coupling was attached to the top of the column in place of the influent feed, along with an ¼ inch ID tube attached to the couple directing backwash flow into the sink. Each column was backwashed daily with a volume of 1 L of deionized water or until particulate matter could no longer be seen leaving the fluidized bed. After backwashing was complete, the influent tee couple was placed back in the top of the column resuming influent flow. The effluent tubing was detached from the peristaltic pump and was placed back over the funnel to allow drainage to the sink at an elevated level.

3.1.6 Sample Collection

Influent and effluent samples were collected from the columns for each time point taken. The tee coupling was placed into a clean beaker for approximately five minutes to collect influent samples. The tubing was removed from the funnel in the sink and was placed into a clean beaker for five minutes to obtain an effluent sample. The tubing remained elevated to maintain positive hydraulic head in the column while collecting effluent samples.

3.1.7 HACH Sample Analysis

HACH reagent sets were utilized for rapid results and help with daily column operation. The 1-(2-pyridylazo)-2-napthol PAN method analysis was used to analyze for Mn (Hach 2016a).

For aluminum analyses, the eriochrome cyanine R method was performed (Hach 2016b). The DPD method was used for the measurement of free chlorine (Hach 2016c). If dilution of a sample was needed, nanopure water was used. Samples were read colormetrically using a bench top spectrophotometer (Hach DR2800).

3.1.8 ICP Sample Analysis

Samples were analyzed for concentrations of Mn and Al in solution using an ICP-MS (Thermo Electron Corporation X-Series). Volumes of 5-10 mL of sample were collected in capped plastic ICP sample tubes. Samples were acidified by adding 2% nitric acid by volume. Samples were analyzed using the laboratory procedure with standard SM-1517-014.

3.1.9 Experimental Conditions for the Mn Desorption Study with Coated Virgin Sand

Column desorption studies (following the setup in Table 3) used FilterSil 0.50 sand media (Table 2), manufactured by Unimin Corporation (New Canaan, CT). The columns contained a six-inch bed depth of uncoated virgin filter sand that was autoclaved on a 20-minute gravity cycle for sterilization prior to addition into the column.

Table 2. FilterSil 0.50 Virgin Filter Sand Characteristics

Parameter	Value
Effective Size	0.5 mm
Uniformity Coefficient	1.63
Specific Gravity	2.65
Extractable Mn	< 0.001 mg/g dry media
Extractable Al	< 0.001 mg/g dry media

Table 3. Experimental Conditions for Coated Virgin Sand Media Experiment

Influent Characteristic	Value
Influent Alkalinity (meq/L)	2.0
Influent Free Chlorine (mg/L as Cl_2)	1.5-2.0
Influent Manganese (μg/L)	200
Influent Aluminum (μg/L)	200
pH	7.15 ± 0.15
Duration of $MnO_{x(s)}$ Coating (days)	5 or 14

3.1.10 Experimental Conditions for the Mn Desorption Study with Harwood Mills Anthracite Media (May 2015)

Anthracite coal media was obtained in May 2015 from Filter 1 of the Harwood Mills Water Treatment Plant (Newport News, VA). The filter had been in service for approximately 28 years and had been backwashed immediately before sample collection. Study details followed the experimental set up detailed in Table 4. The columns contained a six-inch bed depth of the collected anthracite coal. Influent Mn and Al were decreased from 200 μg/L to 50 μg/L after 8 days of column operation. Experimental conditions were identical in duplicate columns, with the exception of pH. Column A had a pH range of 6.3 - 6.6 and Column B had a pH range of 7.0 – 7.3 for the duration of the experiment.

Table 4. Experimental Conditions for Harwood Mills Anthracite Media Experiment

Influent Characteristic	Value
Influent Alkalinity (meq/L)	2.0
Influent Free Chlorine (mg/L as Cl_2)	1.5-2.0
Influent Manganese (μg/L)	50 or 200
Influent Aluminum (μg/L)	50 or 200
pH	6.3 – 6.6 or 7.0 – 7.3
Duration of $MnO_{x(s)}$ Coating (days)	3

3.1.11 Experimental Conditions for the Mn Desorption Study with Mn Reducer Inoculated Harwood Mills (Newport News, VA) Anthracite Media (February 2016)

Anthracite coal media from the upper filter layers of the Harwood Mills Water Treatment Plant (Newport News, VA), was collected in February 2016 from Filter 1. The filter had been online approximately 5.5 hours after the last backwash cycle when the media was collected. Table 5 details the experimental conditions for this column study.

Table 5. Experimental Conditions for Harwood Mills Anthracite Media Experiment

Influent Characteristic	Value
Influent Alkalinity (meq/L)	2.0
Influent Free Chlorine (mg/L as Cl_2)	0.5 – 1.0
Influent Manganese (μg/L)	50
Influent Aluminum (μg/L)	200
pH	6.45 ± 0.15
Duration of $MnO_{x(s)}$ Coating (days)	4
Influent TOC as C (mg/L)	0.5 or 12

One of the columns was inoculated with known Mn-reducing strains, either *S. oneidensis* MR-1 or MB4 (*Bacillus pumilus*) and MB6 (*Bacillus cereus*) together. MB4 and MB6 were isolated from anthracite media from a WTP (Cerrato 2008) and are discussed further in Table 7. The other column had no inoculum.

To prepare the *S. oneidensis* MR-1 inoculum, a 10-μL sterile loop full of culture from an agar plate was added into 100 mL of R2A broth. The flask was incubated for 48 hours in a shaking water bath at 30 °C. *S. oneidensis* MR-1 was then used as the inoculum into a 1 L volume of R2A broth and again incubated for 48 hours in a shaking water bath at 30 °C. The entire volume of culture was allowed to incubate at room temperature for an additional 24 hours as a temperature acclimation step. The culture was centrifuged at 5,000 x g for 20 minutes to concentrate the pellet. The pellet was suspended into a 200 mL volume of Mn-reduction broth, which was poured over the anthracite media in the column. To check for contamination of the inoculum, a t-streak was completed, using standard methods techniques, onto R2A agar. This was to verify that *S. oneidensis* MR-1 was the only organism present in the inoculum. The culture was allowed to flow through the column for a short time, approximately 10 seconds, and then was used to fill the column completely. The column was left undisturbed for 24 hours, at which time it was lightly backwashed. Additional culture was added to the column and was again flowed through for a short time. Culture filled the column and was left undisturbed for an additional 24 hours. After the period of column inoculation, water flow began to the filter.

To prepare the MB4 and MB6 inoculum, a 10-μL sterile loop full of each culture from agar plates were added into separate flasks of 100 mL of R2A broth. The flasks were incubated for 48 hours in a shaking water bath at 30 °C. MB4 and MB6 were then used as the inoculum for separate 1 L volumes of R2A broth and again incubated for 48 hours in a shaking water bath

at 30 °C. The volumes of culture were allowed to incubate at room temperature for an additional 24 hours as a temperature acclimation step. The cultures were centrifuged individually at 5,000 x g for 20 minutes to concentrate the pellets. The pellets were each suspended into a 200 mL volume of Mn reduction broth. A volume of 100 mL of the concentrated MB4 and MB6 culture were mixed together and added into the column. The cultures were allowed to flow through the column for a short time, approximately 10 seconds to ensure full contact with all depths of the media. The column was left undisturbed for 24 hours, at which time it was lightly backwashed. An additional equal volume mixture of MB4 and MB6 cultures were added to the column and flowed through for a short time. The cultures filled the column and were left undisturbed for an additional 24 hours. After the period of column inoculation, water flow began to the filter.

3.2 *In Situ* Mn Reduction Vial Assay

An *in situ* vial assay was developed to semi-quantitatively evaluate the Mn-reduction capability of isolated individual bacterial strains or diverse microbial communities, such as those found in water plant filters. Nealson et al. (1991) used an *in situ* vial assay to evaluate Mn-reduction of strains isolated from the Black Sea. Various modifications, detailed in the following sections, were made from the protocol established by Nealson et al (1991). Modifications to the medium composition were completed to encompass a more diverse microbial population than those that had been isolated from the Black Sea.

3.2.1 $MnO_{x(s)}$ Synthesis

Fresh $MnO_{x(s)}$ was made for use in the *in situ* vial experiments due to concerns of increased $MnO_{x(s)}$ stability over time, which has been thought to decrease bioavailability to microorganisms (Burdige 1992). $MnCl_2$ and 1 meq of alkalinity was reacted with potassium permanganate ($KMnO_4$) using the stoichiometric ratio of 1.92 mg $KMnO_4$ /1 mg Mn. In two of the synthesized $MnO_{x(s)}$ samples, 3 meq of calcium was added to discourage the formation of colloidal $MnO_{x(s)}$. $KMnO_4$ was dissolved into 500 mL of nanopure water and the $MnCl_2$ was dissolved in 250 mL of nanopure water. The $KMnO_4$ solution was added in 50 mL increments to the $MnCl_2$ solution. It can be seen by Equation 1 that this reaction is acid producing, therefore the pH was monitored and adjusted with 50% NaOH after each incremental addition of $KMnO_4$ to maintain a pH of 7.0 ± 0.1 throughout the reaction.

$$3\ Mn^{2+} + 2\ KMnO_4 + 2\ H_2O = 5\ MnO_{2(s)} + 2\ K^+ + 4\ H^+ \quad [1]$$

Once the reaction was complete, the supernatant was visually inspected for clarity so that it was ensured that all $KMnO_4$ had been reacted (Figure 4) and the $MnO_{x(s)}$ was allowed to settle and the supernatant was poured off. The $MnO_{x(s)}$ was centrifuged at 10,000 x g for five minutes to form a pellet and remove excess supernatant. The $MnO_{x(s)}$ samples were washed by resuspension in nanopure water, and re-centrifuged to form a new pellet three times. A single $MnO_{x(s)}$ sample was dried at 103 °C overnight and, using a mortar and pestle, was then ground into a fine powder. All other synthesized $MnO_{x(s)}$ samples were left as a wet "mud."

3.2.2 $MnO_{x(s)}$ Sample Summary

A total of five $MnO_{x(s)}$ samples were used in all Mn reduction soft agar vial experiments. The $MnO_{x(s)}$ samples were either purchased from a chemical supplier or synthesized in house with various treatments or chemicals added (Table 6).

Table 6. Characterization of $MnO_{x(s)}$ Samples

Approximate Synthesis Date "Name"	Origin	Other Notes
2008	Purchased from Sigma-Aldrich in 2008	<5 micron, activated ~85%
7-8-15	In house synthesis on 7-8-15	Dried in oven at 103 °C for 24 hours
7-28-15	In house synthesis on 7-28-15	
11-18-15	In house synthesis on 11-18-15	Added 3 mEq of Ca^{2+}
1-11-16	In house synthesis on 1-11-16	Added 3 mEq of Ca^{2+}

3.2.3 $MnO_{x(s)}$ Chlorine Inactivation

During the course of trial and error when finalizing the $MnO_{x(s)}$ soft agar media, it was hypothesized that the increased heat produced during the autoclave process altered some of the physical properties of the $MnO_{x(s)}$. After $MnO_{x(s)}$ samples were autoclaved, it was increasingly difficult to distribute the solid oxide evenly in the soft agar due to clumping of the $MnO_{x(s)}$ (Figure 4). A chlorine inactivation method was elected since sterilization via autoclave of $MnO_{x(s)}$ was not ideal for even distribution in the vial assay.

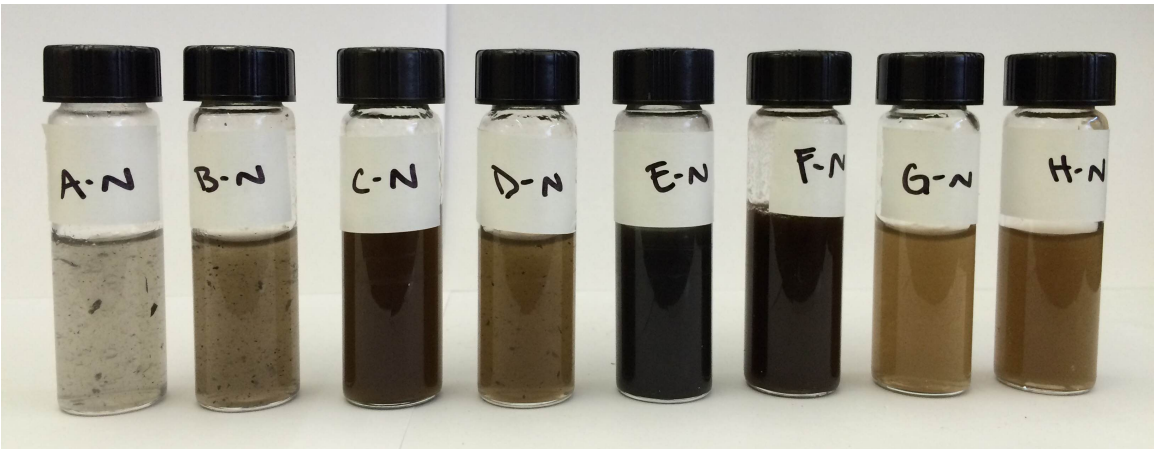

Figure 4. Image of uneven (A-D) and even (E-H) distribution of several $MnO_{x(s)}$ samples after autoclaving (A-D) and chlorine inactivation (E-H)

A goal of 10,000 mg/L*min C_t was targeted for inactivation of any microorganisms that may have been present on the $MnO_{x(s)}$ samples. A 10-ppm free chlorine solution was made using Clorox bleach (8.25% sodium hypochlorite) and deionized water. The desired mass of each $MnO_{x(s)}$ sample being tested was weighed and placed into a sterile 15 mL Falcon tube. A volume of 10 mL of the 10-ppm chlorine solution was added into each tube and the samples were vigorously vortexed. Samples were allowed to maintain chlorine contact for approximately 17 hours overnight to inactivate the microorganisms present. Free chlorine for each sample was measured using HACH DPD methods (Hach 2016c) before and after microorganism inactivation was completed.

3.2.4 Media Composition

A manganese reduction contained the following per liter of 10 mM HEPES buffer (pH 7.4): 0.2 g yeast extract, 2 g sodium acetate and 3 g agar (0.3%). The media was autoclaved on a 20-minute liquid cycle and was allowed to cool before the addition of $MnO_{x(s)}$. $MnO_{x(s)}$ was added, following chlorine inactivation, at a concentration of 0.35 or 0.7 g/L, depending on the color and properties of the oxide. This was done in order to target a starting transmittance of around 4-8%.

$MnO_{x(s)}$ samples that air dried over an extended amount of time or in an oven, were typically darker in color than those left as a wet mud. Because of this, different amounts of the 2008 and 7-8-15 $MnO_{x(s)}$ samples were added into 10 mL of the $MnO_{x(s)}$ reduction soft agar and

transmittance at 540 nm was measured (Figures 5 and 6). Again, the optimal concentration of $MnO_{x(s)}$ for each sample was determined to be concentrations that fell with in the 4-8% transmittance range. The 2008 and 7-8-15 $MnO_{x(s)}$ samples were added into the media at a 0.35 g/L concentration. All other $MnO_{x(s)}$ samples were added at a concentration of 0.7 g/L.

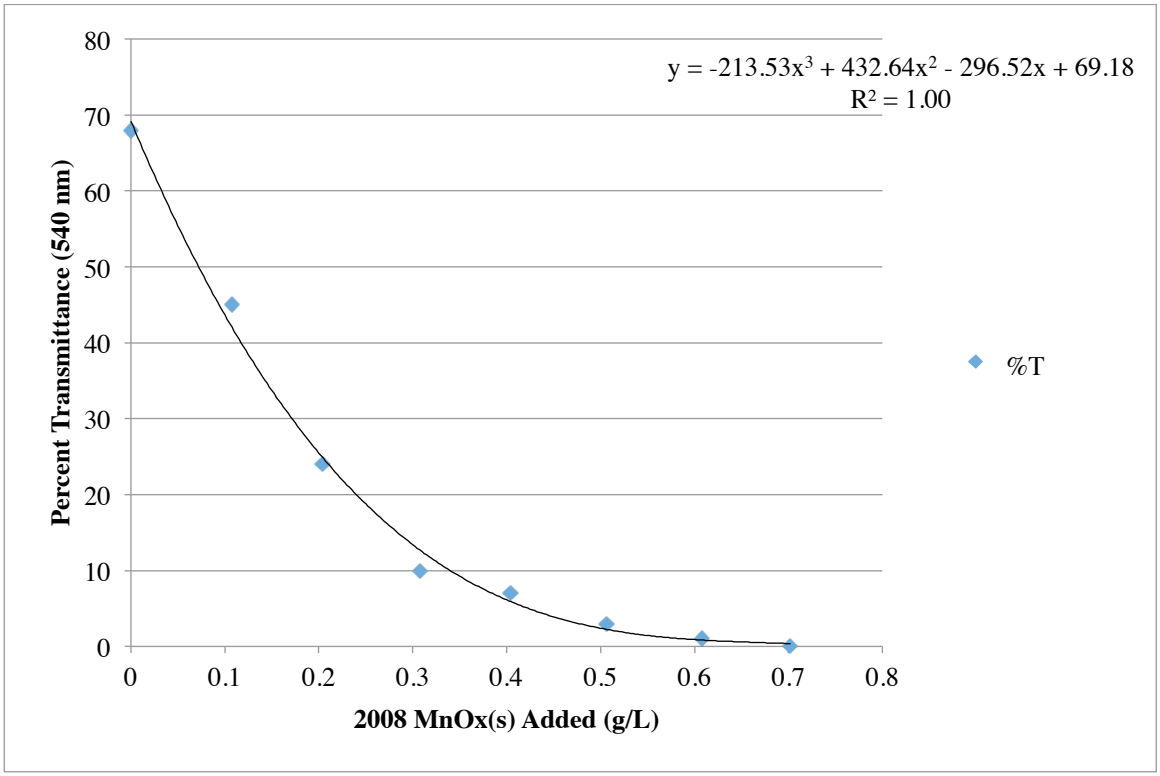

Figure 5. Percent transmittance of 2008 $MnO_{x(s)}$ sample as a function of $MnO_{x(s)}$ concentration added

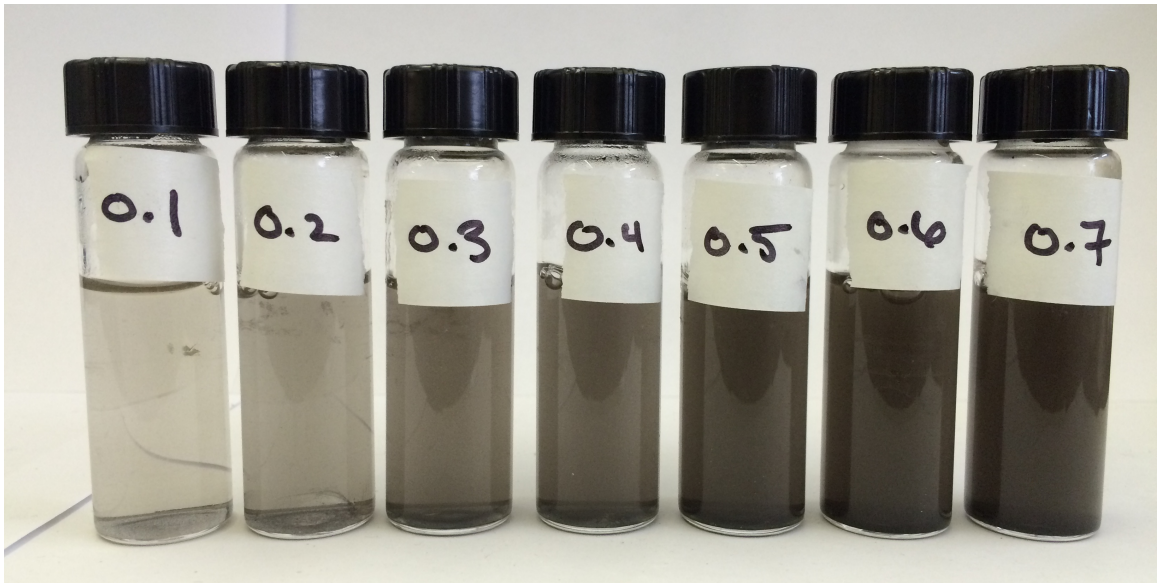

Figure 6. Visual comparison of different concentrations (g/L) of the 2008 $MnO_{x(s)}$ sample

Various concentrations of agar were tested, ranging from 0.2% to 1.0%, including 0.75% agar, following the protocol established by Nealson et al. (1991). The goal of the method development was to measure Mn reduction semi–quantitatively. For this, a lower concentration of agar was needed to allow for adequate distribution and ease of Mn-reducing microorganism motility through the agar for the strains tested. The organisms initially tested in this vial assay, *Bacillus spp*. (Kristoffersen 2007) and *Shewanella oneidensis* (Sun 2014), were known to be motile. A 0.3% agar concentration was chosen and used in all vial experiments as it allowed easy mixing, uniform $MnO_{x(s)}$ distribution, and motility of the microbes in the vial.

3.2.5 Negative and Positive Control Vials

A volume of 100 µL of sterile deionized water was added into a vial of each $MnO_{x(s)}$ sample for the negative control. A percent transmittance curve with differing masses of hydroxylamine sulfate "HAS" were added into vials with 10 mL of 0.7 g/L $MnO_{x(s)}$ soft agar media for determination of the optimal HAS concentration in positive control vials. Percent transmittance was measured to determine the optimal HAS dose for maximum Mn reduction (Figure 7). A concentration of 0.020 g HAS per 10 mL of 0.7 g $MnO_{x(s)}$ reduction soft agar media was shown to produce the highest amount of reduction at the lowest possible dose. For positive control vials, 0.020 g of HAS was added into each vial.

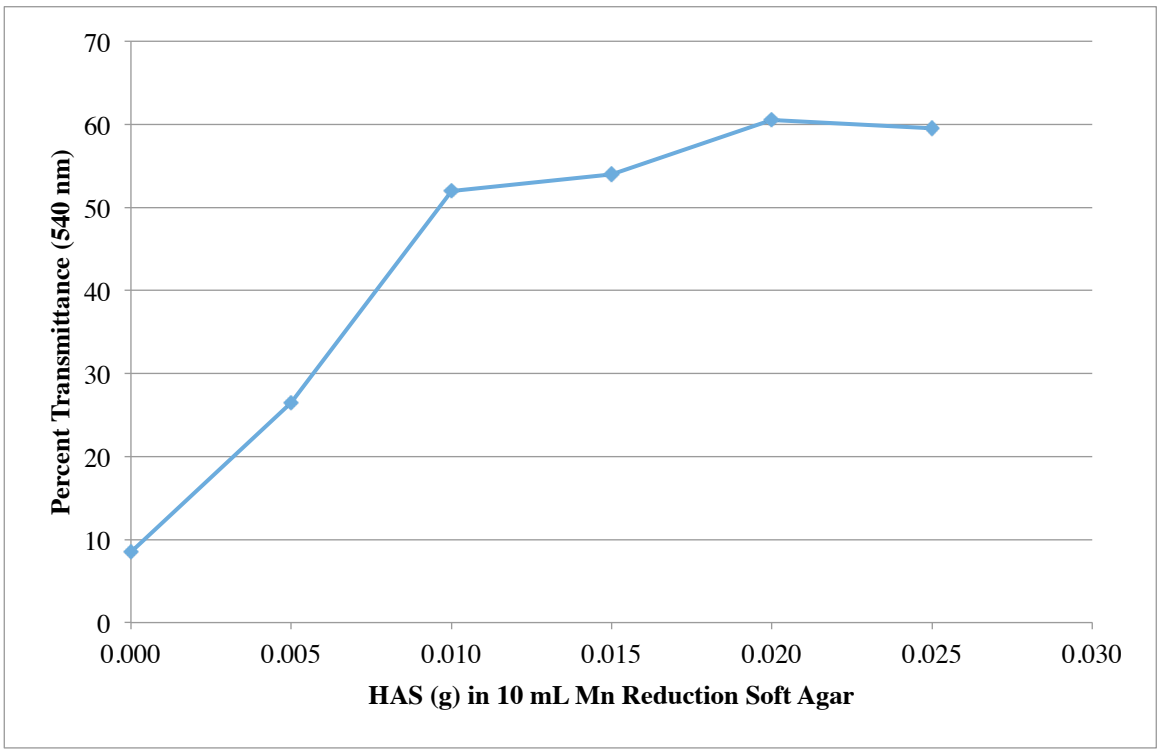

Figure 7. Percent Transmittance for Differing HAS Masses in 10 mL Mn Soft Agar Media

3.2.6 Mn-Reducing Bacteria

One of the microorganisms used for vial and column studies, *Shewanella oneidensis* MR-1, was obtained from Dr. Kenneth Nealson's lab at the University of Southern California. Several mutants of this strain, with deletions in the *mtrA* or *mtrB* gene, along with the wild type strain were received. Wild type is defined as the phenotype of the typical form of a microorganism as it would occur in nature.

The other strains used in these experiments were isolated from various locations in the water treatment built environment (Table 7) (Cerrato 2008). All of the environmental strains used were able to both oxidize and reduce Mn. Mn oxidation or R2A medium was used for culture streaks or enumeration. The Mn oxidation medium contained the following per liter of 10 mM HEPES buffer (pH 7.4): 0.5 g yeast extract, 2 g bacto-peptone, 0.001 $FeSO_4*7H_2O$, 0.15 g $MnSO_4*H_2O$ and 15 g agar (1.5%). The R2A agar, per liter (pH 7.0), contained 0.5 g proteose

peptone, 0.5 g casamino acids, 0.5 g yeast extract, 0.5 g dextrose, 0.5 g soluble starch, 0.3 g K_2SO_4, 0.05 g $MgSO_4*H_2O$, 0.3 g $C_3H_3NaO_3$, and 15 g agar.

Table 7. Water Built Environmental Mn Reducing Isolates

Strain ID	Genus and Species	Isolation Site	Sample Isolation Location	Manganese oxidation capability
MB-4	*Bacillus pumilus*	North Carolina	Filtration Basin - Anthracite Media	Yes
MB-5	*Bacillus cereus*	Honduras	Distribution System Pipe-PVC Pipe	Yes
MB-6	*Bacillus cereus*	Virginia, Newport News	Sedimentation Basin- Top Sludge	Yes
MB-7	*Lysinibacillus fusiformis*	Virginia, Blacksburg	Sedimentation Basin - Top Sludge	Yes

3.2.7 In Situ Vial Inoculation

Vials were inoculated from fresh cultures off of Mn oxidation or R2A agar grown overnight. Cultures were scraped off the plate with a sterile loop and suspended in 1.5 mL of sterile deionized water. If serial dilutions were required, the original culture suspension was diluted as needed by a one-log concentration for each step. If anaerobic conditions were specified for the experimental protocol, all dilutions and inoculation work were performed inside a Coy laboratory anaerobic chamber with an atmosphere of 80% nitrogen, 10% carbon dioxide and 10% hydrogen. A 100-µL aliquot of the culture suspension was added into each vial and was vortexed. Each inoculum was enumerated using standard heterotrophic pour plate methods on R2A agar before the addition into vials.

3.2.8 Percent Transmittance Measurement

Percent transmittance using a spectrophotometer was measured on daily or periodic basis as needed. The spectrophotometer was calibrated at the 540 nm wavelength before each use.

3.2.9 Sampling for Molecular Detection Methods

Samples for DNA extraction and qPCR quantification were also taken from each vial during certain experiments. After percent transmittance was measured, a sample volume of 0.25 mL was taken from each vial and placed in a sterile 1.5 mL microcentrifuge tube and stored at -20 °C until samples were thawed for DNA extraction.

3.3 Molecular Methods Development for *S. oneidensis* MR-1

The ability to identify and quantify *S. oneidensis* MR-1 during vial and column studies using molecular technologies was explored. The ability to enumerate cells numbers of *S. oneidensis* MR-1 in laboratory experiments could provide some insight into the contribution of microbially mediated Mn reduction by that strain.

3.3.1 DNA Extraction

DNA was isolated from pure cultures and environmental samples using the PowerSoil kit from MoBio Laboratories, Inc. (Catalog number 12888). Samples were placed in a Vortex-Genie 2 adapter for the lysing step, according to the protocol established by MoBio (MoBio Laboratories 2016). If there were fewer than 12 samples, a 10-minute vortex time was used, however; if there were more than 12 samples, the vortexing time was increased to 15 minutes to ensure adequate lysing. Extraction protocols established by MoBio for the PowerSoil and UltraClean Microbial DNA Isolation kits were followed exactly, with no modifications. Samples were stored at -20 C after DNA isolation was complete.

3.3.2 qPCR Primers for the Detection of S. oneidensis MR-1

Previous research studying the role of the *mtrA* and *mtrB* genes in *S. oneidensis* MR-1 have demonstrated the necessity of these functional genes in the ability of a microorganism to reduce Mn (Schicklberger 2011). From this study, qRT-PCR primers were developed that were bound in a region of the *mtrB* gene for *S. oneidensis* MR-1. The forward and reverse primers from this study were used in qPCR detection and quantification of *S. oneidensis* MR-1 in vial and column studies are presented in Table 8.

Table 8. *S. oneidensis* MR-1 Forward and Reverse qPCR Primers

Primer Name	Sequence
MR1_Fwd	5'- CGGCTTAAAACAAGCCTCTG – 3'
MR1_Rev	5'- CCAAAGGTGGGGTTAAAAGC– 3'

Schickelberger et al. (2011) used the *S. oneidensis* MR-1 primers in qRT-PCR; therefore, the methods detailed from that study were not directly applicable to completing a qPCR assay. A DNA binding dye protocol was established using the SsoFast EvaGreen Supermix for qPCR quantification (Table 9). The total qPCR reaction volume was 10 µL.

Table 9. *S. oneidensis* MR-1 qPCR Mastermix Components

Reaction Component	Volume Added per Reaction (µL)
EvaGreen	5
Forward Primer (5 µM)	0.8
Reverse Primer (5 µM)	0.8
Molecular Grade Water	2.4
Template	1

3.3.3 qPCR Temperature Gradient for S. oneidensis MR-1

The optimal melting temperature for the *S. oneidensis* MR-1 qPCR primer set program was determined by a temperature gradient and melt curve. Melting temperatures that were tested ranged from 57.0 °C to 51.0 °C (Figure 8). The qPCR program and melt curve program can be seen in Tables 10 and 11. The melting temperature of 57.0 °C yielded the lowest quantification cycles (Cq) and the highest mass of DNA after a melt curve (Figure 9). Therefore, a melting temperature of 57 °C was chosen to for use in this qPCR protocol (Tables 10 and 11).

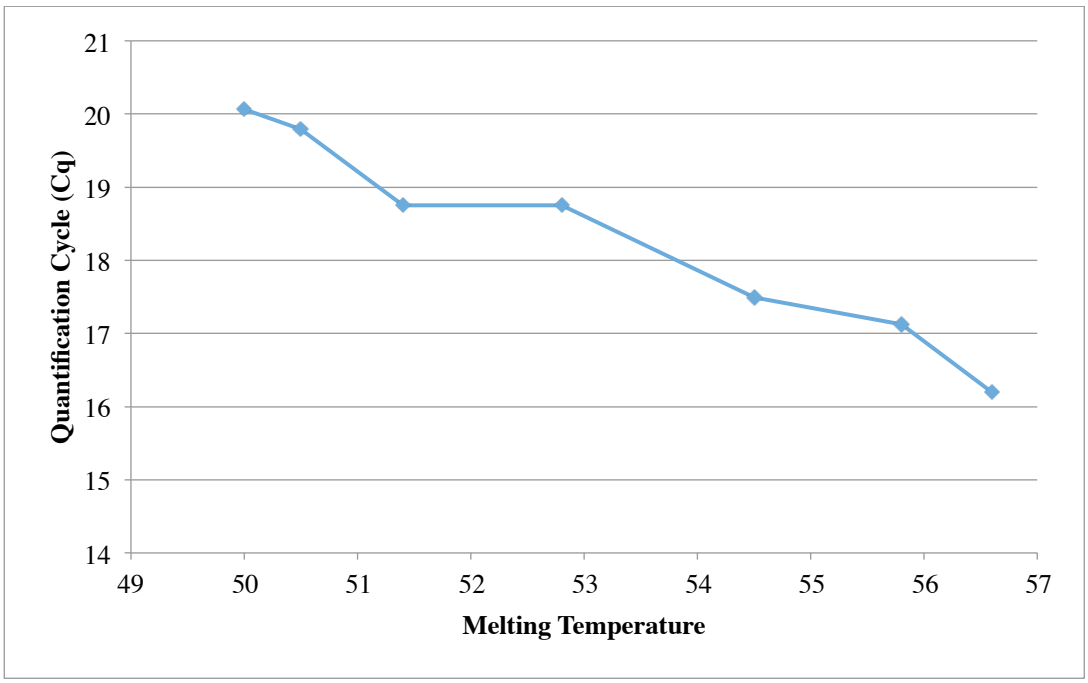

Figure 8. Shewanella oneidensis MR-1 qPCR melting temperature gradient

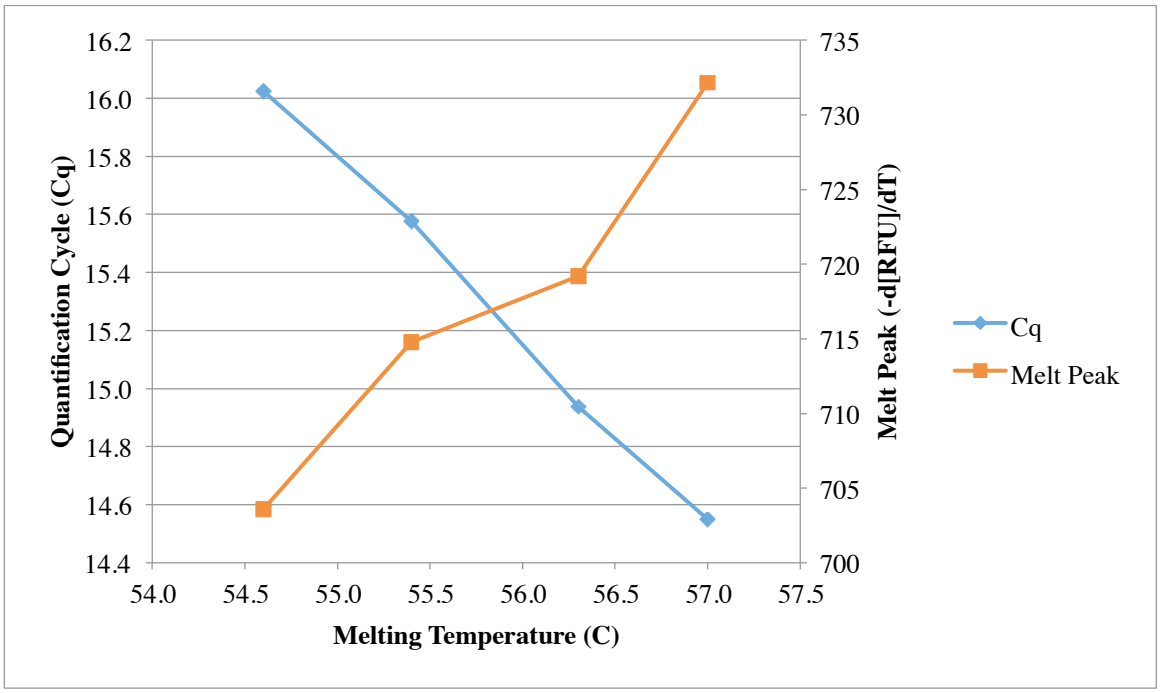

Figure 9. Shewanella oneidensis MR-1 qPCR melting temperature gradient from 54.5 to 57.0 C and corresponding melt peak

Table 10. *S. oneidensis* MR-1 qPCR Program

Cycle Temperature	Cycle Duration	Number of Cycles
98.0 °C	2 minutes	1
98.0 °C	5 seconds	40
57.0 °C	10 seconds	40

Table 11. *S. oneidensis* MR-1 Melt Curve qPCR Program

Cycle Temperature	Cycle Duration	Number of Cycles
98.0 °C	2 minutes	1
98.0 °C	5 seconds	40
57.0 °C	10 seconds	40
82.0 °C	2 minutes	1

3.3.4 *S. oneidensis* MR-1 Standard Curve for Absolute Quantification

Once a qPCR protocol was established, a standard curve for *S. oneidensis* MR-1 was created (Figures 10 and 11). This allowed absolute quantification of *S. oneidensis* MR-1 from laboratory or environmental samples.

The wild type *S. oneidensis* MR-1 was inoculated into 10 mL of R2A liquid broth, which contained, (per liter) at pH 7.0: 0.5 g proteose peptone, 0.5 g casamino acids, 0.5 g yeast extract, 0.5 g dextrose, 0.5 g soluble starch, 0.3 g K_2SO_4, 0.05 g $MgSO_4*H_2O$ and 0.3 g $C_3H_3NaO_3$, and shaken at low RPM in a 30 °C water bath for 48 hours. The inoculum was then serially diluted, stepping down in one-log concentrations until eight total dilutions had been prepared. DNA was extracted using the MoBio Laboratory, Inc. PowerSoil kit from each of the dilutions. A standard plate count method was used for the lowest (most concentrated) three dilutions. All of the serially diluted DNA extractions of *S. oneidensis* MR-1 were analyzed by the qPCR assay. Quantification cycles (Cq) were correlated to actual or back-calculated cell concentrations from the plate counts and translated to CFU/mL (Figures 10 and 11). The standard curve was fit to Equation 2, which could be used to calculate CFU/mL based off of an unknown sample quantification cycle value. The coefficient of variation (R^2) value for this standard curve was 0.99.

[2]

$$y = (2 * 10^{12}) * e^{-0.66x}$$

Where,

y = *S. oneidensis* MR-1 concentration (CFU/mL)

x = Quantification cycle

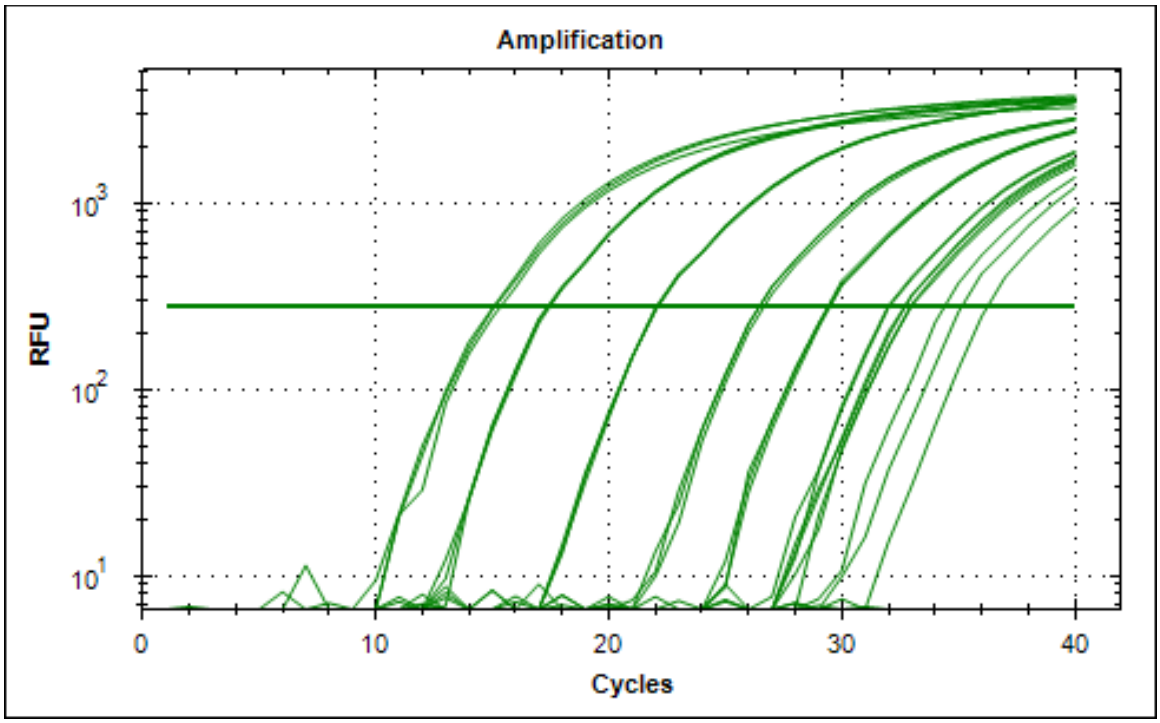

Figure 10. qPCR amplification RFU and quantification cycle data for standard curve samples of *S. oneidensis* MR-1

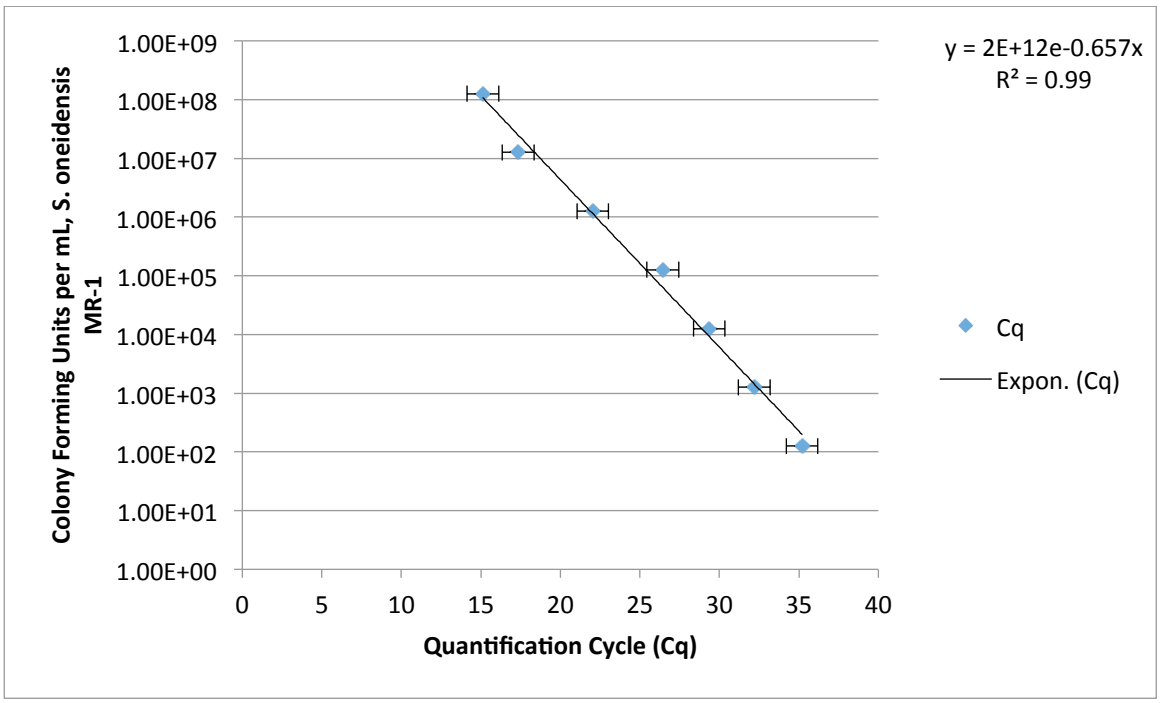

Figure 11. qPCR Standard curve of *S. oneidensis* MR-1 correlating plate enumeration counts (cfu/mL) to quantification cycle (Cq)

3.4 Molecular Methods Development for Detection of the *mtrB* Gene

A qPCR primer that would enable the detection of the *mtrB* gene in environmental and laboratory samples was developed. A molecular method for the detection of Mn reduction capability (tracking the presence of the *mtrB* gene) in a water treatment environment would be useful as this gene is required for Mn reduction (Szeinbaum 2014).

3.4.1 Sequence Selection

From the NCBI GenBank website, a search for the gene name/symbol "mtrB" was conducted resulting in a total of 13 protein sequences matching the search criteria. Ten were chosen for the gene alignment (Table 12) based off of the targeted sequence description.

Table 12. Descriptions of Selected Protein Sequences for MtrB MUSCLE Alignment

Location	Description	Genus and Species
NC-014318.1	Two-component system histidine kinase	*Amycolatopsis mediterranei U32*
NC-014318.1_1	Two-component system histidine kinase	*Amycolatopsis mediterranei U32*
NC-014318.1_2	Two-component system histidine kinase	*Amycolatopsis mediterranei U32*
NC-014318.1_3	Two-component system histidine kinase	*Amycolatopsis mediterranei U32*
NC-014318.1_4	Two-component system histidine kinase	*Amycolatopsis mediterranei U32*
NC-008611.1	Two-component sensory transduction histidine kinase MtrB	*Mycobacterium ulcerans* Agy99
NC-004347.2	Extracellular iron oxide respiratory system outer membrane component MtrB	*Shewanella oneidensis MR-1*
NC-002945.3	Two component sensory transduction histidine kinase MtrB	*Mycobacterium bovis AF2122/97*
NC-002677.1	Two-component system sensor kinase	*Mycobacterium leprae TN*
NC-000962.3	Two component sensory histidine kinase MtrB	*Mycobacterium tuberculosis H37Rv*

3.4.2 MUSCLE Gene Alignment

Multiple sequence comparison by log-expectation "MUSCLE" alignment (Edgar 2004) was chosen as the method to aid in development of the *mtr*B primer set. A nucleotide alignment was performed using the chosen nine sequences detailed in Table 12. Regions for placement of the forward and reverse primers were chosen based off high similarity of base pairs across the nine sequences for a 15-18 base pair length. There were no exact base pair alignments for 15-18 base pairs in a row for the entire length of the submitted *mtrB* gene sequence. Ambiguous base pairs were inserted on an as needed basis because of the variability of the *mtrB* gene. The ambiguous base pair denoted V is equal parts A, C or G for that location. The ambiguous base pair denoted S is equal parts C or G for that location. Table 13 details the final *mtrB* primer set.

Table 13. *mtrB* Forward and Reverse qPCR Primers

Primer Name	Sequence
mtrB_Fwd	5'- CSTTCAACVACATGGCCG – 3'
mtrB_Rev	5'- SGAGATCTCSAGCAGGTC – 3'

3.4.3 DNA Extraction for mtrB Primer Testing

DNA was isolated from the pure cultures of MB4, MB5, MB6, MB7 and *S. oneidensis* MR-1 using a Ultra Clean Microbial Isolation kit from MoBio Laboratories, Inc. (Catalog number 12224). Samples were placed in a Vortex-Genie 2 adapter for the lysing step, according to the protocol established by MoBio. Extraction protocols established by MoBio for the UltraClean Microbial DNA Isolation kits were followed exactly, with no modifications. Samples were stored at -20 °C after DNA isolation was complete.

3.4.4 Temperature Gradient

A temperature gradient using MB4, MB5, MB6, MB7 and *S. oneidensis* MR-1 DNA was completed to determine the optimal melting temperature for the *mtrB* qPCR primer set program. Melting temperatures were tested using DNA isolated from MB4, MB5, MB6, MB7 that ranged from 58.0 °C down to 50.0 °C (Figure 12). Melting temperatures were tested using DNA isolated from MB4, MB5, MB6, MB7 and *S. oneidensis* MR-1 that ranged from 52.0 °C down to 48.0 °C (Figure 13). A melting temperature of 50 °C was chosen based off of the temperature gradient and the data points with the lowest quantification cycle (Table 14).

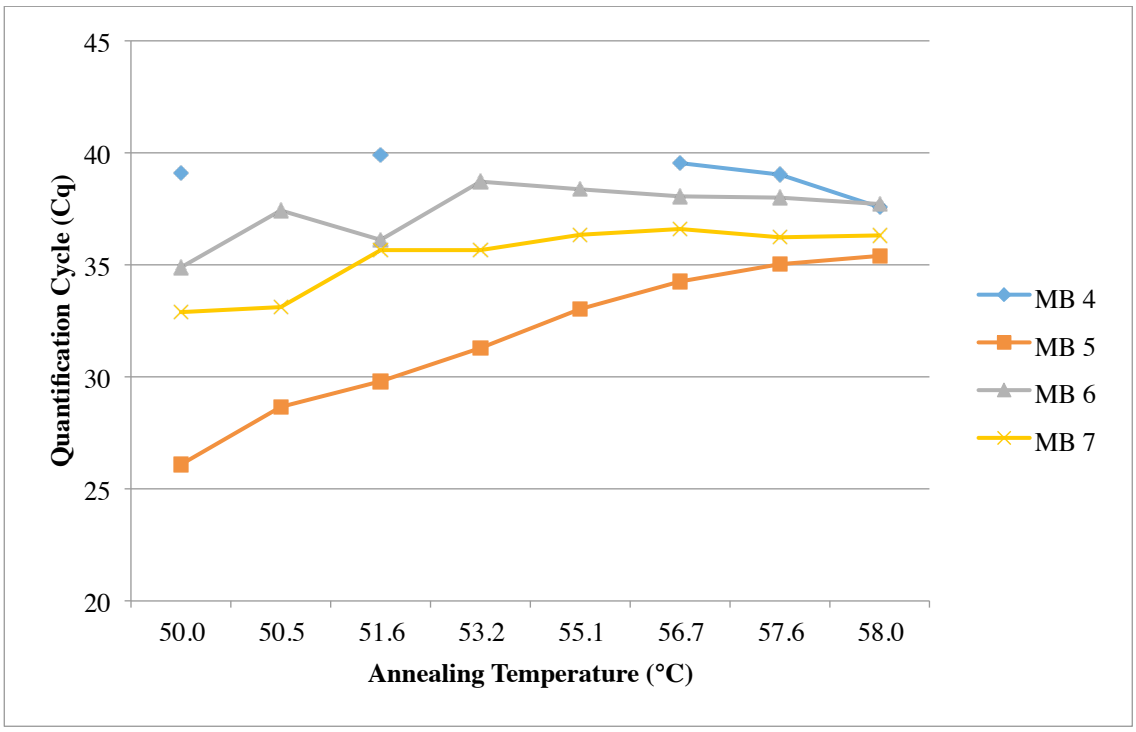

Figure 12. Environmental isolates qPCR melting temperature gradient for 50.0 to 58.0 C for the mtrB primer set

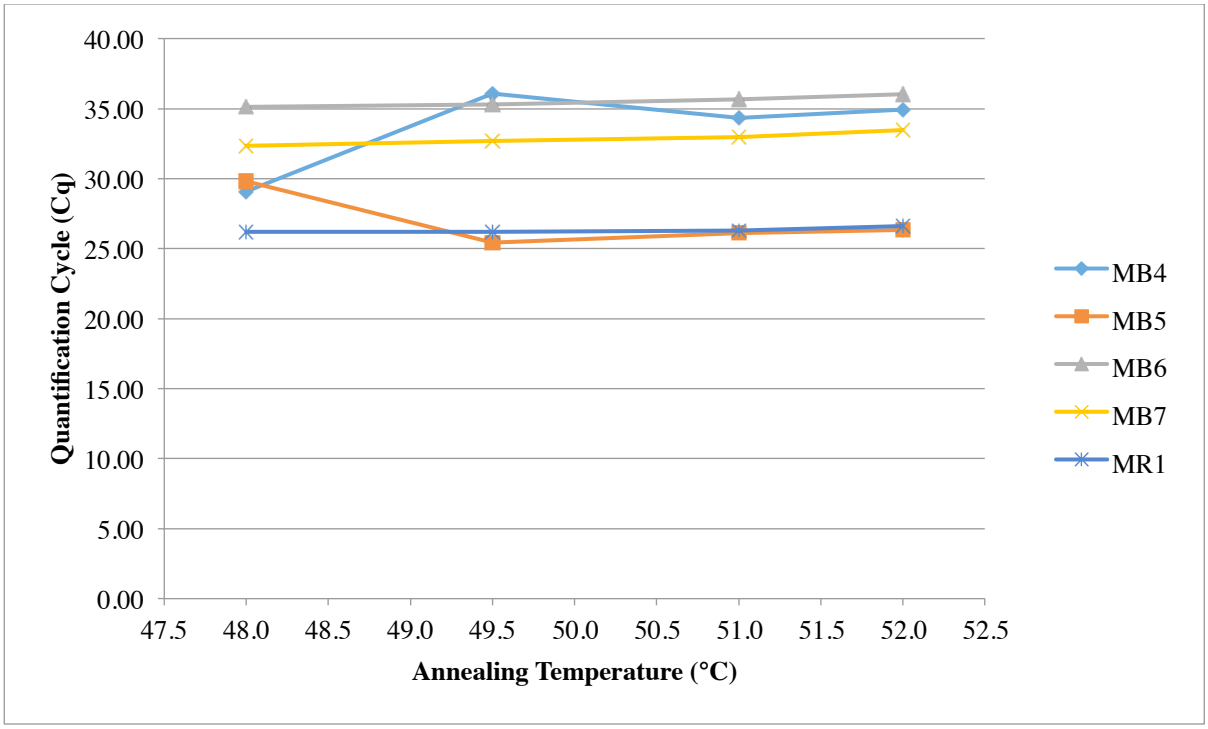

Figure 13. Environmental isolates and *S. oneidensis* MR-1 qPCR melting temperature gradient for 52.0 to 48.0 °C for the mtrB primer set

Table 14. *S. mtrB* qPCR Program

Cycle Temperature	Cycle Duration	Number of Cycles
98.0 °C	2 minutes	1
98.0 °C	5 seconds	40
50.0 °C	10 seconds	40

3.4.5 DNA Normalization

DNA was diluted and added into the wells at approximately the same concentration in order to normalize DNA and check for PCR inhibition. Extraction efficiency of the Ultra Clean kit was lower than that of the PowerSoil kit, so extracted samples had a lower starting concentration of DNA. All samples analyzed in this test were obtained from a pure colony, and were diluted with in the range of 5-15 ng/µL DNA. Taking into account dilution in the plate, final DNA concentrations in each qPCR reaction were between 0.5 and 1.5 ng at the start of the program (Figure 14).

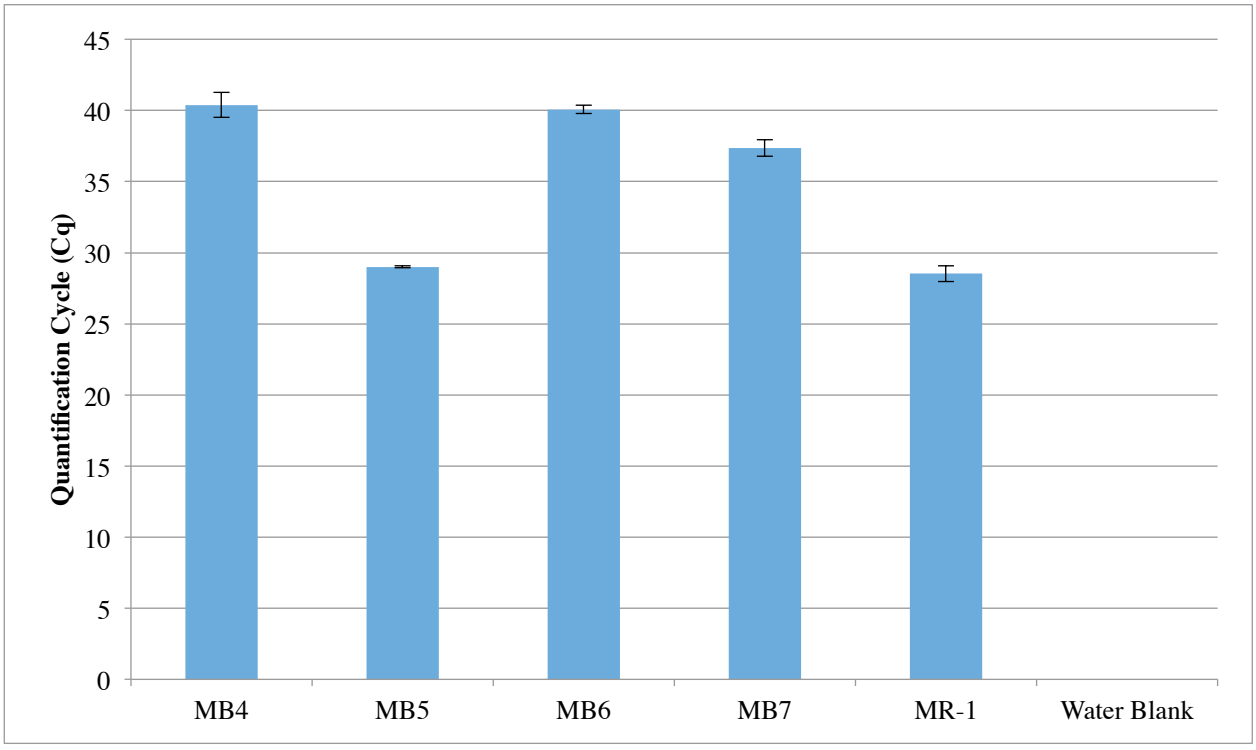

Figure 14. Environmental isolates and *S. oneidensis* MR-1 qPCR quantification cycle for the *mtrB* primer set at a 50 °C melting temperature when loaded DNA is normalized to 5-10 ng/µL

3.5 Shake Flask Study

A shake flask study was conducted to create an environment in which microbially mediated Mn desorption from anthracite coated media could be evaluated. *S. oneidensis* was added into flasks with Mn coated anthracite media and desorption was monitored over time.

3.5.1 Media Preparation

A volume of 245 mL of a modified Mn reduction broth was added into twelve 500 mL Erlenmeyer flasks. The Mn reduction broth contained per liter of 10 mM HEPES buffer (pH 7.4): 0.2 g yeast extract and 2 g sodium acetate. The negative control flasks had 50-μM zinc sulfate added to inhibit microbial growth (Nealson 1991). One pair of flasks also contained 2.5 g of amorphous $MnO_{x(s)}$ as a second type of negative control to investigate spontaneous background release of Mn into solution. Flasks were sterilized on a 15-minute liquid autoclave cycle. After autoclaving, 2.5 +/- 0.1g of anthracite from Harwood Mills (May 2015) was added into each designated flask (Table 15).

3.5.2 *S. oneidensis* MR-1 Inoculation

Three *S. oneidensis* MR-1 strains, the wild type, Δ*mtrA* and Δ*mtrB* were inoculated into R2A broth. The strains were allowed to incubate in a shaking water bath at 30 °C for 48 hours. All cultures were quantified using standard pour plate count methods on R2A agar plates. A volume of 2.5 mL culture was added into the designated flasks (Table 15). Flasks were covered with parafilm to prevent evaporation.

Table 15. Shake Flask Components and Conditions

Flask Component	1	2	3	4	5*	6
Modified Mn Reduction Broth (mL)	245	245	245	245	245	245
Anthracite Media (g)	2.5	2.5	2.5	2.5	2.5	0
***S. oneidensis*, wild type (mL)**	2.5	0	0	0	0	0
***S. oneidensis*, Δ*mtrA* (mL)**	0	2.5	0	0	0	0
***S. oneidensis*, Δ*mtrB* (mL)**	0	0	2.5	0	0	0
Amorphous $MnO_{x(s)}$ (g)	0	0	0	0	0	2.5

* 50 μM zinc sulfate added

3.5.3 Experimental Setup and Sampling

Medium, anthracite or $MnO_{x(s)}$ and cultures were combined in flasks and secured on a tabletop shaker and rotated at 50 RPM. Samples were withdrawn on days 0, 2, 5, 7, 9, 12 and 20 in 5 mL aliquots using 10 mL luer-lock syringes. The samples were filtered through a 0.45 μm Wheaton glass microfiber fiber filter to remove any solid phase or colloidal Mn that may have been sheared off during the shaking process. The filtered samples were preserved using 2% nitric acid for Mn analysis using the ICP.

3.5.4 Anthracite Media Extraction

Measurement of the amount of $MnO_{x(s)}$ coating on the anthracite media was completed following HAS extraction methods described by Knocke et al. (1991). Adaptations and modifications detailed below were conducted as needed for optimal performance and results.

Three aluminum pans were weighed and 1 gram of anthracite media (collected from the Harwood Mills WTP (Newport News, VA)), was placed in each. The media was dried for 24 hours at 103-105 °C and the dry weight of the media was recorded. The media was placed in 250 mL of 2% nitric acid deionized water with 300 mg HAS. After 10 hours, 10 mL samples were withdrawn from each of the triplicates and were diluted 1/50 and 1/100 to fit with in the ICP standard curve. Samples were analyzed via the ICP for Mn. Dissolved Mn was back calculated by using Equation 3.

[3]

$$\left(\frac{\text{mg metal}}{\text{g dry media}}\right) = \frac{\text{Concentration in Extraction Solution} \times \text{Volume Extraction Solution}}{\text{Dry Weight Media}}$$

4.0 EXPERIMENTAL RESULTS

This chapter details results from the experiments that were described in Chapter 3. Mn breakthrough trends are discussed from bench-scale filtration studies that evaluated the effects of influent pH, the duration of $MnO_{x(s)}$ coating and Mn-reducing microbial populations on the media. Then, aerobic and anaerobic vial assay results for five Mn-reducing bacterial strains are described, along with discussion of experimental results for bioavailability of varying $MnO_{x(s)}$ samples. Finally, Mn desorption data from an aerobic shake flask study, inoculated with *S. oneidensis* MR-1, are presented.

4.1 Bench-Scale Column Performance of Coated Sand Media

This section provides results from a filter column test conducted at nearly neutral pH values of 7.0 to 7.3, exposing uncoated sand media to free chlorine for a period of 5 or 15-days to develop a $MnOx_{(s)}$ coating. After the desired exposure time, free chlorine was removed from the filter influent and the potential for Mn breakthrough were measured by comparing soluble influent Mn to effluent Mn concentrations. Mn breakthrough trends for the 5-day and 15-day $MnOx_{(s)}$ coated filters were then compared on the basis of maximum values of Mn through the media bed and how quickly maximum breakthrough values were reached.

4.1.1 Mn Break Through During Chlorine Discontinuation of 5-day $MnO_{x(s)}$ Coated Virgin Sand Media

After five days, free chlorine was removed from the influent and the potential for Mn breakthrough was evaluated by comparing soluble influent Mn to effluent concentrations (Figure 15). An increase in effluent Mn concentration began within one hour of free chlorine removal. The increase continued for approximately 8.4 hours and reached a maximum value of 74% of the influent concentration. Manganese breakthrough values remained around 73-75%, representing steady state conditions within 8.4 hours after chlorine was removed from the filter.

The remaining 27% of the influent Mn that was not passing through the filter represented soluble Mn that was most likely adsorbed onto the $MnO_{x(s)}$ surface, where surface catalyzed oxidation then occurred. At neutral influent pH values (7.0 to 7.3), any appreciable amount of Mn oxidation due to contact with molecular oxygen found in the influent waters was highly improbable (Morgan 1964). A majority of the soluble Mn removed by the column was most

likely adsorbed onto active sites of the filter media and subsequently oxidized. As stated above, $MnO_{x(s)}$ coating on the sand media for this experiment was allowed to develop in the presence of free chlorine for a total of five days before chlorine application ceased. During chlorine application, $MnO_{x(s)}$ active sites were being continuously created and regenerated (Knocke 1991). Once chlorine application stopped, the available active sites continued to adsorb some of the influent Mn and then surface oxidize the soluble Mn.

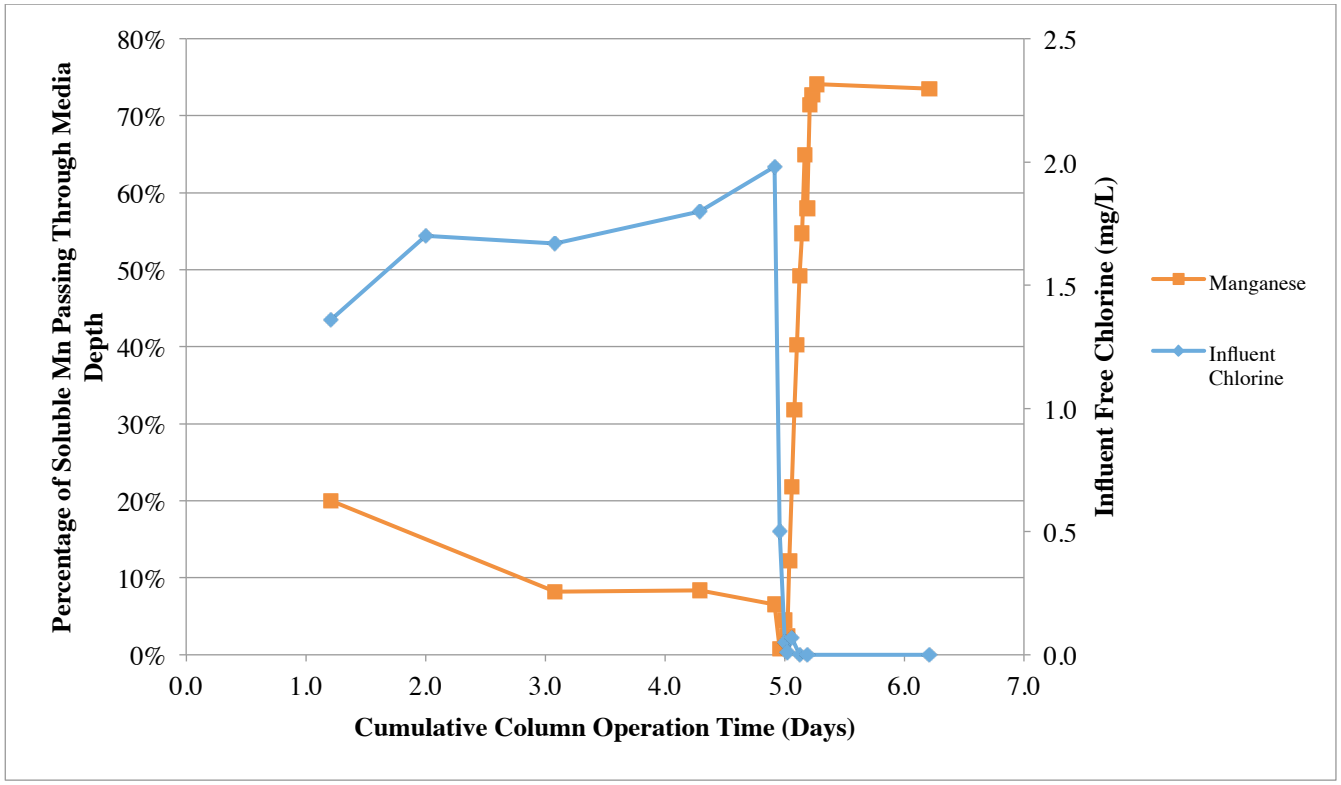

Figure 15. Percentage manganese removal before and after the discontinuation of chlorine of the 5 day $MnOx_{(s)}$ coated sand filter

4.1.2 Mn Break Through During Chlorine Discontinuation of 15-day $MnO_{x(s)}$ Coated Sand Media

After 15 days, free chlorine was removed from the influent and Mn breakthrough was measured by comparing soluble influent Mn to effluent concentrations. Figure 16 shows manganese breakthrough concentrations in the column effluent as a percentage of the influent. After chlorine was removed, effluent Mn concentrations began to rise within one hour. Manganese effluent concentrations increased steadily for 29.5 hours until the percent of

manganese passing through the media depth appeared to have reached a steady state at 82%. On the 17th day of column operation, manganese breakthrough increased suddenly to 98%. The reason for this large increase in manganese release is not known.

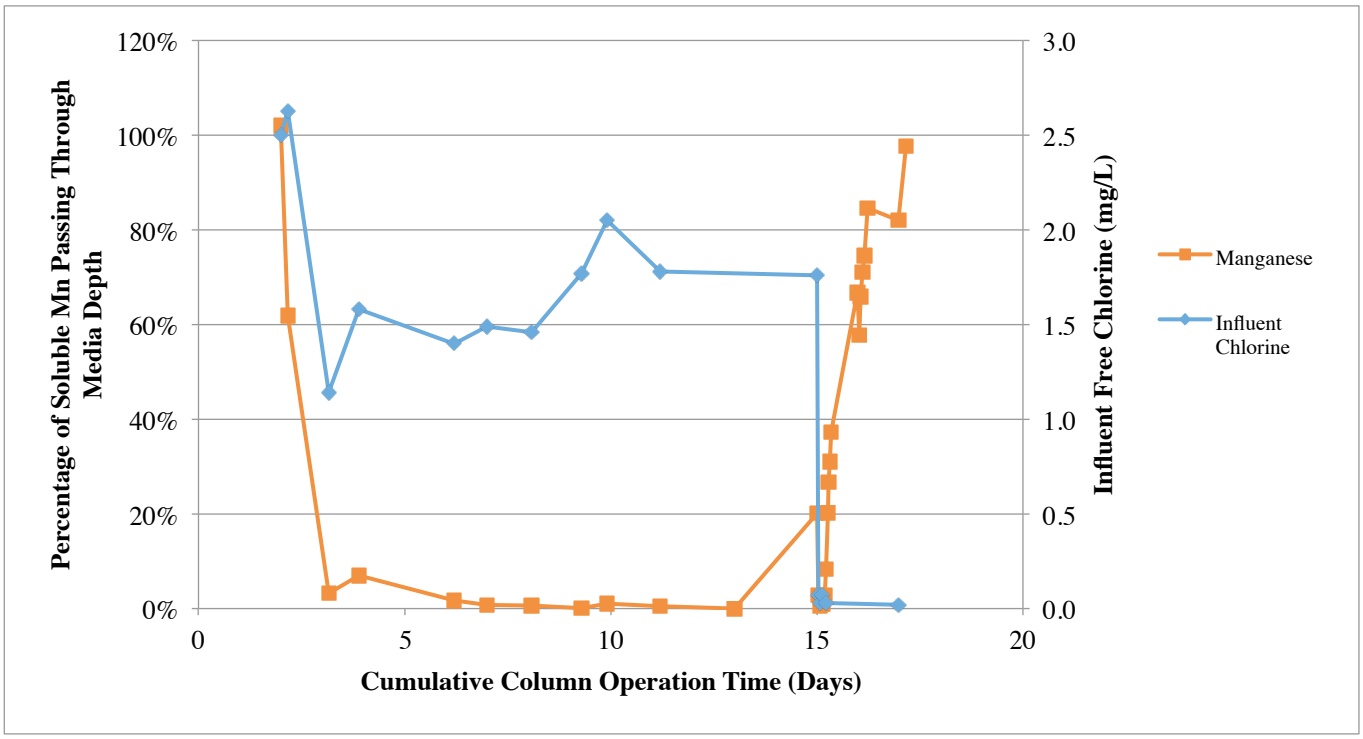

Figure 16. Percentage manganese and aluminum removal before and after the discontinuation of chlorine of the 15-day $MnOx_{(s)}$ coated filter

4.1.3 Comparison of Mn Breakthrough for the 5-day and 15-day $MnO_{x(s)}$ Coated Virgin Sand Media Columns (0.2 mg/L Influent Mn)

The percentage of manganese removal after the discontinuation of chlorine is compared for both the 5-day and 15-day $MnOx_{(s)}$ coated filters (Figure 17). Time zero for Figure 17 was set as the time chlorine was removed from each column. Results show that manganese breakthrough occurs more quickly after chlorine was removed from the 5-day coated column. The rate of soluble Mn removal is directly associated with surface $MnO_{x(s)}$ concentration, which impacts the amount of available active sites on a filter media (Knocke 1991). The average Mn concentration for the 5-day coated media was 1.5 mg Mn/g media compared to 4.9 mg Mn/g media for the 15-day coated media. Mn breakthrough occurred faster from the 5-day coating, which was expected because fewer active sites from the $MnO_{x(s)}$ coating had been developed. Since Knocke et al. (1991) demonstrated more active sites with higher amounts of $MnO_{x(s)}$ and there was more $MnO_{x(s)}$ coating and active sites on the 15-day column, there was increased adsorption capacity on the media surface. This resulted in slowed Mn breakthrough for the 15-day column.

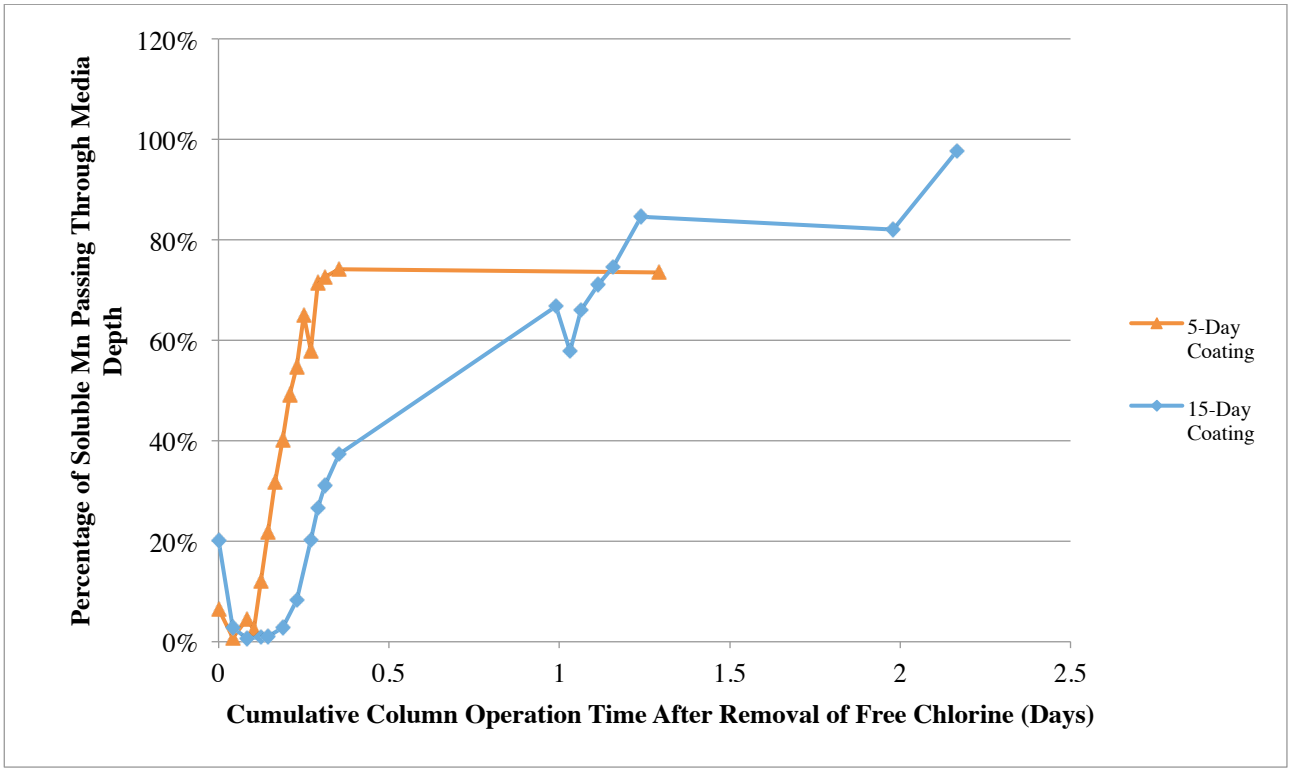

Figure 17. Comparison of the percentage manganese removal (0.2 mg/L influent concentration) after the discontinuation of chlorine of the 5-day and 15-day $MnOx_{(s)}$ coated filters

It is important to note that the percentage of Mn passing through the media depth never exceeded 100% for either the 5-day or 15-day coated columns. The cessation of free chlorine to filters in some full-scale WTP (Gabelich 2006) and laboratory studies (Islam 2010) have shown Mn desorption that results in effluent Mn concentrations exceeding the influent for a period of time. The cause for this Mn release phenomenon has not definitively been determined, but it has been proposed that Mn release is in part facilitated by Mn-reducing microorganisms living on filtration media (Islam 2010). It was critical to demonstrate that Mn breakthrough did not exceed 100% in sand media that had been sterilized before $MnO_{x(s)}$ coating as the current hypothesis was that Mn release might be attributed to microbial activity.

4.2 Bench-Scale Filter Column Performance of May 2015 Harwood Mills Anthracite Media at Different Influent pH Values

This section provides results from parallel filter column experiments conducted at influent pH values of 6.3 - 6.6 or 7.0 - 7.3. The Harwood Mills anthracite media was collected in May 2015 and was exposed to free chlorine for a period of four days. This exposure resulted in a small amount of new $MnO_{x(s)}$ coating. After four days, free chlorine was removed from the influent and Mn breakthrough was measured by comparing soluble influent to effluent Mn concentrations. Mn breakthrough trends for the two different influent pH ranges were then compared on the basis of maximum values of Mn through the media bed and steady state Mn breakthrough percentages.

4.2.1 Mn Break Through During Chlorine Discontinuation of Influent pH 6.3 – 6.6 (Column A)

Percentage Mn coming through the Harwood Mills anthracite media depth for column A (pH of 6.3 – 6.6) was plotted over time (Figure 18). As expected, a sharp increase in effluent manganese was seen after free chlorine was removed on day four. Initially, soluble influent Mn was fed to the column at a concentration of 0.2 mg/L. During this time, Mn breakthrough reached a peak of 80%. After eight days of column operation and four days after the cessation of the free chlorine feed, influent Mn concentration was decreased to 0.05 mg/L. With in 13 hours of decreasing influent Mn, effluent Mn exceeded influent concentrations for several hours,

reaching a maximum value of 109%. Mn breakthrough, after the initial period of Mn breakthrough increase, stayed below 100% for the remainder of the experiment.

A natural microbial population had been established on the media since the anthracite media had been taken directly from the Harwood Mills treatment plant filters while they were been actively in service. The increased Mn breakthrough of 109% could be definitively attributed to a Mn reducing microbial population. When Mn breakthrough has occurred in a full-scale water treatment plant, elevated levels of effluent Mn have been sustained for days or weeks due to stopping the application of free chlorine to filters (Gabelich 2006). When the Mn desorption phenomenon has been observed in a full-scale WTP, Mn release occurs for weeks or months at a time (Figure 2). Elevated effluent Mn levels only lasted for 2.5 hours and then decreased below 100% breakthrough, therefore microbial activity was most likely not the sole reason for the increase seen.

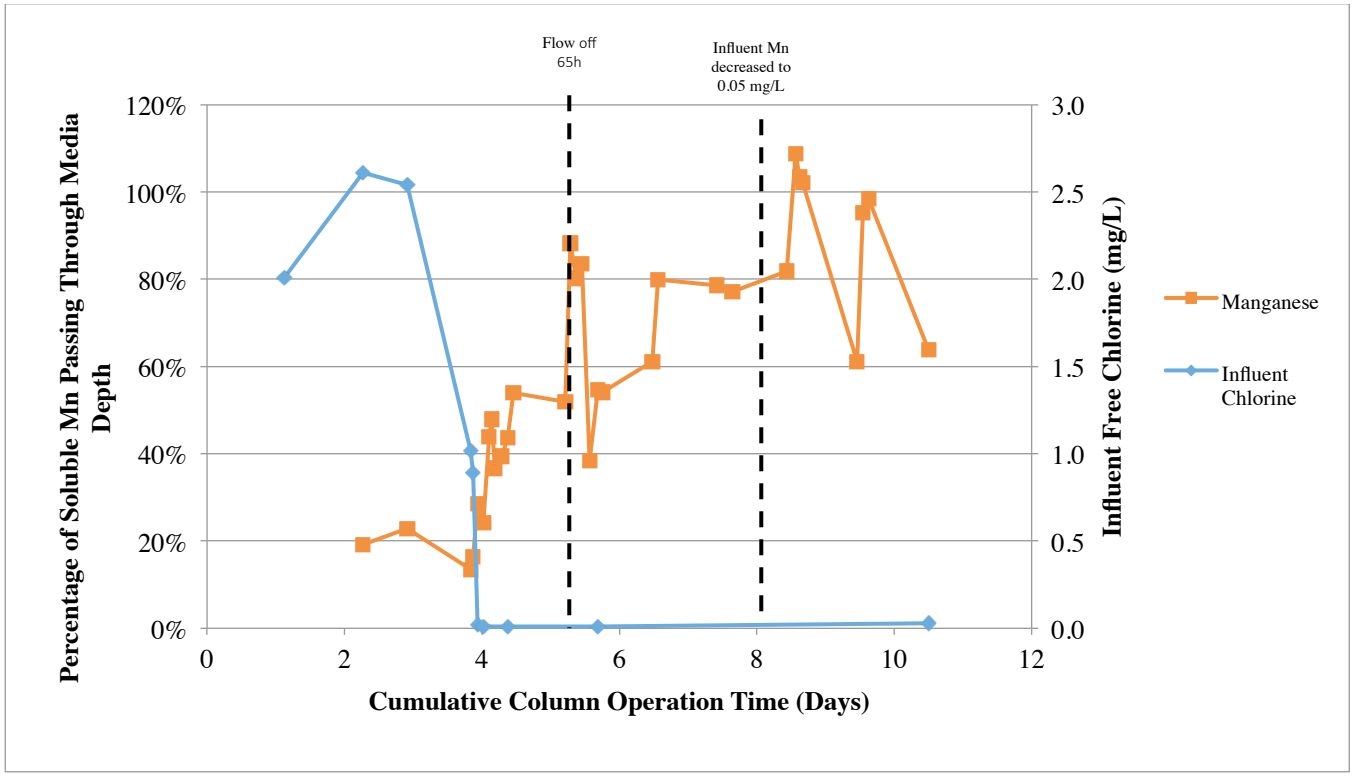

Figure 18. Percentage of manganese through media depth in column A with an influent pH of 6.3 – 6.6

Flow to this column was interrupted on days four and five of operation for 65 hours. Large increases in the amount of effluent Mn were seen immediately after influent flow returned after a period of no flow. Effluent Mn levels returned to expected breakthrough values after a few hours of continuous flow. The reason for the increase in effluent Mn was probably due to reductive dissolution of bioavailable $MnO_{x(s)}$ by Mn-reducing microorganisms living on the media. $MnO_{x(s)}$ on the media surface was reduced and released into the pore waters in soluble form. The increase in Mn released into the pore waters was detected in the effluent once flow was returned.

4.2.2 Mn Breakthrough During Chlorine Discontinuation of Influent pH 7.0 – 7.3 (Column B)

Percentage Mn coming through the Harwood Mills anthracite media depth for column B (pH of 7.0 – 7.3) was plotted over time (Figure 19). As previously noted, a sharp increase in effluent manganese was seen after free chlorine was removed on day four. Corresponding to column A (pH 6.3 - 6.6), soluble influent Mn was initially fed to the column at a concentration of 200 ppb for eight days. During this time, Mn breakthrough reached a peak of 66%. On the 8th day of column operation, influent Mn concentration was decreased to 0.05 mg/L. Within 13 hours of decreasing the influent Mn, breakthrough reached a maximum value of 99%. Effluent Mn concentrations never exceeded influent concentrations after the application of free chlorine had ceased for four days and when the influent Mn concentration was lowered to 0.05 mg/L. Flow to this column was also interrupted on days four and five of operation for 65 hours. Large decreases in the amount of Mn breakthrough were seen when flow was turned off for the same reason of reductive dissolution, which was detailed in section 4.2.1.

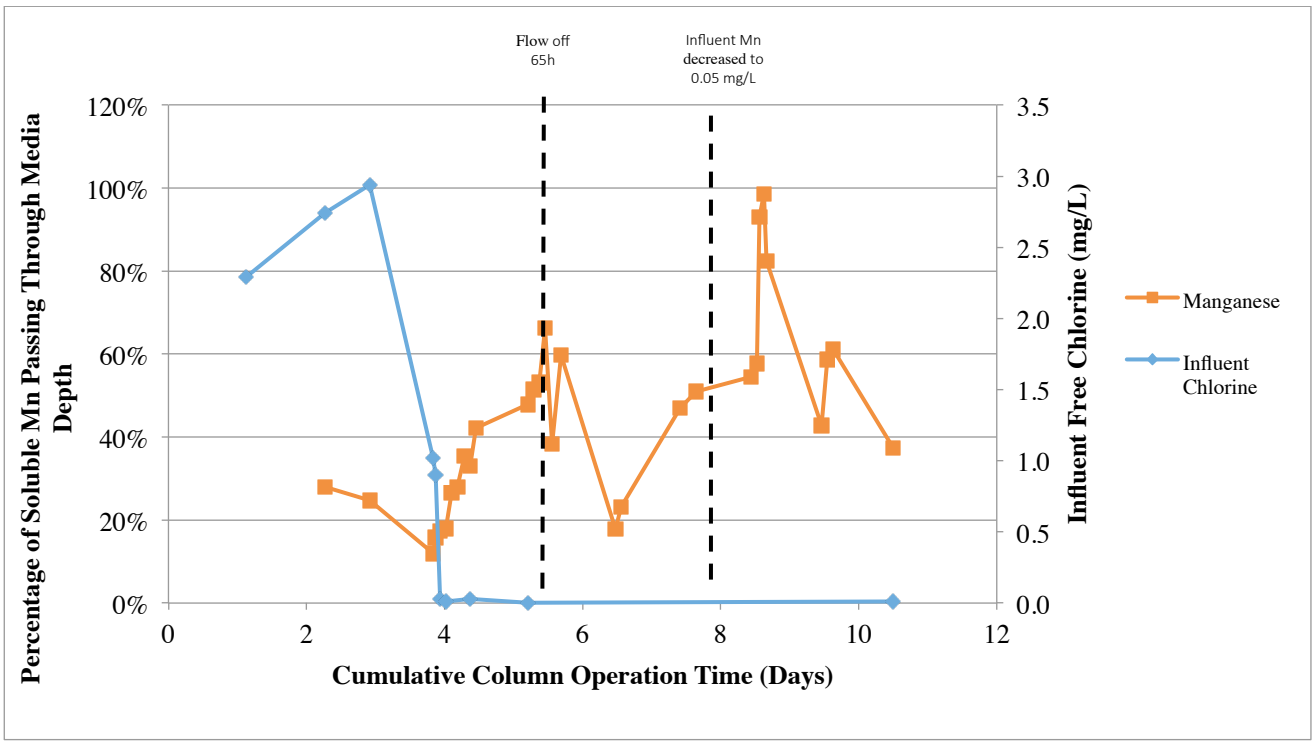

Figure 19. Percentage of manganese through media depth in column B with an influent pH of 7.0 – 7.3

4.2.3 Comparison of Manganese Break Through During Chlorine Discontinuation of Influent pH 6.3- 6.6 (Column A) and 7.0 – 7.3 (Column B)

Figure 20 compares the percentage Mn coming through media depth in columns A (pH 6.3 – 6.6) and B (pH 7.0 – 7.3). Both columns had the highest percentage breakthrough values with the lower influent manganese loading concentration of 0.05 mg/L. Mn breakthrough trends for both columns were similar for the first 24 hours after free chlorine removal. However, large differences in Mn breakthrough can be seen after six days of column operation, where column A demonstrated 14% more manganese breakthrough than column B.

Several mechanisms including surface regeneration by molecular oxygen, $MnO_{x(s)}$ concentration and Mn oxidation kinetics are mediated by pH and, therefore, directly affected Mn breakthrough in column studies. Increases in pH have been shown to improve Mn oxidation (Morgan 1964). Knocke et al. (1991) were able to demonstrate that the absorptive capacity of the $MnO_{x(s)}$ surface increases with pH as well. Molecular oxygen in the influent waters is able to better regenerate active sites on the $MnO_{x(s)}$ surface as the pH increases, which also helps promote the uptake of Mn (Knocke 1991).

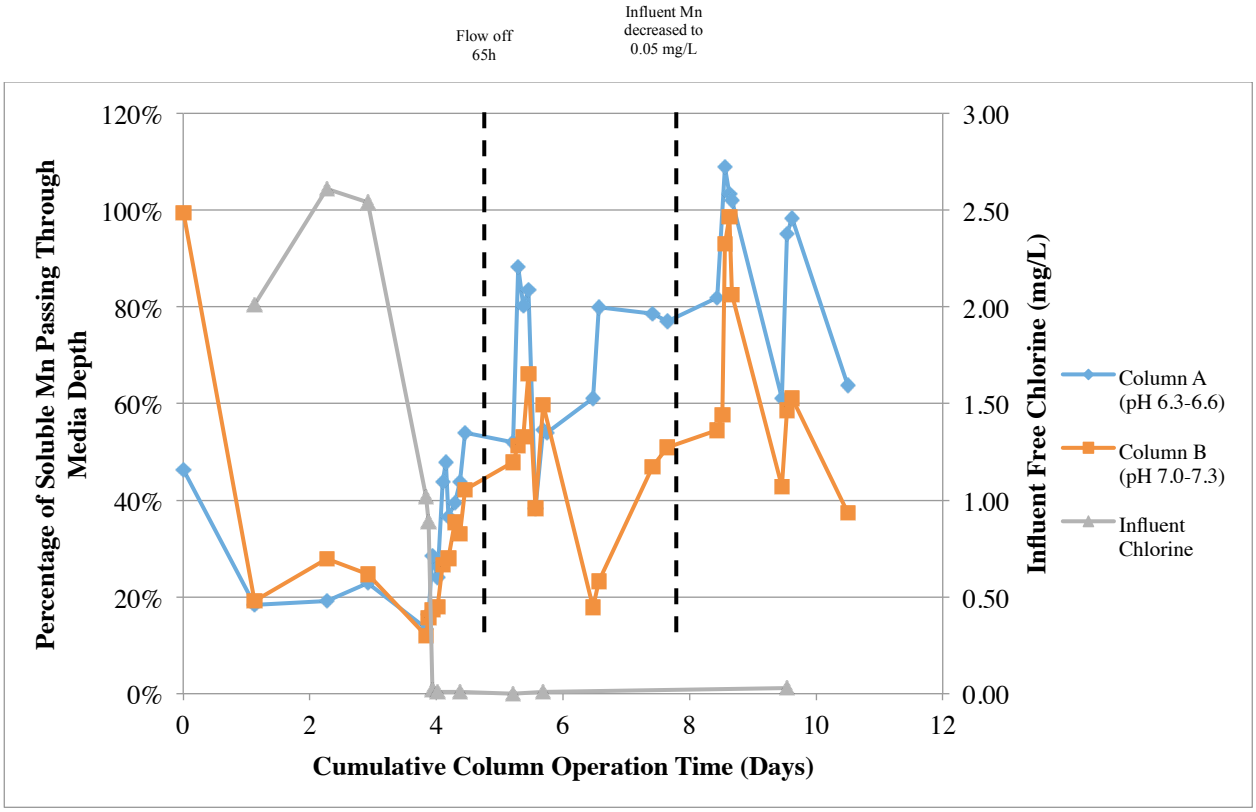

Figure 20. Comparison of percentage manganese through media depth in Columns A and B

Laboratory studies have shown that manganese oxide coatings on media increase as the pH increases from 6.0 to 8.0 (Tilak 2013). Column A, at an influent pH of 6.3 - 6.6, would have formed less of a coating during the application of free chlorine than column B with an influent pH 7.0 – 7.3. As already stated, there is a direct correlation to soluble Mn absorption and the amount of $MnO_{x(s)}$ coating that has been formed. Because column B had a higher pH, the amount of coating and active sites formed would be greater and the soluble Mn absorptive capacity would also be greater. This would also result in a lower percentage of Mn breakthrough occurring through the filter, which supports the results from this column experiment.

4.3 Bench-Scale Filter column Performance of March 2016 Harwood Mills Anthracite Media Inoculated with Mn Reducers

This section provides results from parallel filter column experiments, with an influent pH range from 6.3 – 6.6, that had one Mn-reducing microorganism inoculated and one non-inoculated column. The Harwood Mills anthracite media (collected in February 2016) was exposed to 0.3 – 0.4 mg/L free chlorine for a period of 5 days. After 5 days, free chlorine was removed from the influent and Mn breakthrough was measured by comparing soluble influent Mn to effluent concentrations. TOC was also applied to the column at a concentration of 0.5 mg/L as C for the first 17 days and increased to 12 mg/L after day 18. Mn breakthrough trends for the inoculated and non-inoculated columns were compared on the basis of maximum values of Mn through the media bed and average steady state Mn breakthrough. Patterns of Mn breakthrough are also discussed in relation to TOC entering the column.

4.3.1 *S. oneidensis* MR-1 Inoculum Experiment

Percentage of Mn through the anthracite media filter depth for both column A (*S. oneidensis* MR-1 inoculum) and B (no inoculum) is represented in Figure 21. During the initial 5 days when free chlorine was applied, a consistent difference in Mn breakthrough was seen in column A when compared to column B. Column A had a maximum difference of 23% from column B in Mn passing through the filter media while chlorine was applied. Experimental conditions between columns A and B remained the same through the duration of the experiment. The difference in Mn breakthrough can be attributed to the Mn reduction activity of the *S. oneidensis* MR-1 inoculum. *S. oneidensis* MR-1 was exposed to a C_t value of 4,400 mg/L*min.

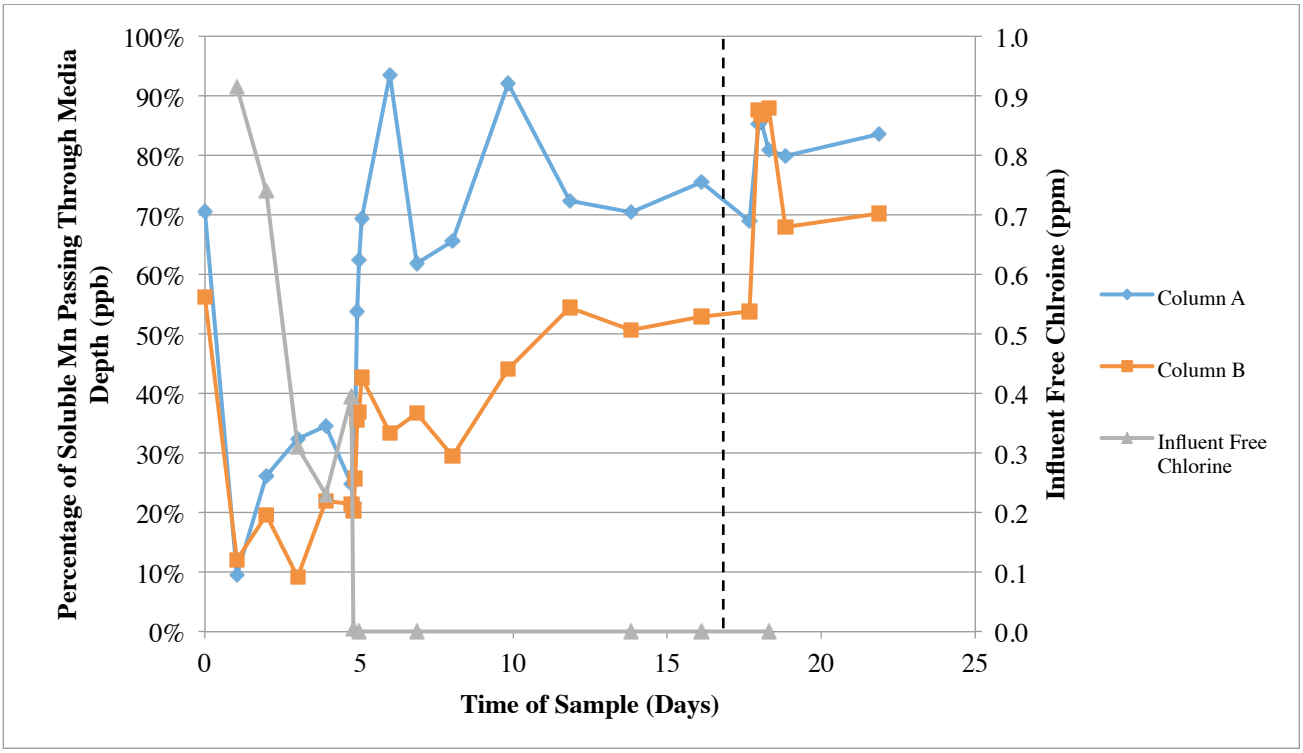

Figure 21. Percentage of Mn through the media depth for column A (*S. oneidensis* MR-1) and B (no inoculum); Dashed line indicates an increase in influent TOC from 0.5 mg/L to 12 mg/L

TOC was added to each column for the first 17 days of operation at a concentration of 0.5 mg/L as C. On day five, when free chlorine was removed, an increase in Mn breakthrough was seen in both columns. Column A had a much larger percentage breakthrough for the duration of the time after chlorine was removed than noted in column B. With in 24 hours of chlorine removal, column A had a peak breakthrough of 94%, where column B had a peak breakthrough of 43%. The maximum difference in breakthrough between the two columns occurred on day 6 with column A having 60% greater breakthrough than column B. After several days, steady state Mn breakthrough for both columns was established. Columns A and B had steady state breakthroughs of 76% and 54%, respectively. Column A had a much larger amount of effluent Mn passing through the column, which could be again attributed to the reduction activity of the *S. oneidensis* MR-1 inoculum.

On day 18, influent TOC loading was increased to 12 mg/L as C. Mn passing through the filter bed increased substantially over the established steady state value for both columns.

Column A had a maximum breakthrough of 86%, while column B had a value of 87% of influent Mn reaching the effluent. Both columns had similar maximum breakthrough values, with a 1% difference in percentage of Mn passing through the filter media after the addition of additional influent carbon. Column B had the largest increase in Mn breakthrough when TOC was increased from 0.5 mg/L to 12 mg/L as C. When TOC was increased in column B, 32% more Mn release over steady state conditions occurred within eight hours. After the TOC concentration increased, Mn breakthrough in column A only increased by 10%. The exact reason as to why the increase of TOC loading into the filter columns increased the amount of Mn seen in the effluent is unclear. The reason why the addition of TOC into column B created such a large increase in the amount of Mn in the effluent is also unclear. Islam (2010) demonstrated that the addition of 4-μL sodium acetate to filter columns facilitated Mn release. When the sodium acetate was no longer fed into the columns, Mn release ceased (Islam 2010).

A differing steady state condition occurred after the increase in TOC for both columns. Mn breakthrough for column A appeared to remain around 84% for several days after the increase in TOC. Column B Mn breakthrough remained around 70% after the initial increase in TOC. These new steady state values were higher than the steady state values achieved before with the lower TOC concentration.

Since both of the columns contained anthracite media, which had an active natural microbial population, it appeared that some unknown microbiological mechanisms were occurring during column operation. Column A had additional Mn-reducing microorganisms (*S. oneidensis* MR-1) added onto the media in addition to the existing natural microbial population. This could explain the differences in Mn removal for the first 17 days of the experiment when TOC was loaded at 0.5 mg/L. The presence of *S. oneidensis* MR-1 in column A could also explain the elevated and sustained Mn breakthrough after the influent TOC concentration was increased. Additional carbon, above the initial TOC of 0.5 mg/L, may have been required for the naturally existing population of Mn-reducing microorganisms to begin to actively reduce more of the accumulated $MnO_{x(s)}$ present on the anthracite.

The columns that were inoculated with *S. oneidensis* MR-1 showed a greater percentage in Mn breakthrough for the duration of the experiment when compared to the column that did not have any additional inoculum. Lovely and Philips (1988) showed that *S. oneidensis* MR-1 coupled the oxidation of electron donors, similar to the acetate supplied in the columns, to Mn

reduction. This is the probable reason for why Mn release in both columns increased when TOC was increased. The oxidation of TOC was coupled to and promoted the reduction of $MnO_{x(s)}$ from the media surface by the Mn-reducing microorganisms. The types and quantity of naturally occurring Mn-reducing microorganisms residing on the Harwood Mills WTP were not known. Studies have shown that microorganisms have preferences for one carbon source over another (Jones 2009). *S. oneidensis* MR-1 may have had a competitive advantage over the naturally occurring Mn-reducing microorganisms for acetate as the carbon source in filter studies.

Mn reduction kinetics and Mn-reducing microbial populations may also have played roles in the differences in Mn reduction seen between the inoculated and non-inoculated columns. Differences in Mn reduction kinetics are seen between differing microorganisms, with some organisms able to reduce faster than others (Cerrato 2008). *S. oneidensis* MR-1 Mn reduction kinetics could have been faster than the naturally occurring Mn-reducing microorganisms on Harwood Mills WTP media. Figure 22 shows the mtrB gene qPCR quantification cycle values for the top, middle and bottom two-inch sections of the *S. oneidensis* MR-1 inoculated (Column A) and non-inoculated columns (Column B). Results show that the *S. oneidensis* MR-1 inoculated columns contained more microbes that possessed the *mtrB* gene, therefore, the column contained more Mn-reducing microorganisms. The increase in the number of Mn-reducing microorganisms is likely an additional reason why increased Mn release was seen from this Column A. It is not known which of the above discussed factors (TOC concentration, Mn reduction kinetics or Mn-reducing microorganism population) has the greatest effect on Mn release or what combination of these conditions would be necessary to see Mn release in a full-scale WTP. Detection of *S. oneidensis* MR-1 was confirmed at all depths in Column A at an average density of $3.9x10^2$ CFU/mL and was not detected at any depth in Column B (Figure 23). The density of *S. oneidensis* MR-1 in Column A appears to increase as the depth increases in the column.

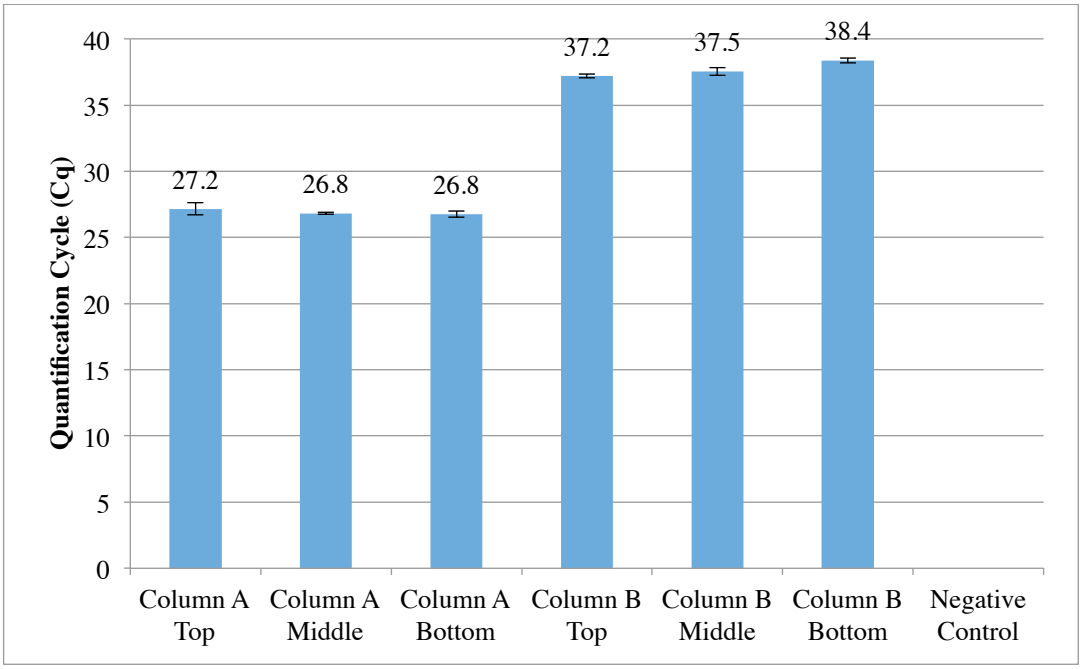

Figure 22. Comparative quantification cycle number for the top, middle and top two inch depths of Column A (*S. oneidensis* MR-1 inoculated) and Column B (non-inoculated) for microorganisms that contain the *mtrB* gene

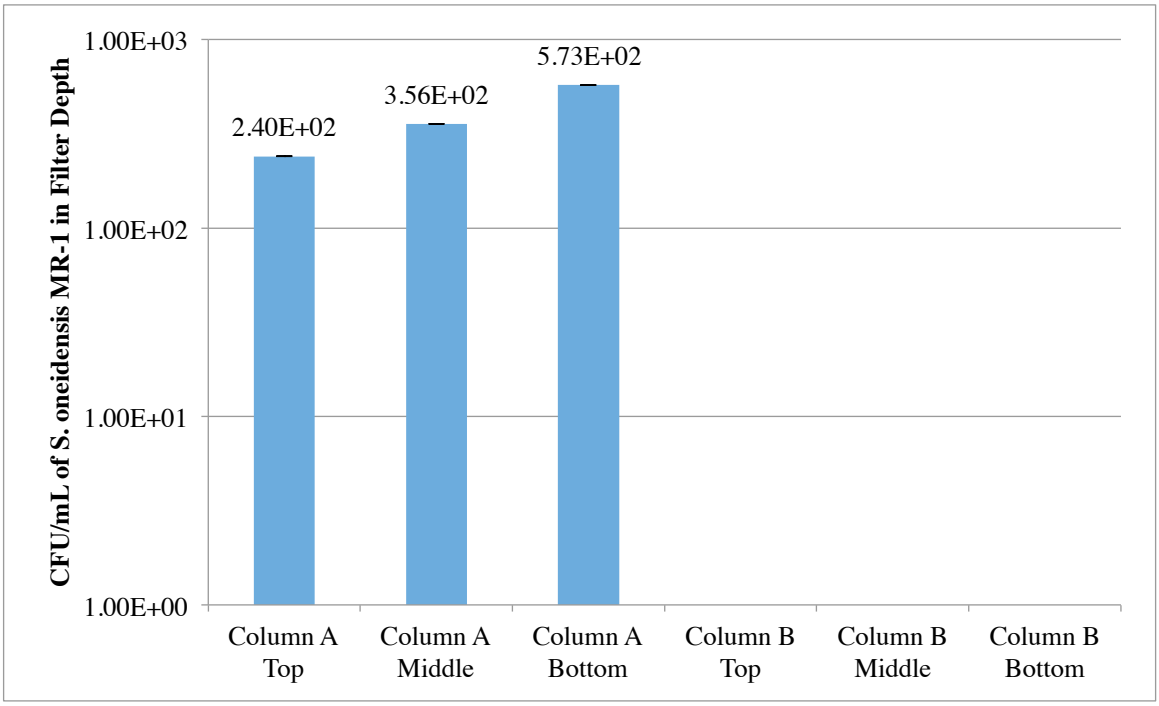

Figure 23. *S. oneidensis* MR-1 concentration in the top, middle and top two inch depths of Column A (*S. oneidensis* MR-1 inoculated) and Column B (non-inoculated)

Figure 24 compares the average concentration of extractable Mn in mg per gram of the anthracite media in the top and bottom two inches of Column A (inoculated with *S. oneidensis* MR-1) and Column B (non-inoculated). Results show that there is a possibly significant difference in the amount of Mn coating in the top and bottom sections in Column A. The amount of extractable Mn was 9 mg Mn lower in the top 2-inch section compared to the bottom section for Column A. This results in a percent difference for Column A of 23%. In a study by Tobiason et al. (2008), natural variability of the concentration of Mn coatings had a standard variation of +/- 20% Mn content. The differences in Mn coating seen in Column A between the top and bottom depths could represent real world variability in Mn coatings. Since the difference in Mn coating between the top and bottom of the column was larger than 20% for Column A, the difference could be considered small to moderate but significant. For Column B, the amount of Mn coated on the anthracite media is approximately the same at the top and bottom sections of the column.

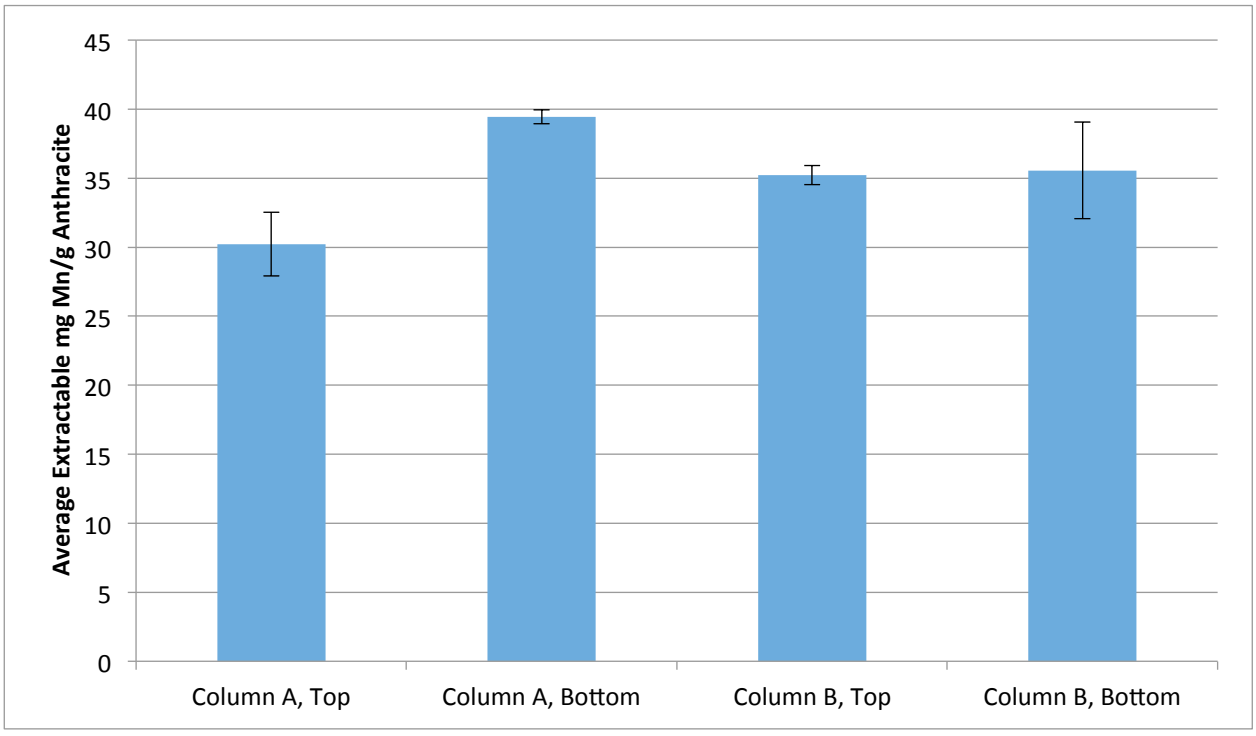

Figure 24. Average concentration of extractable Mn (mg) per gram of anthracite media from Column A (inoculated with *S. oneidensis* MR-1) and Column B (non-inoculated)

4.3.2 MB4 and MB6 Inoculum Experiment

Figure 25 shows the percentage of Mn through the anthracite media filter depth for both column A (MB4 and MB6 inoculum) and B (no inoculum). For the five days when free chlorine was applied, on average, 10% more Mn breakthrough was seen in column A when compared to column B. Influent free chlorine was removed on day five and, as expected, effluent Mn levels increased steadily in both columns.

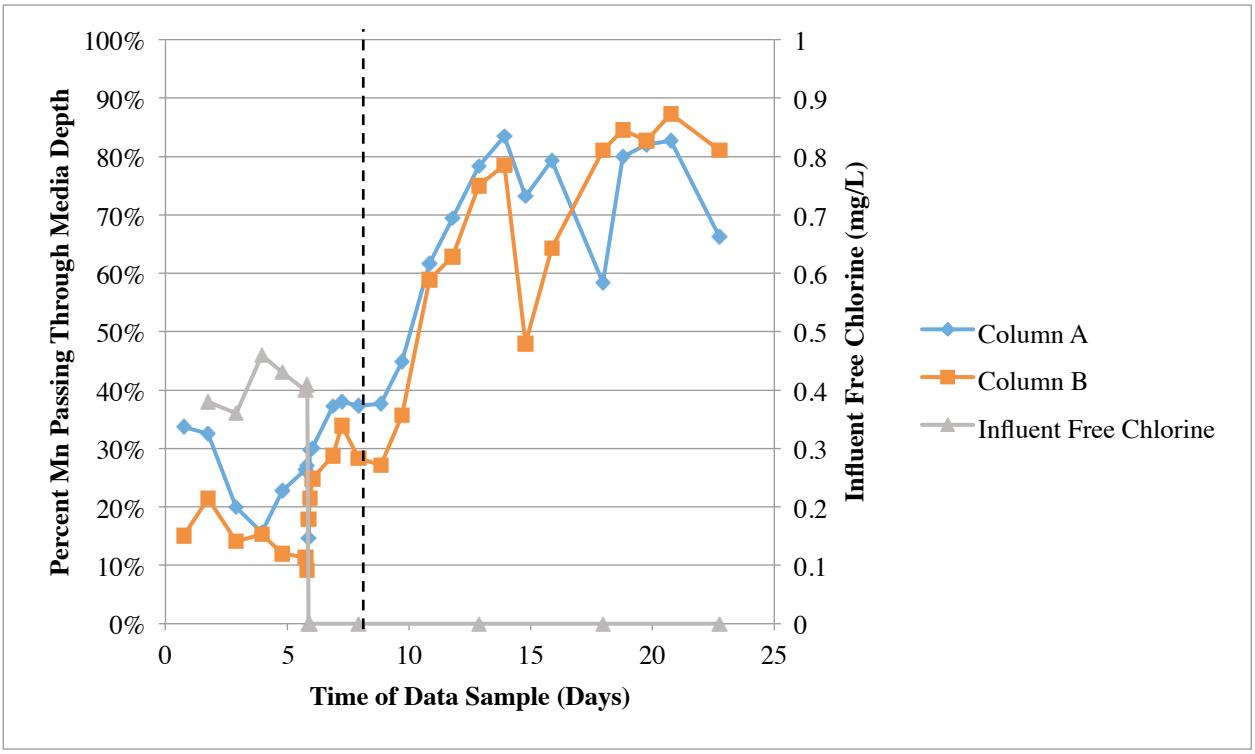

Figure 25. Percentage of Mn through the media depth for column A (MB4 and MB6 inoculated) and B (no inoculum); Dashed line indicates an increase in influent TOC from 0.5 mg/L to 12 mg/L

On day seven, effluent Mn levels for both columns stopped increasing and began to reach a steady state for Mn release. After chlorine was removed (TOC was 0.5 mg/L as C), the steady state Mn breakthrough values were 38% and 34% for columns A and B, respectively. On day eight, TOC was increased from 0.5 mg/L to 12 mg/L as C. Again, Mn passing through the filter bed increased substantially over the established steady state value for both columns. Mn breakthrough for both columns continued to increase until day 14 when Mn release started to

slow and level off. On average, column A had a 5% greater Mn breakthrough than column B for the duration of the experiment. Column A had a small but consistently greater amount of Mn breakthrough than column B, with the exception of days 16 through 23. From days 17 to 23, the percentage of Mn breakthrough in column B exceeded column A.

After the influent TOC was increased to 12 mg/L as C, the maximum Mn breakthrough value for both columns was 84%. The Mn breakthrough percentage for column A increased 38% after the increase in TOC, where column B Mn breakthrough increased 43%. After day 16, Mn breakthrough for column B began to exceed column A for the remainder of the experiment (six days). The MB4 and MB6 inoculum was exposed to a Ct of 3,400 mg/L*min.

Again, both columns contained anthracite media collected from the Harwood Mills WTP (February 2016) with an active native microbial population. Column A had additional Mn reducing organisms, MB4 and MB6, inoculated onto the media in addition to the native microbial population. The small increase in Mn breakthrough seen for most of this column experiment could be contributed to the presence of the additional inoculated Mn-reducing microorganisms. Although, the amount of sustained Mn breakthrough compared to the column study with *S. oneidensis* MR-1 inoculum was much lower. The average increase in Mn breakthrough over the non-inoculated column for the S. oneidensis MR-1 study was 21% compared to a 5% increase in Mn breakthrough over the non-inoculated column for the MB4/MB6 column experiment. The lower amount of Mn breakthrough seen in the MB4/MB6 columns was somewhat expected as these Mn-reducing microorganisms were repeatedly shown to reduce Mn at a much slower rate than *S. oneidensis* MR-1 in the *in situ* vial assays.

The relative presence of the *mtrB* gene was also quantified from the bottom, middle and top two-inch sections of the anthracite media in the inoculated (Column A) and non-inoculated columns (Column B) (Figure 26). There were insignificant differences seen between Cq values for either column, which suggests at first glance that the amount of microorganisms that possessed the *mtrB* gene were similar between the columns. Figure 14 demonstrates the Cq values for each of the built environment Mn-reducing microorganisms. MB4 and MB6 both had average Cq values of 40 when the *mtrB* primer set was used. This result demonstrated that the designed *mtrB* primer set was able to weakly bind to the extracted *mtrB* gene of MB4 and MB6 during qPCR. It is plausible that the MB4 and MB6 strains were completing reductive Mn dissolution and reducing the bioavailable fraction of the $MnO_{x(s)}$ surface. This reductive

dissolution resulted in the average 5% increase in Mn breakthrough seen during the experiment compared to the non-inoculated column. Since DNA from MB4 and MB6 did not bind strongly to the *mtrB* primer set, qPCR results did not show an increase in the presence of the *mtrB* gene for the inoculated column.

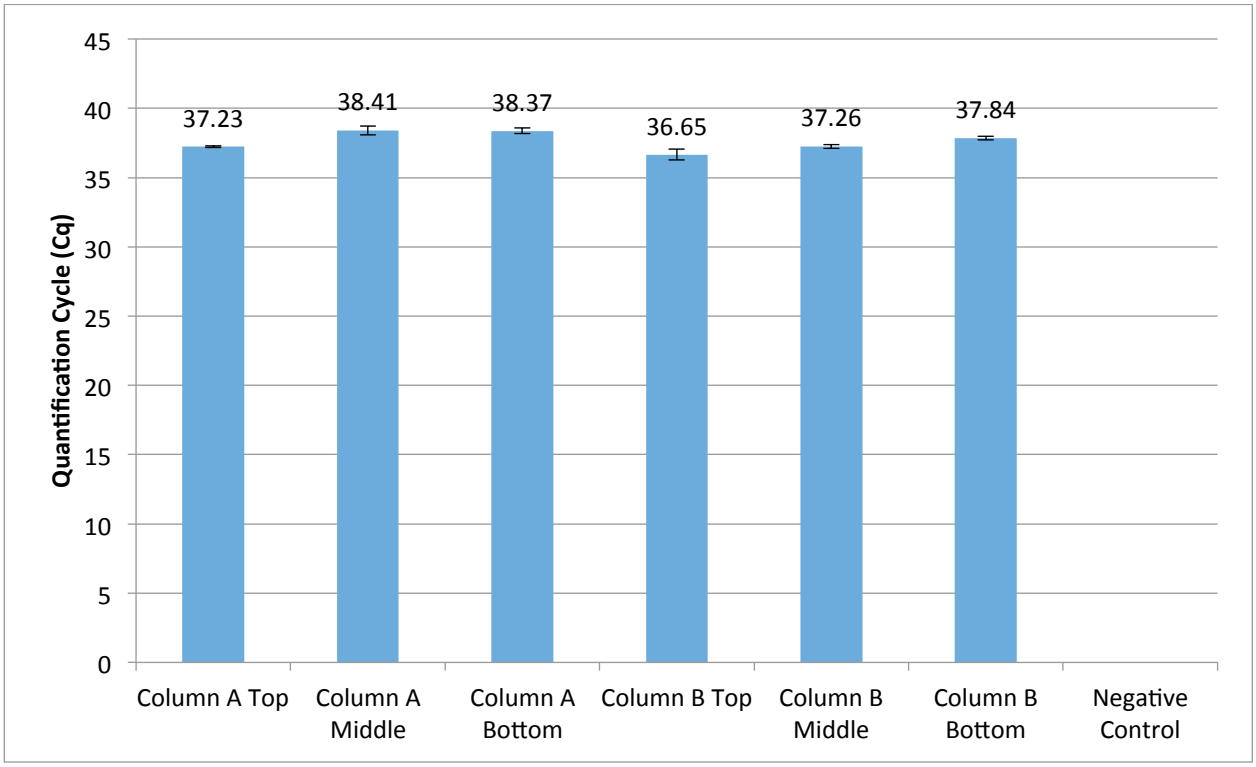

Figure 26. Comparative quantification cycle number for the top, middle and top two inch depths of Column A (MB4 and MB6 inoculated) and Column B (non-inoculated) for microorganisms that contain the *mtrB* gene

Figure 27 compares the average concentration of extractable Mn in mg per gram of the anthracite media in the top and bottom two inches of Column A (inoculated with MB4 and MB6) and Column B (non-inoculated). Comparable to extractable Mn concentrations from the *S. oneidensis* MR-1 inoculated column, results show that there is a difference in the amount of Mn coating in the top and bottom sections in Column A (MB4 and MB6 inoculum). The amount of extractable Mn was 6 mg Mn lower in the top 2-inch section compared to the bottom section for Column A. This difference amounts to 16% less Mn coating on the top of the media depth. Again, in the study by Tobiason et al. (2008), real world variability of Mn coatings for media at

the same depth was +/- 20%. The difference in the Mn coating seen in Column A for this experiment may or may not be significant due to the measured variability by Tobiason et al (2008). For Column B, the amount of Mn coated on the anthracite media is approximately the same at the top and bottom sections of the column.

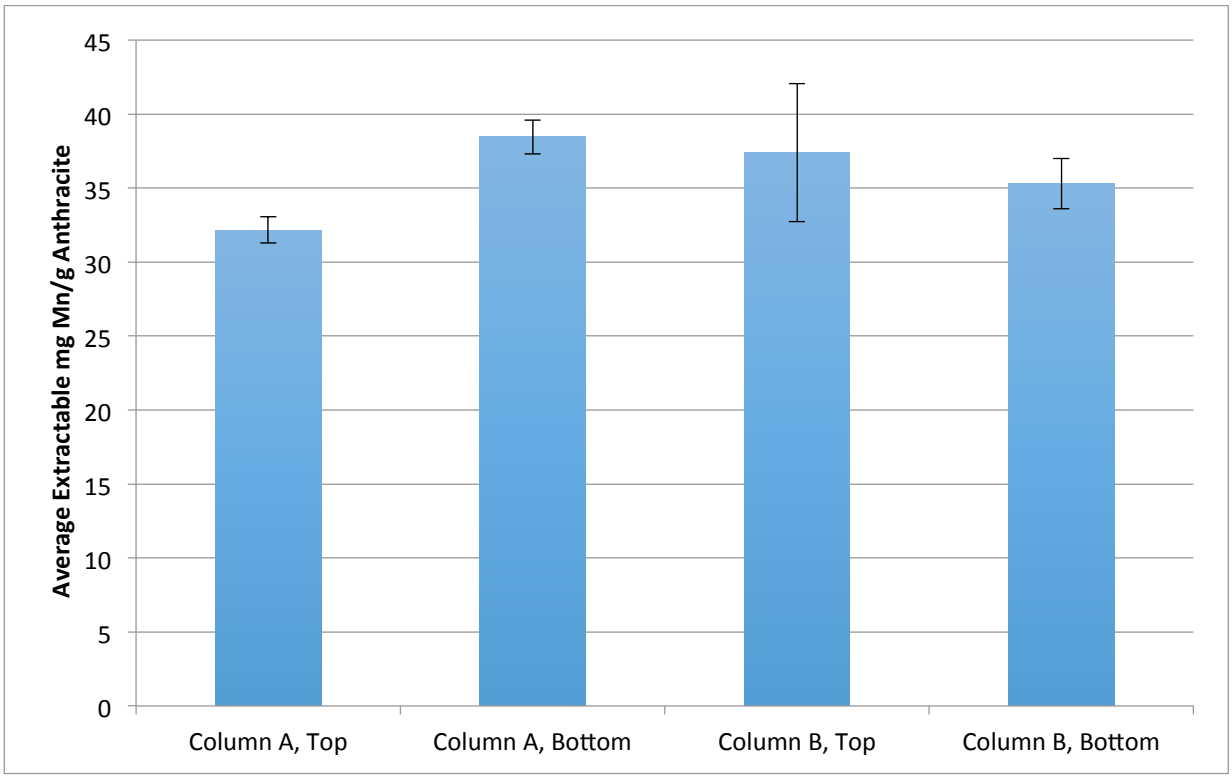

Figure 27. Average concentration of extractable Mn (mg) per gram of anthracite media from Column A (inoculated with MB4 and MB6) and Column B (non-inoculated)

4.4 *In Situ* Mn Reduction Vial Assay Results

Vial assays were completed that confirmed and evaluated anaerobic and aerobic Mn reduction capability of five different Mn reducing strains (MB4, MB5, MB6, MB7 and *S. oneidensis* MR-1). $MnO_{x(s)}$ reduction and bioavailability experiments using five different $MnO_{x(s)}$ samples of various dates of synthesis were also completed. Corresponding inoculum was added into semi-solid agar vials with $MnO_{x(s)}$ samples and light transmittance at 540 nm was measured over time. Percent transmittance was used as a measurement tool in the vial assays for evaluating the extent of observed Mn reduction.

4.4.1 *S. oneidensis* MR-1 Inoculum Concentration Correlation

The purpose of this study was to determine relationships between Mn reduction and Mn-reducing microorganism concentration. *S. oneidensis* MR-1 inoculum was added into the Mn reduction agar vials and incubated anaerobically at 30 °C for 7 days before light transmittance was measured. The starting inoculum was quantified by plate count methods and was $50.5x10^7$ CFU/mL. This inoculum was serially diluted as needed and the desired CFU/mL added into each vial was back calculated from the undiluted inoculum value. The final cell counts for the *S. oneidensis* MR-1 inoculum added into vials was $50.5x10^5$, $50.5x10^4$, $50.5x10^2$, 50.5, and 0 CFU/mL. Mn reduction in the vial resulted in $MnO_{x(s)}$ clearing, which increased light transmission. Visually, an increase in $MnO_{x(s)}$ clearing was seen as the inoculum concentration increased (Figure 28).

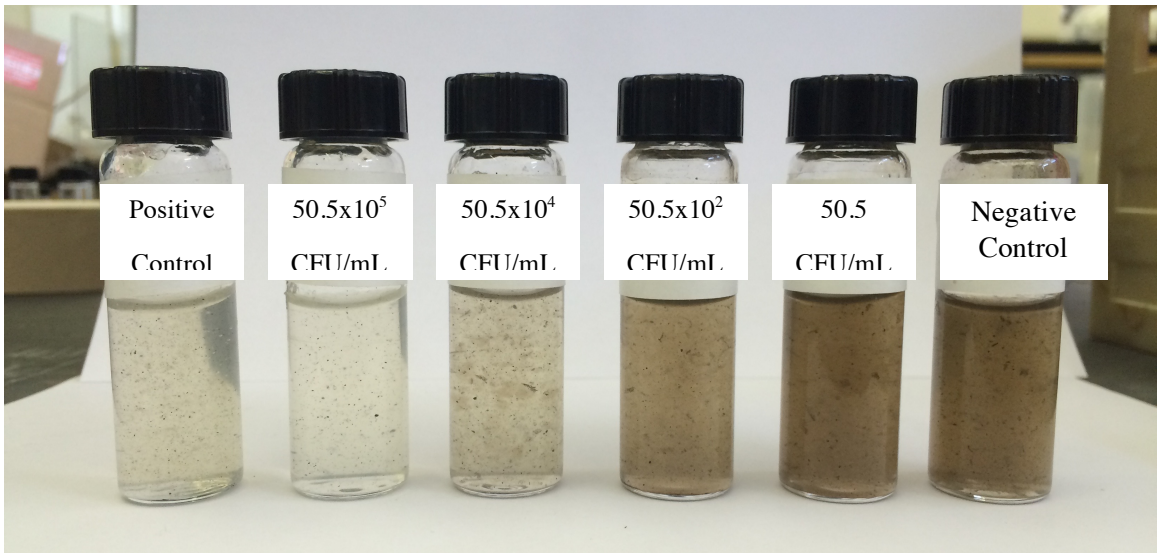

Figure 28. Visual inspection of Mn reduction anaerobic vial assay results from differing concentrations of *S. oneidensis* MR-1 inoculum after 7 days of incubation

S. oneidensis MR-1 inoculum concentrations in each vial were graphed against the percent light transmittance measured at 540 nm in Figure 29. A direct correlation between the concentration of the *S. oneidensis* MR-1 inoculum and apparent extent of Mn reduction was seen.

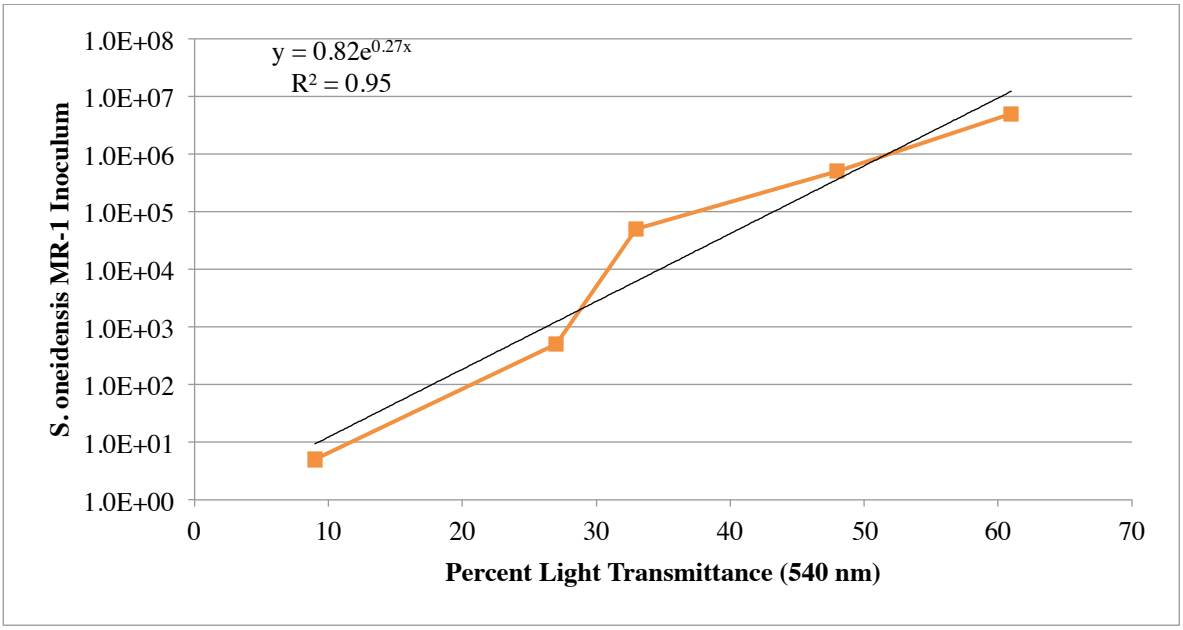

Figure 29. Correlation of *S. oneidensis* MR-1 inoculum concentration to percent light transmittance at 540 nm in the Mn vial assay after 7 days of incubation

4.4.2 Anaerobic Mn Reducing Bactria Inoculum Concentration Correlation

The first purpose of this study was to verify that the five Mn reducing strains being tested in this research study were able to reduce Mn under anaerobic conditions. This experiment also determined if there were any correlations of Mn reduction to Mn reducing microorganism concentration. For this study, Mn reduction vials were inoculated with MB4, MB5, MB6, MB7 or *S. oneidensis* MR-1 in an anaerobic chamber and then incubated at 30 °C in Gas-Pak anaerobic jars. Figure 30 shows the increase in percent light transmittance over time for various inoculum concentrations of MB4 in anaerobic vials. The MB4 vials were inoculated with $6.95x10^5$, $6.95x10^3$, $6.95x10^1$ and 0 CFU. As expected, the vials with the highest concentration of inoculum were able to reduce Mn more quickly. Percent light transmittance for the highest inoculum concentration, $6.95x10^5$ CFU, was 27%.

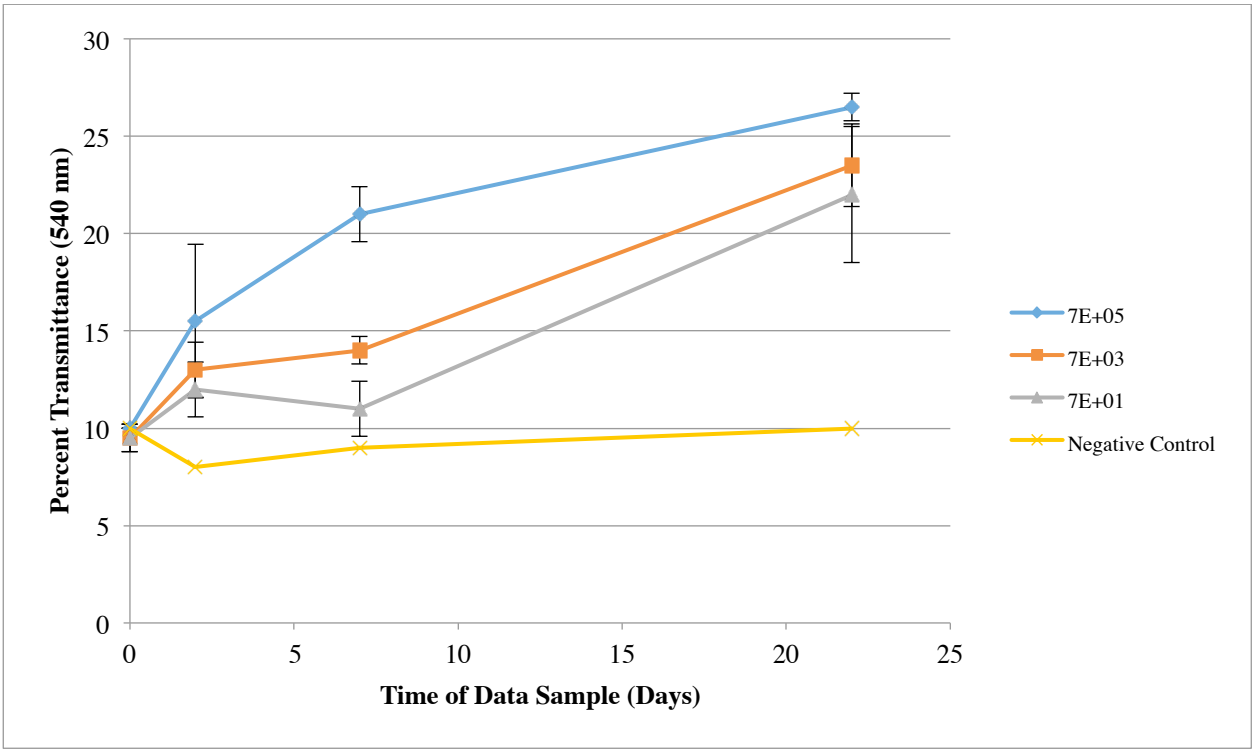

Figure 30. Percent light transmittance in anaerobic vial assay for MB4 based on inoculum concentration (CFU)

Figure 31 represents the increase in percent light transmittance over time for differing inoculum concentrations of MB5 in anaerobic vials. The MB5 vials were inoculated with $1.20x10^6$, $1.20x10^4$, $1.20x10^2$, and 0 CFU. The vials with the highest concentration of inoculum did not reduce Mn faster, as predicted. Before the last time point at 22 days, the $1.20x10^4$ inoculum surpassed the higher inoculum concentration light transmittance, demonstrating higher Mn reduction. Percent light transmittance for $1.20x10^4$ CFU inoculation concentration was 18%, where as for the $1.20x10^6$ CFU it was only 15%. The negative control for the MB5 strain increases slightly over time and has a slightly greater percent light transmittance than the $1.20x10^2$ CFU vials. This can be attributed to possible contamination with a low level of MB5 or variability in this testing procedure.

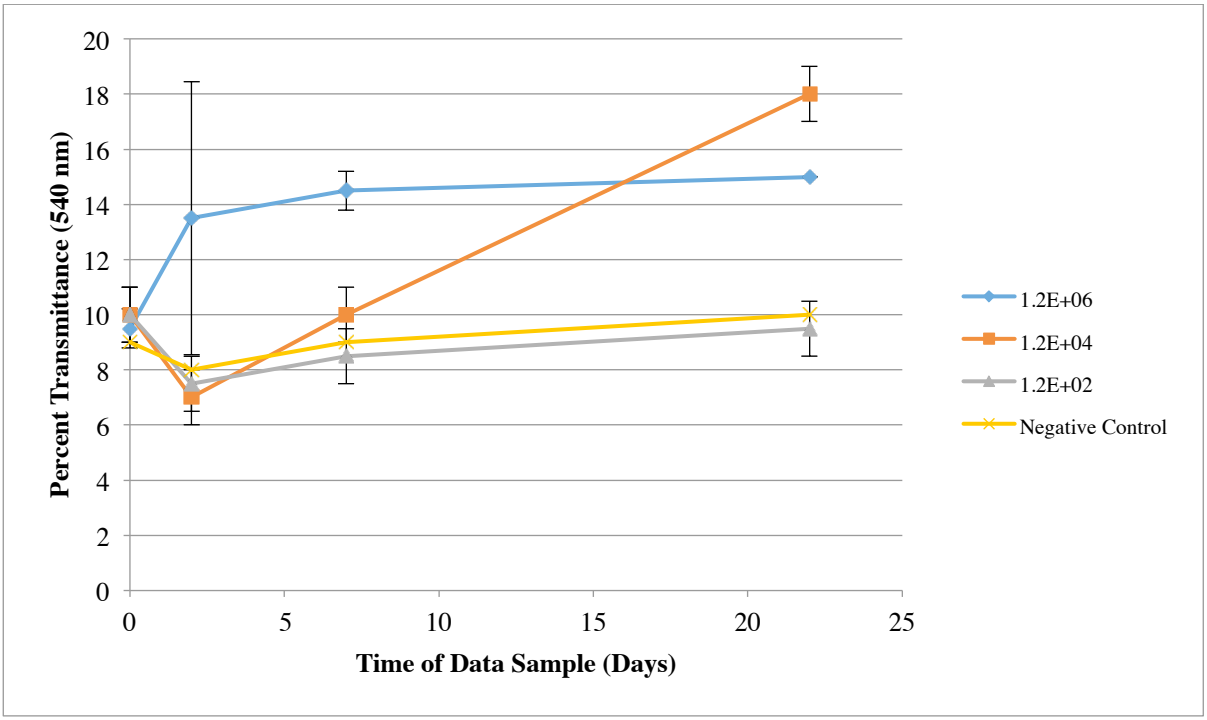

Figure 31. Percent light transmittance in anaerobic vial assay for MB5 based on inoculum concentration (CFU)

Increase in percent light transmittance over time for differing inoculum concentrations of MB6 in anaerobic vials is depicted (Figure 32). The MB6 vials were inoculated with $4.60x10^6$, $4.60x10^4$, $4.60x10^2$, and 0 CFU. As predicted, the vials with the highest concentration of inoculum were able to reduce Mn more quickly. Percent light transmittance for the highest inoculum concentration, $4.60x10^6$ CFU, was 28%.

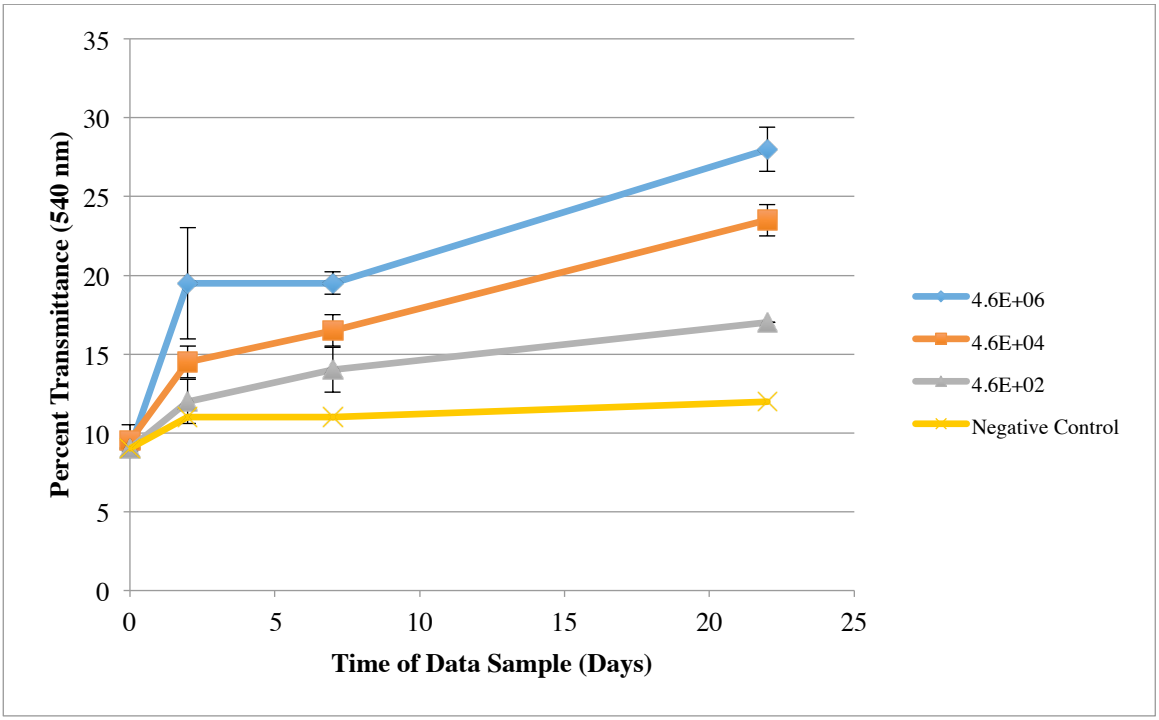

Figure 32. Percent light transmittance in anaerobic vial assay for MB6 based on inoculum concentration (CFU)

Figure 33 shows the increase in percent light transmittance over time for various inoculum concentrations of MB7 in anaerobic vials. The MB7 vials were inoculated with $1.35x10^6$, $1.35x10^4$, $1.35x10^2$, and 0 CFU. The vials with the highest concentration of inoculum were able to reduce Mn more quickly. Percent light transmittance for the highest inoculum concentration, $1.35x10^6$ CFU, was 21%. For the MB7 inoculum, it appeared that Mn reduction capability was hindered at the $1.35x10^4$ CFU or lower concentrations of inoculum.

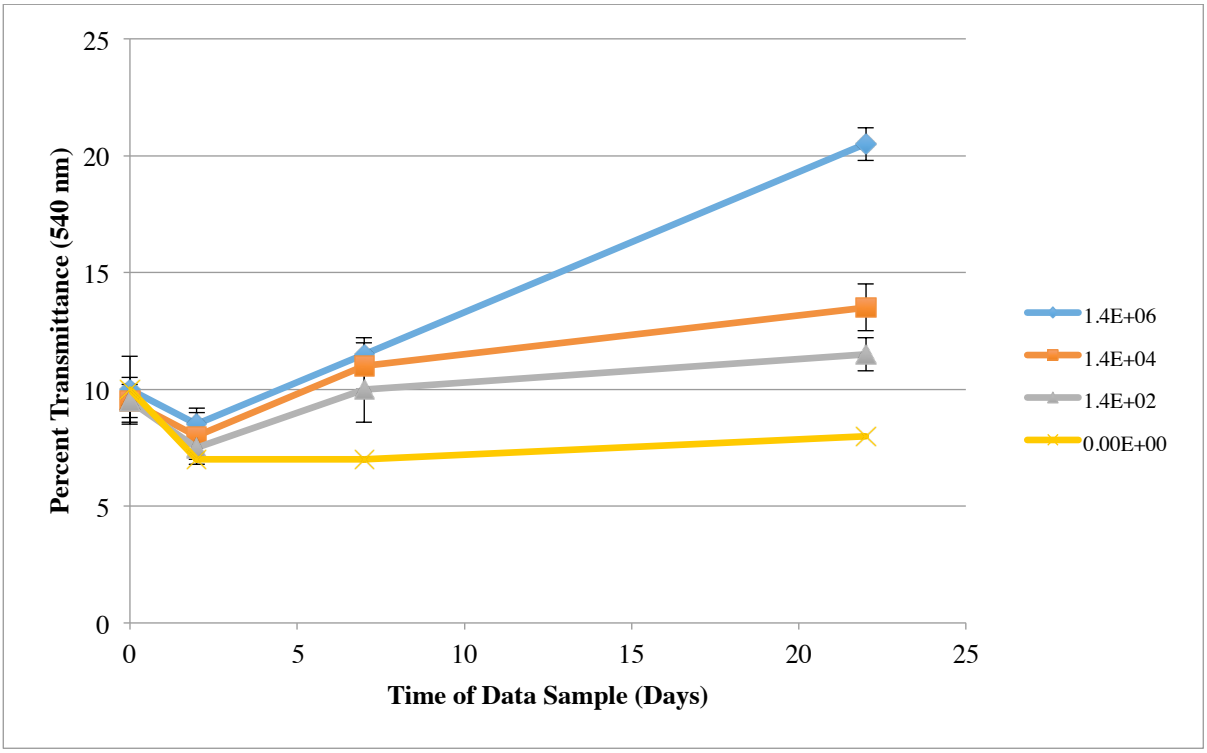

Figure 33. Percent light transmittance in vial assay for MB7 based on inoculum concentration (CFU)

The percent light transmittance over time for various inoculum concentrations of *S. oneidensis* MR-1 in anaerobic vials is shown in Figure 34. The *S. oneidensis* MR-1 vials were inoculated with $5.05x10^6$, $5.05x10^4$, $5.05x10^2$, and 0 CFU. As expected, the vials with the highest concentration of inoculum were able to reduce Mn more quickly. Percent light transmittance for the highest inoculum concentration, $5.05x10^6$ CFU, was 61%. The highest inoculum concentration was able to reach the maximum amount of Mn reduction after 7 days. After 22 days of incubation, the $5.05x10^4$ CFU vials were able to reach a maximum light transmittance value of 60% and reduce as much Mn as the highest inoculum concentration. The increase in light transmittance for the $5.05x10^2$ CFU vials appeared to be linear in nature, with a peak transmittance value of 54% after 22 days incubation.

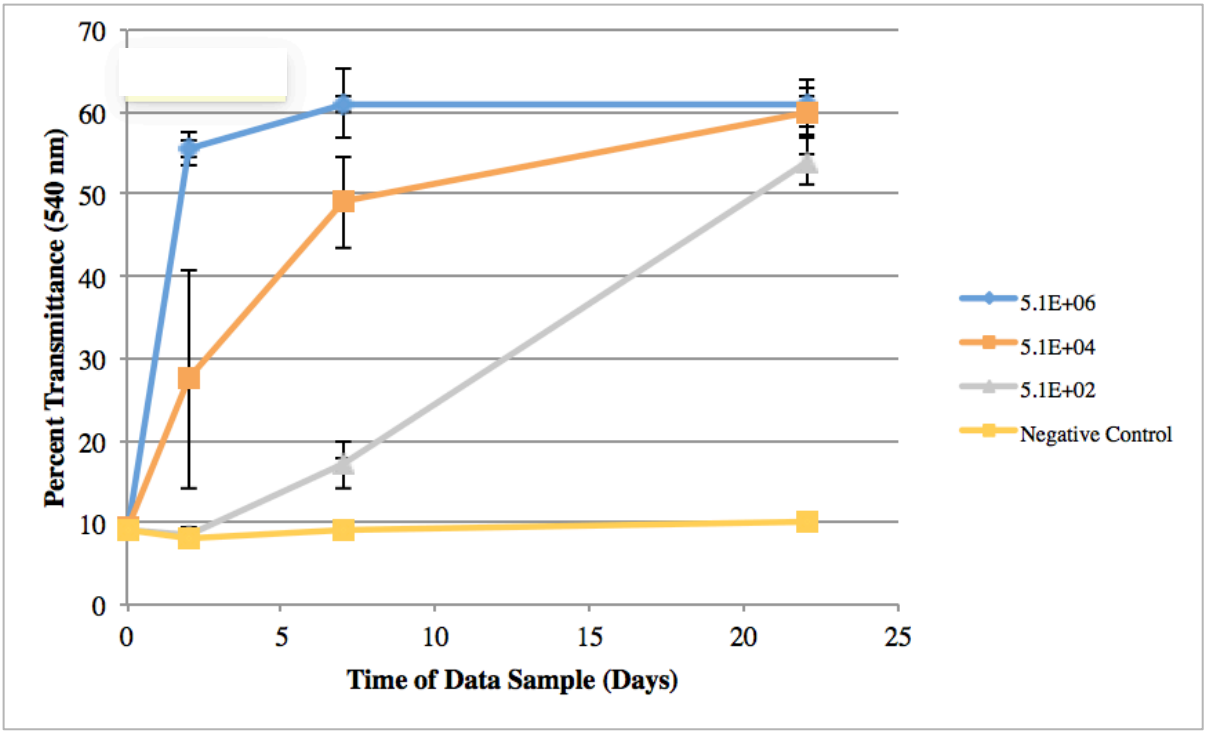

Figure 34. Percent light transmittance in anaerobic vial assay for *S. oneidensis* MR-1 based on inoculum concentration (CFU)

4.4.3 Aerobic Mn-Reducing Bacteria Vial Assay

This experiment investigated the ability of the five Mn-reducing strains to reduce Mn aerobically. Mn reduction vials were inoculated aerobically with MB4, MB5, MB6, MB7 or *S. oneidensis* MR-1 and incubated aerobically at 30 °C. Vial inoculum counts for the Mn-reducing strains MB4, MB5, MB6, MB7 and *S. oneidensis MR-1* can be found in Table 16. The 7-28-15 $MnO_{x(s)}$ sample was used to make the agar media for this experiment. The data represented in Figure 35 shows that *S. oneidensis* MR-1 had the highest level of reduction for the duration of the experiment, with a peak percent transmittance of 66%. MB4 had the next highest final peak transmittance value of 22%, followed by MB5 at 16%. MB6 and MB7 had final peak transmittance values of 12% and 14%, respectively. This vial assay demonstrated that all of the Mn-reducing strains tested were able to reduce Mn aerobically, at least to some extent. Aerobic Mn reduction was demonstrated by a greater percent transmittance value when compared to the negative control. Results demonstrated that MB4, MB5, MB6 and MB7 appeared to reduce at rates significantly less than what was observed with *S. oneidensis* MR-1

Table 16. Manganese Reducing Bacteria Vial Inoculum Count

Inoculum Counts	Final CFU in Vial
MB4	7.50×10^6
MB5	1.20×10^7
MB6	2.80×10^6
MB7	1.00×10^7
***S. oneidensis* MR-1**	7.33×10^6

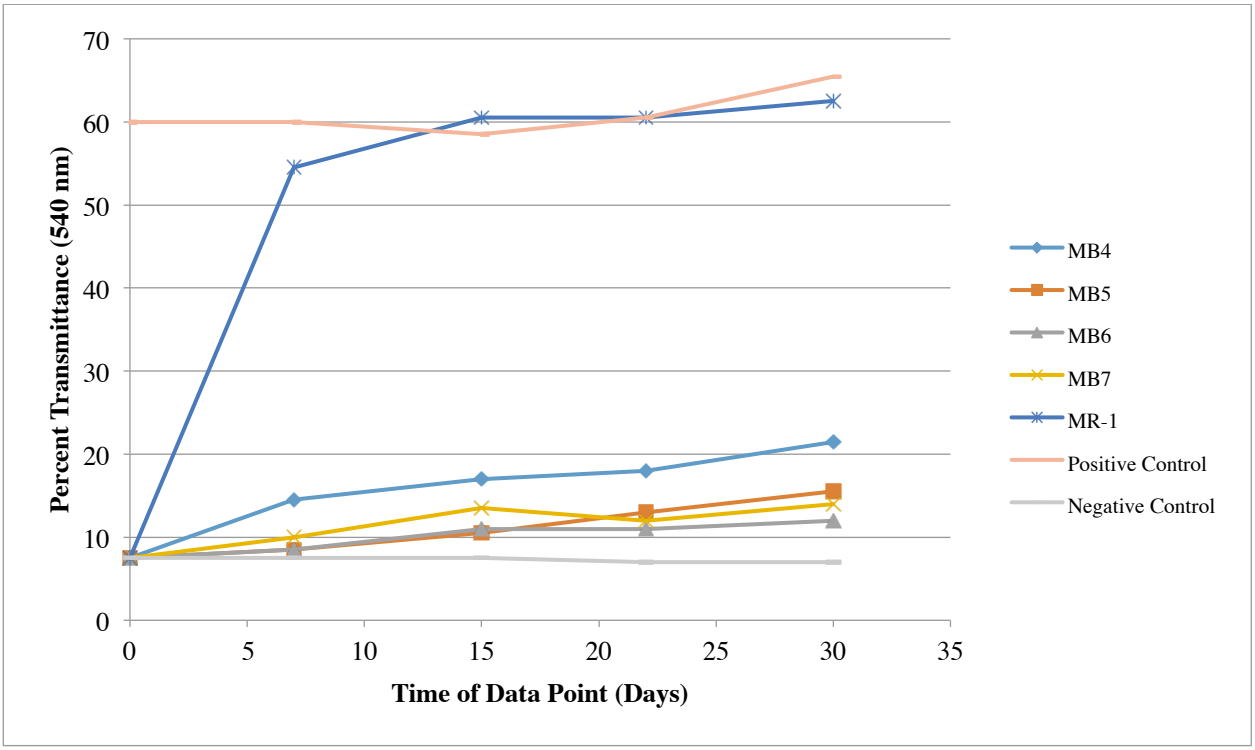

Figure 35. Percent light transmittance in aerobic vial assay for inoculated Mn reducing bacteria

4.4.4 Aerobic Mn Reducing Bactria Vial Assay

S. oneidensis MR-1 and MB5 aerobic reduction performance was comparable to anaerobic results (Table 17). The percent light transmittance for *S. oneidensis* MR-1 in the aerobic vials surpassed anaerobic vials by 2.5%. The MB4, MB6 and MB7 strains were all able to reduce Mn aerobically, but at a lower level than that seen anaerobically. The aerobic vials were allowed to incubate for eight more days than the anaerobic vials and all of the strains, except *S. oneidensis* MR-1, still had lower amounts of Mn reduction. This demonstrated that,

while aerobic Mn reduction is possible, the kinetics and mechanisms for microorganisms to do would probably be slower than when in an anaerobic environment.

Table 17. Maximum Light Transmittance for Anaerobic and Aerobic Mn Reduction Vial Assays

Inoculum Name	Maximum Light Transmittance, Anaerobic (22 days)	Maximum Light Transmittance, Aerobic (30 days)
MB4	27%	22%
MB5	18%	16%
MB6	28%	12%
MB7	21%	14%
S. oneidensis MR-1	60%	63%

4.4.5 *S. oneidensis* MR-1 $MnO_{x(s)}$ Age Study Results

The purpose of this study was to investigate bioavailability of $MnO_{x(s)}$ samples for Mn-reducing microorganisms, starting with *S. oneidensis* MR-1. *S. oneidensis* MR-1 was added into Mn reduction vials containing five different $MnO_{x(s)}$ samples of various ages and treatments. The 2008 sample had presumably lost waters of hydration due to age and the 7-8-15 sample had lost waters of hydration due to drying at 103 °C for 24 hours in an oven. The other $MnO_{x(s)}$ samples had similar properties and relative age was denoted by date synthesized.

Figure 36 represents the raw percent light transmittance data, which correlates to Mn reduction over time for all five different $MnO_{x(s)}$ samples. For the initial 50 hours, the 7-28-15 and 11-18-15 samples had the highest amount of Mn reduction. After 150 hours, all samples had similar transmittance values around 58%, with the exception of the 2008 $MnO_{x(s)}$ sample. After 50 hours, the 2008 $MnO_{x(s)}$ sample had consistently lower Mn reduction, with a transmittance value of 45%, compared to all of the other vials for the remainder of the study.

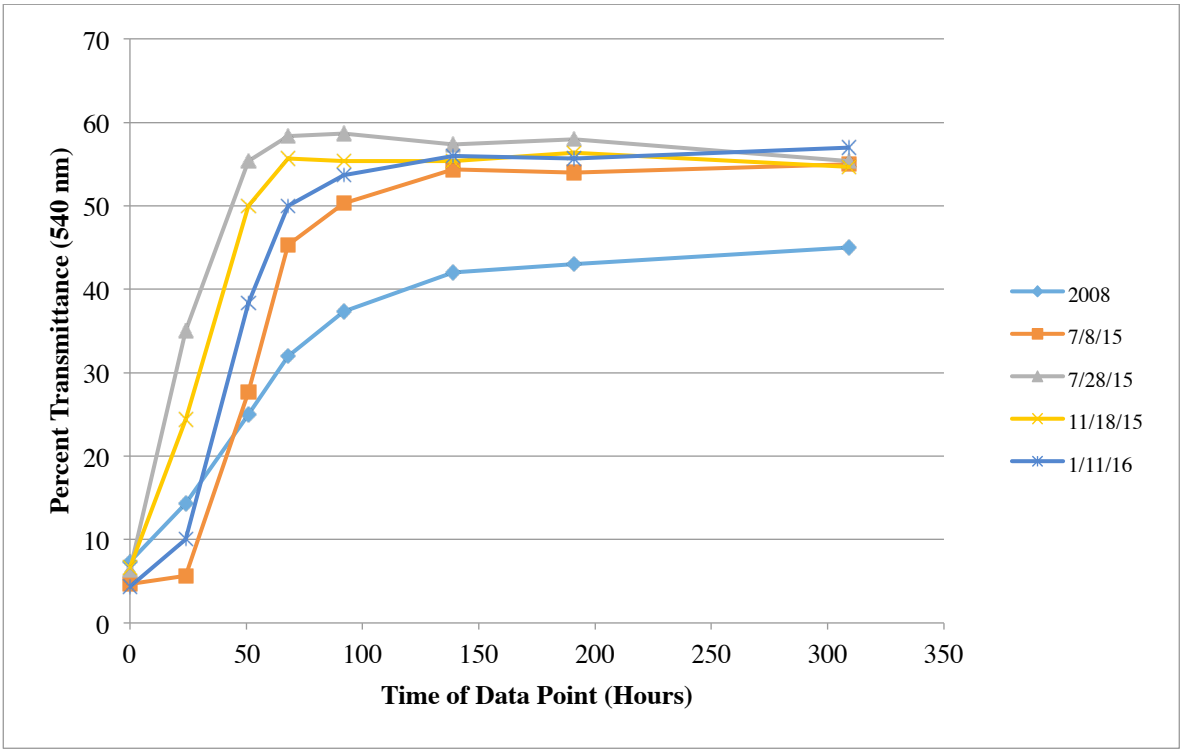

Figure 36. Percent transmittance at 540 nm of different MnOx(s) samples over time with *S. oneidensis* inoculum

Figure 37 normalized the percent transmittance data to the equivalent transmittance for a 1 g/L $MnO_{x(s)}$ sample vial. Because the 2008 and 7-8-15 $MnO_{x(s)}$ samples were significantly darker in color than the other samples, they were mixed into the agar at 0.35 g/L instead of 0.7 g/L. Normalization of the data was completed in an attempt to compare reduction capacity, as a measure of change in transmittance, at equal $MnO_{x(s)}$ concentrations. When the data was normalized, significant differences in Mn reduction can be seen between certain samples. The 2008 and 7-8-15 samples had an overall lower amount of Mn reduction for the duration of the study. All of the other $MnO_{x(s)}$ samples were comparable in Mn reduction or percent transmittance. Figure 38 also demonstrated that the percent transmittance of the negative controls remained constant and did not increase through this study.

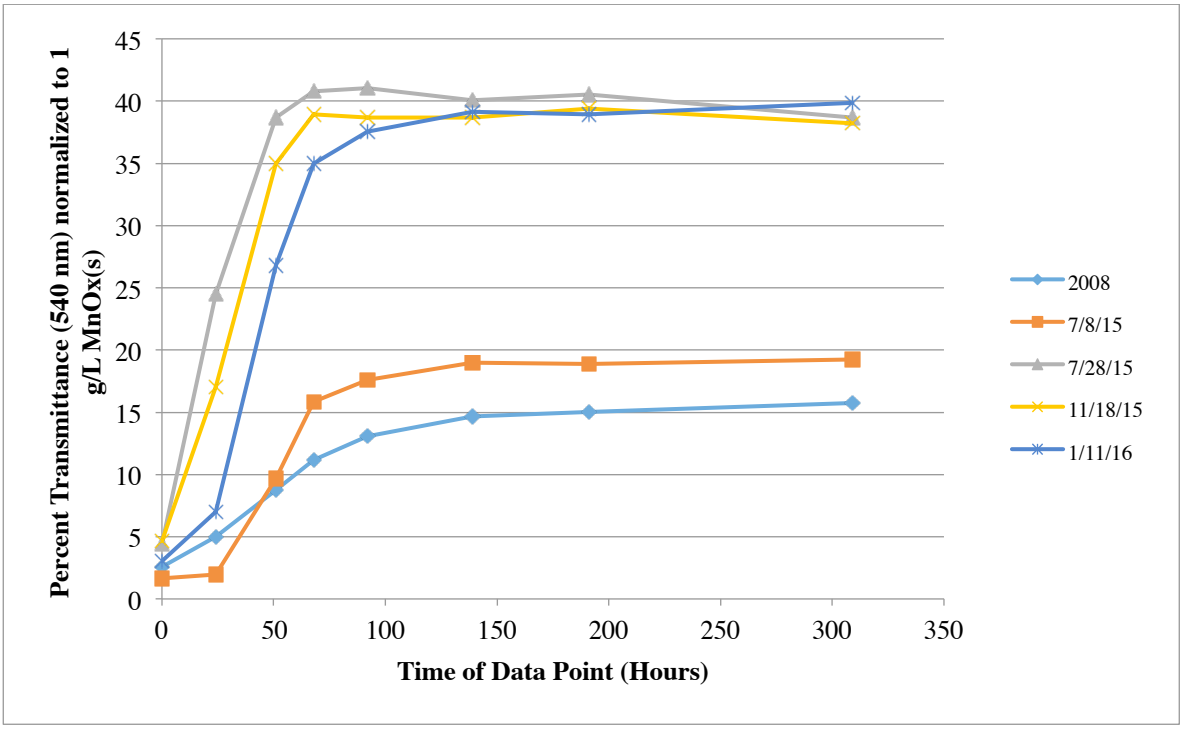

Figure 37. Percent transmittance data normalized to 1 g/L of different $MnO_{x(s)}$ samples over time with *S. oneidensis* inoculum

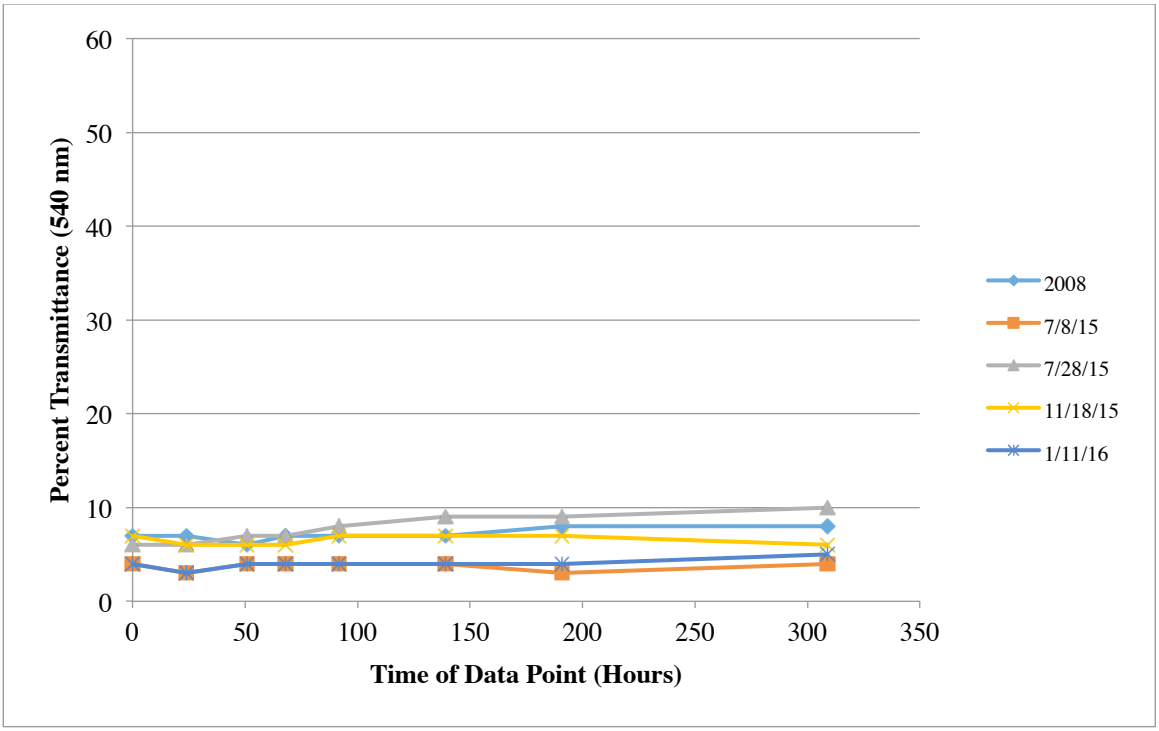

Figure 38. Percent transmittance negative control data normalized to 1 g/L of different $MnO_{x(s)}$ samples

Average *S. oneidensis* MR-1 cell counts for each vial were compared through the course of this study (Figure 39). The cell concentrations found were very similar at each time point in all of the vials for the duration of the experiment. Figures 3-22 through 3-26 show *S. oneidensis* MR-1 concentrations with normalized 1 g/L $MnO_{x(s)}$ percent transmittance data. Distinguishable differences in Mn reduction can be seen, even though *S. oneidensis* MR-1 counts are similar in all vials (Figure 3-22). For the 2008 and 7-8-15 $MnO_{x(s)}$ samples, even though the *S. oneidensis* MR-1 count increases over time, Mn reduction is much slower than the other samples. The 7-28-15, 11-18-15 and 1-11-16 $MnO_{x(s)}$ samples have the same concentration of *S. oneidensis* MR-1 but are able to reduce more $MnO_{x(s)}$. Because the 2008 and 7-8-15 vials have similar *S. oneidensis* MR-1 counts but lower Mn reduction, this points to a lack of bioavailability of the more aged $MnO_{x(s)}$ samples.

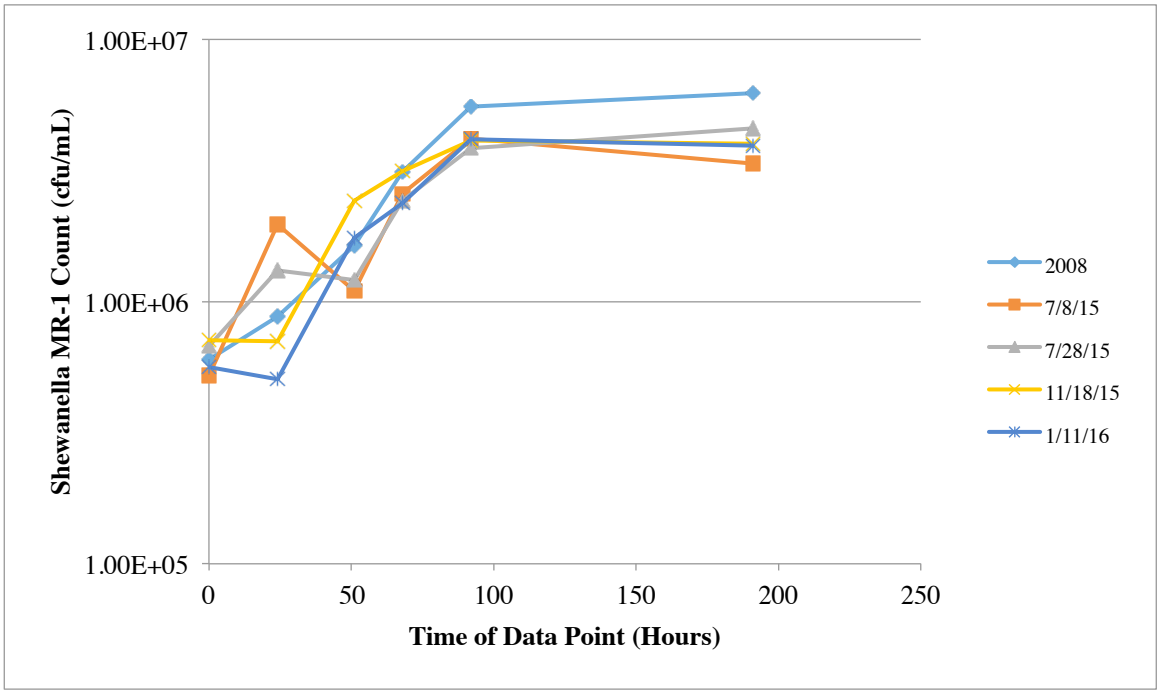

Figure 39. Average *S. oneidensis* MR-1 count (CFU/mL) of triplicate vials via qPCR analysis

4.4.6 Aerobic MB4 and MB6 $MnO_{x(s)}$ Age Study Results

The purpose of this study was to investigate bioavailability of $MnO_{x(s)}$ samples for Mn-reducing microorganisms isolated from the water treatment built environment. MB4 and MB6 were inoculated into Mn reduction vials that contained the 2008, 7-28-15 and 1-11-16 $MnO_{x(s)}$ samples. To measure Mn reduction, the percent light transmittance was measured over time. Figure 40 shows the raw percent light transmittance data for three different $MnO_{x(s)}$ samples with MB4 inoculum. For the initial 7 hours, Mn reduction for all of the samples are similar. After 30 days, the 1-11-16 sample had the greatest percent light transmittance value at 14%. The 7-28-15 sample had the next highest light transmittance at 10% and the 2008 sample had the lowest value at 8%.

The percent transmittance data was normalized to the equivalent transmittance for a 1 g/L $MnO_{x(s)}$ sample vial (Figure 41). When the data was normalized, a greater difference in Mn reduction was seen between the three samples. The 2008 sample consistently had the lowest amount of Mn reduction for the duration of the study, while the 1-11-16 sample had the highest amount of Mn reduction for the entire study. The 7-28-16 sample had been dried at 103 °C for 24 hours, which promoted aging. A decrease in MB4 Mn reduction capability was seen due to aging that occurred due to the heating process. These results help to support the hypothesis that aged $MnO_{x(s)}$ samples have lower bioavailability and directly affect the Mn reduction capability of microorganisms.

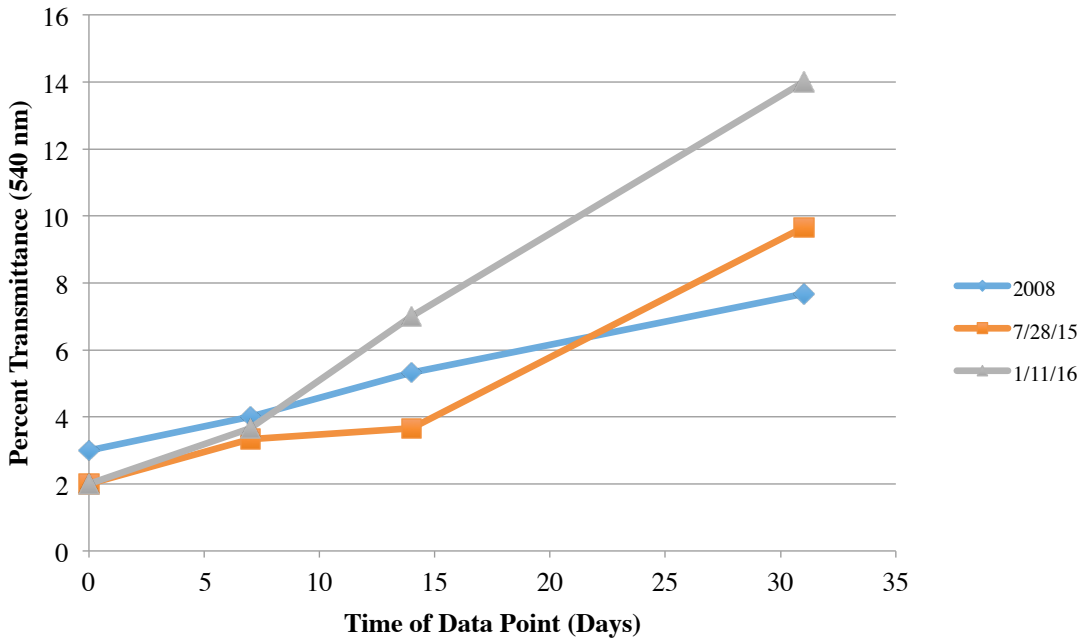

Figure 40. Percent transmittance at 540 nm of different $MnO_{x(s)}$ samples over time with MB4 inoculum

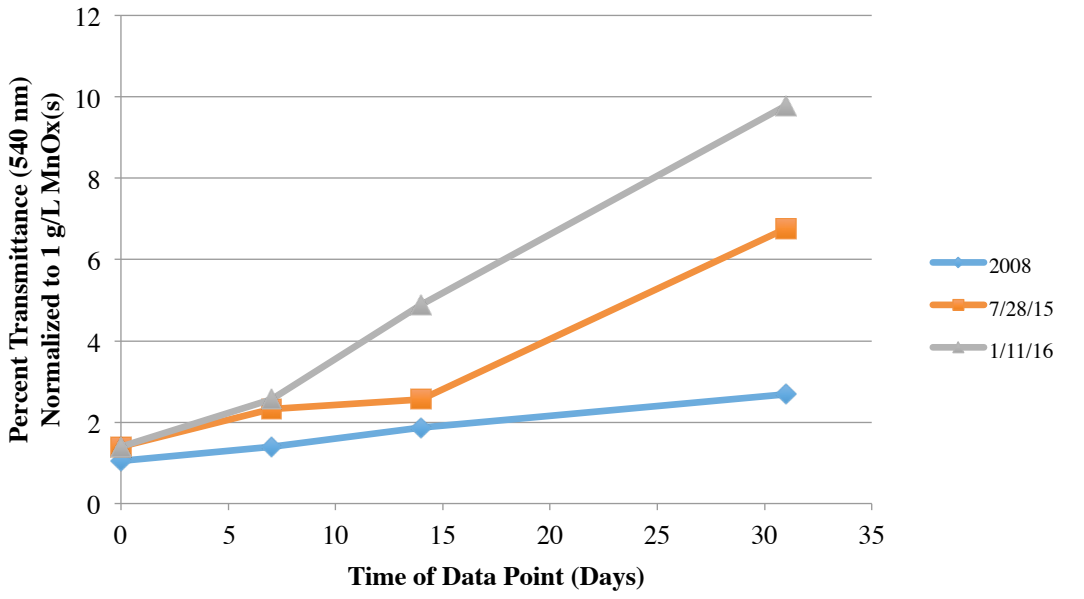

Figure 41. Percent transmittance data normalized to 1 g/L of different $MnO_{x(s)}$ samples over time with MB4 inoculum

The raw percent light transmittance data was graphed for three different $MnO_{x(s)}$ samples with MB6 inoculum (Figure 42). After 30 days, the 1-11-16 sample had the greatest percent light transmittance value at 11%. The 7-28-15 sample had the next highest light transmittance at 8% and the 2008 sample had the lowest value at 7%. Figure 43 normalizes the percent transmittance data to the equivalent transmittance for a 1 g/L $MnO_{x(s)}$ sample vial. As with the MB4 sample vials, when the data was normalized, a larger difference in Mn reduction was seen between the three samples. Again, the 7-28-15 sample was dried, which promoted aging, therefore a lower Mn reduction was seen in the vials. The 2008 sample consistently had the lowest amount of Mn reduction while the 1-11-16 sample had the highest amount of Mn reduction for the entire study. The MB6 results further supported the hypothesis that the aged samples had low bioavailability and affected the Mn reduction capability of microorganisms.

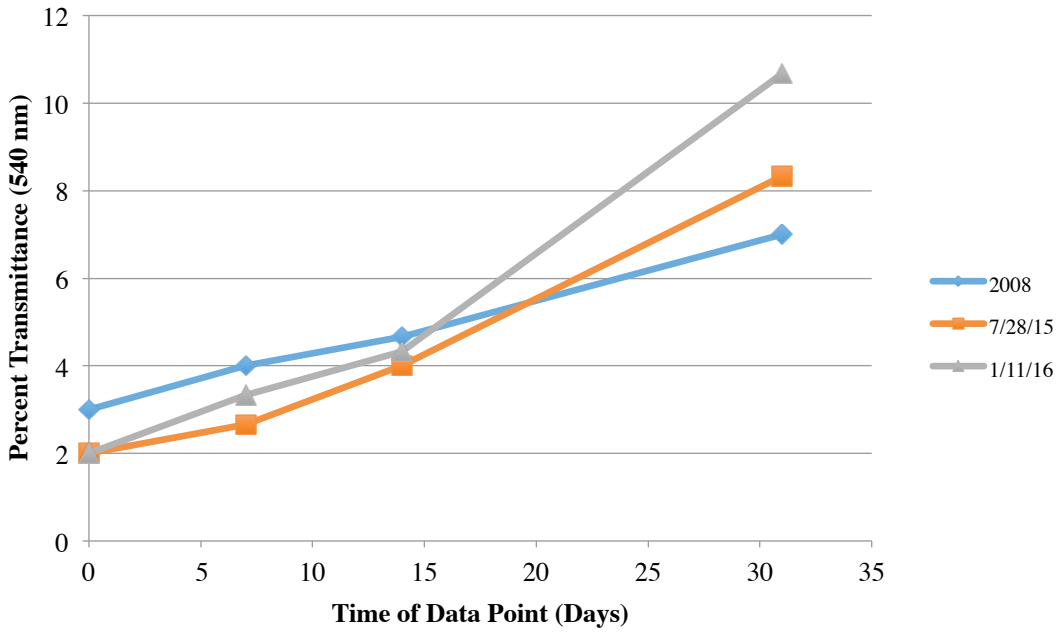

Figure 42. Percent transmittance at 540 nm of different $MnO_{x(s)}$ samples over time with MB6 inoculum

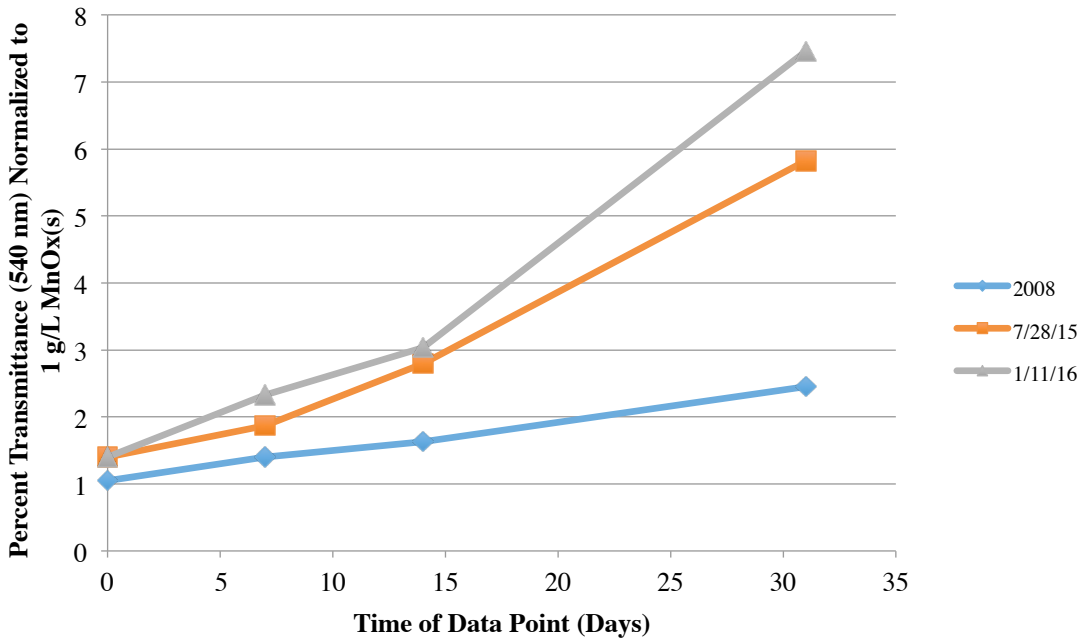

Figure 43. Percent transmittance data normalized to 1 g/L of different MnOx(s) samples over time with MB6 inoculum

It can also be noted that MB6 was able to reduce less $MnO_{x(s)}$ than MB4 in this study. For the normalized percent transmittance trials, the MB4 vials reached a maximum percent light transmittance of 10% compared to 8% for MB6.

Before each time point was measured on the spectrophotometer, each vial was visually inspected. Clearing zones formed on the top of the 7-28-15 and 1-11-16 Mn reduction vials that were inoculated with MB4 (Figure 44) and MB6 (not shown). From these results, it appeared that MB4 and MB6 prefer to reduce Mn at the top of the vial. Semi-solid agar forms a dissolved oxygen air gradient and the highest concentration of dissolved oxygen is found at the surface of the agar (Claus 1989). Because the agar used was very fluid in nature, MB4 and MB6 were able to locate to preferential areas with higher oxygen content with in the vial. There is no immediate explanation as to why these microorganisms would prefer to reduce Mn in an area where higher oxygen concentrations are probable. Since previous results showed a lower amount of aerobic Mn reduction when compared to anaerobic Mn reduction (Table 17), these findings seem to be contradictory to previous experiments.

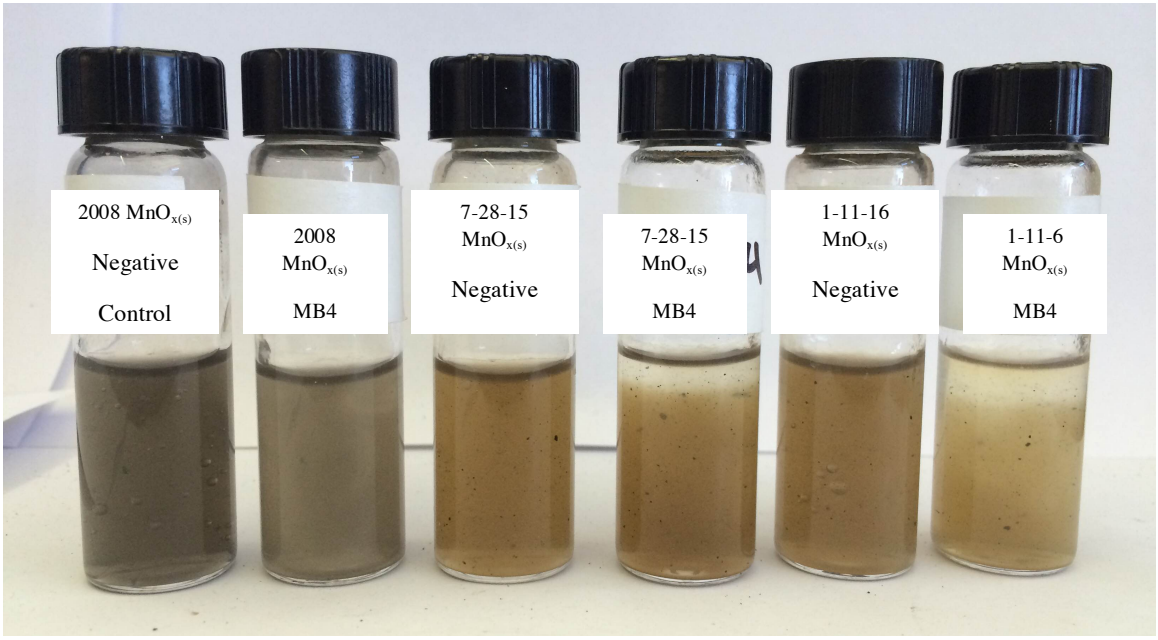

Figure 44. Visual inspection of clearing zones at the top of the Mn reduction vials

4.5 Shake Flask Study

This study evaluated microbially mediated Mn desorption from anthracite media in an aerobic environment using shake flasks inoculated with *S. oneidensis* MR-1 and two *S. oneidensis* strains with mutations in genes (*mtrA* and *mtrB*) required for Mn reduction. Soluble Mn release was monitored from the anthracite media in the bulk liquid. Mn extraction results of the May 2015 Harwood Mills anthracite media showed that 36.5 mg Mn/mg anthracite was previously coated onto the media at the water treatment plant. 2.5 g of the anthracite media was added into each flask, resulting in a total of 91.1 mg Mn/mg anthracite available for biological Mn reduction. The amount of inoculum added into each flask, enumerated from the plate count method, is represented in Table 18. The volume removed for each sampling point was recorded so the total volume in the flask would be known at all times and was considered mass balanced related to soluble Mn released.

Table 18. Inoculum Concentrations for Shake Flask Study

Inoculum Counts	Final CFU in Flask
S. oneidensis MR-1	$2.12x10^6$
S. oneidensis MR-1 ΔmtrA	$1.9x10^5$
S. oneidensis MR-1 ΔmtrB	$3.6x10^6$

The amount of Mn released during the shake flask study from the May 2015 Harwood Mills anthracite media is presented in Figure 45. Data was analyzed as a percentage of Mn released from the anthracite media as soluble Mn in the bulk liquid. The y-axis for Figure 41 was scaled to have a maximum value of 0.5% desorption to depict the negligible release and took place in the shake flask study.

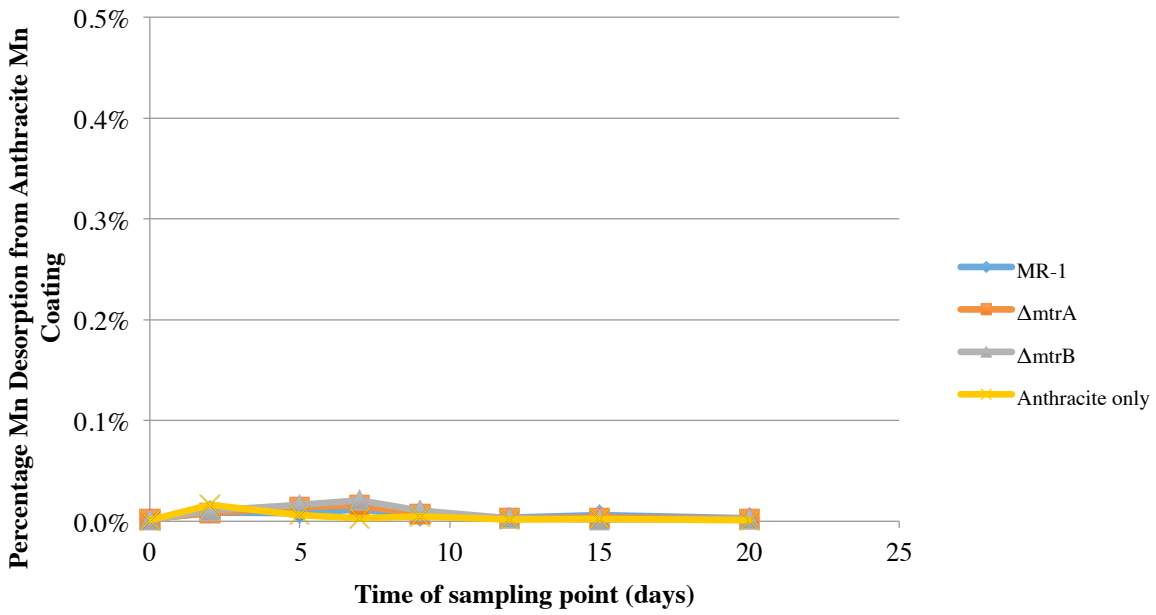

Figure 45. Soluble Mn mass release (sized 0.45 µm or less) as a fraction of Harwood Mills WTP accumulated Mn anthracite coating

5.0 DISCUSSION

The main objective of this research was to examine the role of Mn-reducing microorganisms in desorption of soluble Mn from $MnO_{x(s)}$ -coated filters once free chlorine had been removed from the filter influent. This was accomplished through the completion of bench-scale filter column studies along with development of a qPCR detection method for Mn-reducing organisms. In addition to bench-scale laboratory filter studies, in situ Mn reduction vial assays were completed to investigate Mn reduction capacity of several strains in aerobic and anaerobic conditions. Vial assays were also used to determine the effects of Mn-reducing microorganism populations on the kinetics of Mn reduction and to investigate the bioavailability of various $MnO_{x(s)}$ samples.

The beginning of the discussion chapter will detail the pieces of research that most appropriately relate to examining the role of Mn-reducing microorganisms in bench-scale filter studies. Other noteworthy experimental outcomes that tangentially relate to microbially related Mn reduction will then be discussed towards the end of the chapter.

5.1 Evidence for Microbially Mediated Reductive Dissolution of Mn in Bench-Scale Filter Column Studies

5.1.1 *S. oneidensis* MR-1 Inoculated Bench-Scale Column Studies

Evidence of reductive Mn dissolution was seen in the bench-scale filter column experiment where the Harwood Mills anthracite media (collected March 2016) was inoculated with *S. oneidensis* MR-1 (Figure 21). For example, a 10% increase in effluent Mn was seen in the *S. oneidensis* MR-1 inoculated column over the non-inoculated column even while free chlorine was applied to the filter. After free chlorine was removed from the column, the average concentration of effluent Mn seen in the *S. oneidensis* MR-1 column was 20% greater than the non-inoculated column. The observed Mn breakthrough for the non-inoculated column could have been due to exhaustion of active sites on the media combined with a low amount of Mn reduction from the native Mn-reducing microorganism present on the media. The differences in Mn release between the inoculated and non-inoculated release can be attributed to the true reductive Mn dissolution of the $MnO_{x(s)}$ surface by *S. oneidensis* MR-1.

From qPCR analysis, qualitatively there were more organisms that contained the *mtrB* gene on the columns inoculated with *S. oneidensis* MR-1 than on the non-inoculated column. The average Cq value for the *S. oneidensis* MR-1 inoculated columns was 27 compared to non-inoculated column, which had an average Cq value of 38 (Figure 22). These findings demonstrated that there were more microorganisms that had the ability to reduce Mn on the inoculated column. *S. oneidensis* MR-1 was also recovered and quantified from all sections of the anthracite media in the laboratory-scale columns and was not detected via qPCR methods from the non-inoculated media (Figure 32). These findings verified the presence of *S. oneidensis* MR-1 on the inoculated filter media for the duration of the experiment. Therefore, the increase in Mn breakthrough can be attributed to the presence of *S. oneidensis* MR-1, a Mn reducing organism.

The correlation of increased Mn in the column effluent and demonstration that *S. oneidensis* MR-1 was present on the $MnO_{x(s)}$ surface at the end of experiment indicated that Mn-reducing microorganisms were most likely responsible for the additional Mn desorption. Results are in agreement with the study by Islam (2010), which concluded that Mn release from filter media was caused by microbial activity. This research provided additional evidence that the presence of Mn-reducing microorganisms on $MnO_{x(s)}$ media in a full-scale WTP could likely be contributing to the observed Mn desorption phenomenon when free chlorine is removed.

5.1.2 MB4 and MB6 Inoculated Bench-Scale Column

For the column that was inoculated with MB4 and MB6 cultures, a small amount of increased Mn breakthrough compared to the non-inoculated column was seen (Figure 25). This increase in Mn breakthrough again demonstrates true reductive Mn dissolution caused by the presence of Mn-reducing microorganisms. The percent differences in Mn breakthrough were not as large when compared to the *S. oneidensis* MR-1 inoculum study (Figure 21). On average, the inoculated column with MB4 and MB6 had a 5% greater Mn breakthrough percentage when compared to the non-inoculated column when free chlorine was being applied. When the application of free chlorine stopped, an average increase of 4% Mn breakthrough was seen in the MB4/MB6 inoculated column compared to the non-inoculated column. Similar to the *S. oneidensis* MR-1 inoculated column experiment, the observed Mn breakthrough for the non-inoculated column was likely due to exhaustion of active sites on the media combined with a low

amount of Mn reduction from the native Mn reducing microorganism present on the media. Event though differences in Mn release between the inoculated and non-inoculated columns were small, the increase in Mn breakthrough was attributed to the true reductive Mn dissolution of the $MnO_{x(s)}$ surface by MB4 and MB6.

The qPCR analysis for this column study was less conclusive when compared to molecular results from the *S. oneidensis* MR-1 study. Evidence of increased concentrations of the *mtrB* gene (Mn reducing microorganisms) was not seen. The Cq values for both columns at all three depths were very similar in value. This result could either demonstrate that the amount of Mn-reducing microorganisms were the same in both columns or that the *mtrB* primer set was not able to adequately bind to the *mtrB* gene sequence of MB4 and MB6. It is more probable that that the latter is true based off of prior qPCR analyses (Figure 14), where the Cq values for both MB4 and MB6 were low. Experimental evidence of an increase in reductive Mn dissolution in the columns inoculated with MB4 and MB6 helps to support this hypothesis.

It is also noteworthy to comment on the fact that MB4 and MB6 both have Mn oxidation capability in addition to the capacity to reduce Mn. The environmental conditions, mechanisms and reasons behind whether a microorganism chooses to oxidize or reduce Mn are not known. During the MB4 and MB6 inoculated column experiment, for the last five days the non-inoculated column had consistently greater Mn breakthrough values. The possibility that the inoculated MB4 and MB6 microorganisms began to oxidize influent Mn or Mn adsorbed to the $MnO_{x(s)}$ surface should not be ruled out.

5.1.3 Kinetic Differences in Bench-Scale Column Reductive Dissolution

The reasons for the large differences seen in Mn breakthrough results between the *S. oneidensis* MR-1 and MB4/MB6 inoculated columns are unclear (Figures 21 and 25). Sizeable differences in the amount of Mn reduction between *S. oneidensis* MR-1, MB4 and MB6 were also observed in the *in situ* vial assays (Table 17). *S. oneidensis* MR-1 reduced a much larger amount of Mn (both aerobically and anaerobically) and in a shorter time frame when compared to MB4 and MB6. The dissimilatory Mn reduction mechanisms of MB4 and MB6 have yet to be studied and it could be possible that those mechanisms are distinctive from that of *S. oneidensis* MR-1. Organic carbon oxidation is often linked to Mn reduction (Lovley 1988) and some microorganisms may prefer one carbon source over another. *S. oneidensis* MR-1 may have had a

competitive advantage or preference over MB4 and MB6 for acetate as the carbon source in filter studies. More research is needed to discern why and under what conditions that certain microorganisms are able to reduce $MnO_{x(s)}$ from filter media.

5.1.4 Mn-Reducing Microorganism Viability in the Presence of Chlorine

For the column study with *S. oneidensis* MR-1 inoculum, the inoculum and any organisms present on the media were exposed to a free chlorine Ct of 4,400 mg/L*min. *Shewanella* species are Gram negative and are therefore non-spore-forming (Venkateswaran 1999). This is in contrast to MB4 and MB6, which are gram-positive *Bacillus* sp. that are spore-formers. There was a 5-log reduction in qPCR detectable cell counts of *S. oneidensis* MR-1 from the time of inoculation until the end of the study. Only $3.9x10^2$ CFU/mL of *S. oneidensis* MR-1 remained on the $MnO_{x(s)}$ surface at the end of that study even though large differences in Mn breakthrough are still seen when compared to the column with no additional inoculum. This leads to the conclusion that small numbers of Mn-reducing microorganisms, even if not able to form spores, are able to remain viable on the $MnO_{x(s)}$ surface and reduce a detectable amount of Mn in the presence of free chlorine. It should be noted that the average amount of pre-filter free chlorine typically applied to the Harwood Mills WTP filters is 2.9 mg/L (Hawkins 2016). This concentration of free chlorine is about five times greater than the amount of free chlorine applied to the filter in the bench-scale filter column studies with added Mn reducer inoculum. The presence of Mn-reducing microorganisms on the Harwood Mills WTP $MnO_{x(s)}$ media coating was confirmed with a low level of detection of the *mtrB* gene via qPCR. It is notable that the Mn-reducing microbes present on the $MnO_{x(s)}$ surface were able to remain viable while the filter was in service in the presence of much higher chlorine Ct values. The formation of biofilms protects microorganisms from the effects of chlorine (LeChevallier 1988). The formation of a biofilm on the surface of the anthracite media could have helped to promote the viability of some of the inoculated *S. oneidensis* MR-1 organisms.

5.2 Factors that Affected Mn Breakthrough in Bench-Scale Filter Column Studies

5.2.1 MnOx(s) Coating Age and Bioavailability

Much is still unknown about the forms and phases of $MnO_{x(s)}$ that are present in filter media coatings; further this might affect the bioavailability of Mn for reductive dissolution.

Typical anthracite or sand filtration media beds have a long service life due to media durability (Edzwald 2011), which allows for a large amount of $MnO_{x(s)}$ coating to form during many years of operation. $MnO_{x(s)}$ coatings on anthracite media have been shown to form a tree-ring-like structure (Tobiason 2008). Little is known about the differing characteristics of the $MnO_{x(s)}$ coating layers, as aging inevitably occurs through in service use. As in the Harwood Mills WTP, the anthracite media from Filter 1 had been in operation and accumulating an $MnO_{x(s)}$ coating for 28 years. Differing rates of Mn reactivity have been seen in laboratory testing because of variations in $MnO_{x(s)}$ crystalline structure and surface area (Stone 1987). Burdige et al. (1992) showed that *S. oneidensis* MR-1 was able to reduce a greater amount of two less "aged" crystalline forms of Mn oxide (birnessite and 6-$MnO_{2(s)}$) when compared to a highly crystalline form $MnO2_{(s)}$, pyrolusite. The conclusion from the Burdige et al. (1992) study was that mineralogy, crystalline structure and surface area all play an important role in the bioavailability of Mn oxides and the rate of biotic Mn reduction.

When the Mn desorption phenomenon has been observed in a full-scale WTP, typically there is a period of effluent Mn concentrations exceeding influent Mn. Over time, the amount of Mn released in the effluent ceases to exceed the influent and evidence of outright Mn release from the media is no longer evident. In comparison to this trend, the column studies that utilized the Harwood Mills WTP filter media did experience a periodic increase in effluent Mn and an eventual return to a steady state condition of Mn release. Even though, effluent Mn never exceeded the influent concentration, microbially mediated Mn reduction of bioavailable $MnO_{x(s)}$ from the anthracite media was taking place. An acceptable working hypothesis is that the $MnO_{x(s)}$ layers present on the coating had undergone changes in chemistry such that progression towards a more crystalline structure was seen the longer that the coating had been present in the system. The Mn-reducing microorganisms were potentially able to reduce the less crystalline or less "aged" forms of $MnO_{x(s)}$ on the media surface, which caused the initial rise of effluent Mn. This result is supported by the demonstration that Mn reduction of the more aged 2008 $MnO_{x(s)}$ sample was substantially lower in the *in situ* vial assays (Figures 36 and 37). Once the bioavailable forms of $MnO_{x(s)}$ had been exhausted, the $MnO_{x(s)}$ that was left on the surface was hypothetically more crystalline in nature and was less bioavailable. Effluent Mn levels then decreased from a decline in microbially mediated Mn reduction of the $MnO_{x(s)}$ surface due to lack of bioavailability.

It is possible that the concentration of Mn-reducing microorganisms and forms of bioavailable $MnO_{x(s)}$ that were present during the inoculated filter column studies were not suitable for the observation of the Mn desorption phenomenon where the effluent Mn exceeds influent Mn concentration. The kinetics or concentration of Mn-reducing bacteria may not have been high enough to establish conditions where effluent Mn exceeded the influent.

It is notable that the amount of extractable Mn was significantly lower in the top 2-inches of the anthracite media for both the *S. oneidensis* MR-1 and MB4/MB6 inoculated columns. As noted in Chapter 4, natural variability of Mn coating concentration can be as great as +/- 20% (Tobiason 2008). It is known $MnO_{x(s)}$ deposition is a function of depth, with the greatest $MnO_{x(s)}$ concentrations being found at the top of a column depth (Tobiason 2008). This presumably means that the $MnO_{x(s)}$ formed there is less aged and would be more bioavailable. Since this trend was seen in both column studies, it could be hypothesized that the Mn reducing microorganisms were able to readily reduce the less aged $MnO_{x(s)}$ formed at the top of the column. This resulted the decrease in extractable Mn at the top of the *S. oneidensis* MR-1 and MB4/MB6 inoculated columns. The decrease in extractable Mn at the top of the column was not observed in either of the non-inoculated columns for both *S. oneidensis* MR-1 and MB4/MB6 experiments.

5.2.2 pH

$MnO_{x(s)}$ surface regeneration by molecular oxygen (in the absence of free chlorine) and microbial processes are both affected by pH. Some of the changes in abiotic release of Mn from the media can be attributed to the effects of pH on the regeneration of active sites. The impact of pH dependence on microbially mediated Mn reduction is not known and should be considered in evaluation of observed increases or decreases in Mn release. The behavior of Mn oxidizing microorganisms that are present on filtration media have been shown to be effected by pH (Hoyland 2014). The authors showed that Mn oxidizing microorganisms were able to begin to oxidize Mn earlier at pH conditions between 6.3 - 6.7 when compared to 7.0 – 7.3, which demonstrated that pH was directly tied to microbial Mn oxidation mechanisms and possible enzymatic activity. Therefore, the possibility of increased or decreased Mn reduction due to pH conditions should not be ruled out.

5.2.3 TOC

Bioavailable DOC loading into a filtration process is typically around 0.5 – 2.0 mg/L (Yapsakli 2010). All of the carbon loading (acetate) for experiments in this research for column studies was considered 100% BDOC. For the Harwood Mills WTP, the average TOC demand across Filter 1 was 0.59 mg/L TOC (Hawkins 2016). Consequently, the initial TOC loading of 0.5 mg/L as C was considered a representative BDOC across a WTP filter during operation. When 0.5 mg/L as C was added into the inoculated filter, maximum Mn breakthrough values of 54% were seen. A large increase in Mn breakthrough in the inoculated column to 86% was seen when TOC loading was increased to 12 mg/L as C. The surge in Mn breakthrough, which correlated to the increase in TOC, could be credited to the increased reductive Mn dissolution activity of *S. oneidensis* MR-1 on the media. Simple carbon containing compounds, like sugars or amino acids, can be fully oxidized by Mn-reducing microorganisms in a reducing environment (Lovley 2004). Lovely and Philips showed that *S. oneidensis* MR-1 coupled the oxidation of electron donors, similar to the acetate supplied in the columns, to Mn reduction. It should be noted that the environment with in the column would probably not be considered reducing since oxygen entrained in the influent waters would be present. Additionally, a large majority of organic matter that is oxidized in sedimentary environments is directly linked to Fe or Mn reduction (Burdige 1992). The columns that were inoculated with *S. oneidensis* MR-1 showed a greater percentage in Mn breakthrough for the duration of the experiment when compared to the column that did not have any additional inoculum.

It is plausible that the influent concentration of 0.5 mg/ and 11 mg/L TOC as C were not at high enough carbon concentrations to see evidence of effluent Mn exceeding influent Mn concentrations. In the bench scale laboratory study by Islam (2010) where Mn desorption was seen, carbon dosing was 4-μM sodium acetate (56 mg/L as C). As stated above, typical influent TOC loading in a treatment plant is 25 to 100 times lower than the carbon concentration used in Islam's laboratory study. True Mn desorption was seen in the study by Islam, but application of the results in a full scale WTP could be questioned. Interestingly in Islam's study, when carbon was removed from the filter, Mn desorption ceased.

It is apparent that some amount of bioavailable carbon is required for Mn desorption to be seen in laboratory experiments and full-scale treatment facilities. Effluent concentrations of Mn did not exceed influent concentrations in research conducted for this thesis where 0.5 or 11

mg/L as C was added into the columns. This leads to the assumption that bioavailable carbon may be incorporated into observed Mn desorption phenomenons but the nature and role of carbon concentration and Mn bioavailability is unclear.

5.2.4 Mn Reducing Microorganisms and Required $MnO_{x(s)}$ Contact

Results from the shake flask study failed to demonstrate reductive Mn dissolution from $MnO_{x(s)}$ coated Harwood Mills' anthracite filter media (Figure 45). The shake flask environment into which the *S. oneidensis* MR-1 were placed did not force the organism to attach to the $MnO_{x(s)}$ media surface. In contrast for in bench-scale laboratory filter column studies, the naturally occurring microbes or added inoculum (*S. oneidensis* MR1 or MB4/MB6) were forced to adhere to the $MnO_{x(s)}$ surface or be washed out through downflow or upflow hydraulics. For *S. oneidensis* MR-1 to reduce Mn, the organism must be in direct contact with the oxide surface (Meyers 1988). This experiment most likely did not succeed because *S. oneidensis* MR-1 was not required to stay attached to the surface of the anthracite media and could reside in the bulk liquid media.

5.3 Molecular Detection Methods

A qPCR detection method was created to qualitatively compare amounts of the *mtrB* gene in laboratory and environmental samples. Overall, this detection method was able to relatively compare the amount of microorganisms in a sample that contained the *mtrB* gene (Figures 23 and 26). Consequently, this qPCR method was able to compare samples to determine which contained higher quantities of Mn reducing microorganisms. This method appeared to detect certain Mn-reducing organisms at greater levels than others. The *mtrB* primers demonstrated strong detection for *S. oneidensis* MR-1 and MB5 (*Bacillus cereus*). The *mtrB* primers did not detect MB4 (*Bacillus pumilus*), MB6 (*Bacillus cereus*) or MB7 (*Lysinibacillus fusiformis*) well. The reason for the preferential binding of primers for certain microorganisms, even when identified as the same genus and species (MB5 and MB6), is not known. The most likely reason for this would be due to sequence dissimilarities in the *mtrB* gene for those organisms. Sequences for the mtrB gene from the NCBI GenBank database contained a moderate level of variability, which could demonstrate low conservation of that gene or uncertainty in gene sequence. None of the sequences found from the NCBI GenBank were Bacillus *sp.* which could be another reason why detection for some Bacillus sp. is low. A much

larger subset of *mtrB* gene sequences would be required for additional MUSCLE alignments to strengthen the binding of the *mtrB* primers to Bacillus *sp*. and others.

5.4 Mn Desorption Prevention for Full-Scale WTP

This research demonstrates that the Mn-reducing microorganism population residing on the $MnO_{x(s)}$ surface play an important role in desorption of Mn from filter media. If a WTP desires to cease pre-filter chlorination and maintain a biologically active filter process instead, the occurrence of the Mn desorption phenomenon could be of concern. The application of a sustained high dose of chlorine as a shock treatment to the filter media could help to reduce viability of the Mn-reducing microorganisms on the media. Outright replacement of the filter media could also be an option. The cost of the replacement of the media would have to be considered in lieu of a shock chlorine treatment, which would be the most cost effective option.

6.0 CONCLUSIONS

6.1 Conclusions

Bench-scale filter column studies have demonstrated the potential of Mn reducing microorganisms to contribute to the Mn desorption phenomenon seen in WTPs when pre-filtration free chlorine is removed. The exact conditions under which effluent will Mn exceed influent Mn concentrations are not known but the following conclusions can be made from the experimental results:

1. Microbially mediated desorption is possible when sufficient Mn-reducing microbial populations are present on $MnO_{x(s)}$ surfaces in column setups
2. Microbially mediated desorption is likely a major contributor to the Mn desorption phenomenon seen in full-scale WTPs
3. Mn-reducing microorganism population and reduction kinetics affect how $MnO_{x(s)}$ is desorbed from filter media
4. Both gram positive and gram negative Mn-reducing microorganisms residing on the $MnO_{x(s)}$ surface are able to remain viable and reduce Mn after contact with free chlorine
5. $MnO_{x(s)}$ age and crystalline structure plays an important role in bioavailability to Mn-reducing organisms
6. $MnO_{x(s)}$ bioavailability could affect the duration of elevated effluent Mn during times of observed Mn desorption

6.2 Future Research

This research provided evidence that Mn-reducing microorganisms do play an important, but undefined role, in the Mn desorption phenomenon. The operational and plant conditions that causes the Mn desorption to occur are still not known. Investigation into these following areas would help to further understand the causes of Mn desorption seen in WTPs when pre-filter free chlorine is removed:

1. Isolation of a variety of Mn-reducing microorganisms in order to collect numerous *mtrB* sequences for a more complete and encompassing MUSCLE alignment
2. Development of molecular methods for detecting the expression of the *mtrB* gene

3. Further investigation of the roles that pH, carbon loading and Mn-reducing bacteria concentration play in microbially mediated $MnO_{x(s)}$ reduction
4. Advanced analysis and identification of the structure and bioavailability of coated $MnO_{x(s)}$ on a media as to predict Mn desorption patterns

7.0 WORKS CITED

Bierlein, K. A. (2012). Modeling manganese sorption and surface oxidation during filtration. Blacksburg, Va University Libraries, Virginia Polytechnic Institute and State University.

Burdige, D. D., Surya; Nealson, Kenneth (1992). "Effects of manganese oxide mineralogy on microbial and chemical manganese reduction." Geomicrobiology Journal **10**(1): 27-48.

Burdige, D. J. (1993). "The biogeochemistry of manganese and iron reduction in marine sediments." Earth-Science Reviews **35**: 249-284.

Burnes, B. S. (2000). Identification and Characterization of Genes Required for Mn(IV) Reduction by Shewanella putrefaciens, Georgia Institute of Technology. **Doctor of Philosophy**.

Carlson, K. H. K., William R. (1999). "Modeling Manganese Oxidation with KMnO4 for Drinking Water Treatment." Journal of Environmental Engineering **125**(10): 892-896.

Cerrato, J. M. F., Joseph O.; Dietrich, Andrea M., Knocke, William R.; McKinney, Chad W.; Pruden, Amy (2008). "Manganese-oxidizing and reducing microorganisms isolated from biofilms in chlorinated drinking water systems." Water Research **44**: 3935-3945.

Cerrato, J. M. R., Lourdes P.; Alvarado, Carmen N.; Dietrich, Andrea M. (2006). "Effect of PVC and iron materials on Mn(II) deposition in drinking water distribution systems." Water Research **40**(14): 2720-2726.

Claus, W. (1989). Understanding Microbes: A Laboratory Textbook for Microbiology. New York, NY, W. H. Freeman and Company.

Costa, L. G. A., Michael (2015). Manganese in health and disease. Cambridge, The Royal Society of Chemistry.

Edgar, R. C. (2004). "MUSCLE: multiple sequence alignment with high accuracy and high throughput." Nucleic Acids Research **32**(5): 1792-1797.

Edzwald, J. (2011). Water Quality and Treatment: A Handbook of Drinking Water.

EPA (1979). National Secondary Drinking Water Regulations. **143.3**.

Gabelich, C. G., Fredrick W; Knocke,William R.; Connie C. Lee (2006). "Sequential Manganese Desorption and Sequestration in Anthracite Coal and Silica Sand Filter Media." American Water Works Association **98**(5): 116-127.

Hach (2016a). "Determination of Low Range Manganese by the PAN method." from http://www.hach.com/manganese-reagent-set-lr-pan-10-ml/product?id=7640180304.

Hach (2016b). "Aluminum by the Eriochrome Cyanine R (ECR) Method." from http://www.hach.com/aluminum-reagent-set-eriochrome-cyanine-r-ecr-method-50-ml/product?id=7640178472.

Hach (2016c). "Free chlorine determination by the DPD Free Chlorine method." from http://www.hach.com/dpd-free-chlorine-reagent-powder-pillows-10-ml-pk-300/product?id=7640187689&callback=qs.

Hawkins, R. (2016). L. Swain.

Haynes, E. N. S., Heidi; Kuhnell, Pierce; Alden, Jody; Barnas, Mary; Wright, Robert O.; Parsons, Patrick J.; Aldous, Kenneth M.; Praamsma, Meredith L.; Beidler, Caroline (2015). "Manganese Exposure and Neurocognitive Outcomes in Rural School-Age Children: The Communities Actively Researching Exposure Study (Ohio, USA)." Environmental health perspectives **123**(10): 1066-1071.

Hinds, G. (2015). The Impact of Aluminum on the Initiation and Development of MnOx(s) Coatings for Manganese Removal. Virginia Polytechnic Institute and State University **Master of Science, Environmental Engineering**.

Hoyland, V. K., William; Falkinham, Joseph III; Pruden, Amy; Singha, Gargi (2014). "Effect of drinking water treatment process parameters on biological removal of manganese from surface water " Water Research **66**: 31-39.

Islam, A. A. (2010). Manganese removal by media filtration: Release and Complexation. Civil and Environmental Engineering, University of Massachusets. **Doctor of Philosophy**.

Johnson, K. S. (2006). "Manganese Redox Chemistry Revisited." Science **313**(5795): 1896-1897.

Jones, S. N., Ryan; McMahon, Katherine (2009). "Evidence for structuring of bacterial community composition by organic carbon source in temperate lakes." Environmental Microbiology **11**(9): 2463-2472.

Knocke, W. R., Occiano, Suzanne C., Hungate, Robert (1991). "Removal of Soluble Manganese by Oxide-coated Filter Media: Sorption Rate and Removal Mechanism Issues." Journal (American Water Works Association) **83**(8): 64-69.

Knocke, W. R. O., Suzanne C.; Hungate, Robert (1991). "Removal of Soluble Manganese by Oxide-coated Filter Media: Sorption Rate and Removal Mechanism Issues." American Water Works Association **83**(8): 64-69.

Kristoffersen, S. M. R., Solveig; Tourasse, Nicolas J.; Økstad, Ole Andreas; Kolstø, Anne-Brit; Davies, William (2007). "Low concentrations of bile salts induce stress responses and reduce motility in Bacillus cereus ATCC 14579 [corrected]." Journal of Bacteriology **189**(14): 5302-5313.

LeChevallier, M. C., C; Lee, R (1988). "Factors promoting survival of bacteria in chlorinated water supplies." Applied and Environmental Microbiology **54**(3): 649-654.

Lin, H. S., Nadia H.; DiChristina, Thomas J. ; Taillefert, Martial (2012). "Microbial Mn(IV) reduction requires an initial one-electron reductive solubilization step." Geochimica et Cosmochimica **99**: 179-192.

Lovley, D. H., Dawn.; Nevin, Kelly (2004). Dissimilatory Fe(III) and Mn(IV) Reduction. England, Elsevier Science & Technology. **49:** 219-286.

Lovley, D. P., E. (1988). "Novel mode of microbial energy metabolism: organic carbon oxidation coupled to dissimilatory reuction of iron or manganese." Applied Environmental Microbiology **51**: 683-689.

Madison, A. S. (2012). Biogeochemical cycling of soluble manganese(III) in marine (pore)waters. University of Delaware. **Doctor of Philopsophy**.

Meyers, C. a. N., K. (1988). "Bacterial manganese reduction and growth with manganese oxide as the sole electron acceptor." Science **240**: 1319-1321.

MoBio Laboratories, I. (2016). "PowerSoil DNA Isolation Kit." from https://mobio.com/powersoil-dna-isolation-kit.html.

Morgan, J. S., Werner (1964). "Colloid-Chemical Properties of Manganese Dioxide." Journal of Colloid Science **19**: 347-359.

Nealson, K. H. M., C. R. ; Wimpee, B. B. (1991). "Isolation and identification of manganese-reducing bacteria and estimates of microbial Mn(IV)-reducing potential in the Black Sea." Deep-Sea Research **38**(2): S907-S920.

Osterman, A. L. R., Jennifer L; Beliaev, Alexander S; Zhulin, Igor B; Auchtung, Jennifer M; Driscoll, Michael E; Tiedje, James M; Pinchuk, Grigoriy; Romine, Margaret F; Serres, Margrethe H; Rodionov, Dmitry A; Saffarini, Daad A; Spormann, Alfred M; Gardner, Timothy S; Rodrigues, Jorge L. M; Nealson, Kenneth H; Fredrickson, James K (2008). "Towards environmental systems biology of Shewanella." Nature Reviews Microbiology **6**(8): 592 - 603.

Ross, D. E. (2009). Kinetic and biochemical analysis of electron transfer in dissimilatory metal reduction by Shewanella oneidensis MR-1. Biochemistry and Molecular Biology, Pennsylvania State University. **Doctor of Philosophy**.

Sain, A. G., Ashley; Dietrich, Andrea M. (2014). "Assessing taste and visual perception of Mn(II) and Mn(IV)." Journal of the American Water Works Association **106**(1): E32-E32.

Schicklberger, M. B., Clemens; Schuetz, Bjoern; Heide, Heinrich; Gescher, Johannes (2011). "Involvement of the Shewanella oneidensis Decaheme Cytochrome MtrA in the Periplasmic

Stability of the Alpha-Barrel Protein MtrB." Applied and Environmental Microbiology **77**(4): 1520-1523.

Sly, L. I., M. C. Hodgekinson and V. Arunpairojana (1990). "Deposition of manganese in a drinking water distribution system." Applied and Environmental Microbiology **56**(3): 628-639.

Stone, A. (1987). "Microbial metabolites and the reductive dissolution of manganese oxides: Oxalate and pyruvate." Geochimica et Cosmochimica Acta **51**(4): 919-925.

Sun, L. D., Yangyang; Shi, Miaomiao; Jin, Miao; Zhou, Qing; Luo, Zhao-Qing; Gao, Haichun (2014). "Two residues predominantly dictate functional difference in motility between Shewanella oneidensis flagellins FlaA and FlaB." The Journal of biological chemistry **289**(21): 14547-14559.

Szeinbaum, N. J. L. B. a. T. J. D. (2014). "Electron transport and protein secretion pathways involved in Mn(III) reduction by Shewanella oneidensis." Environmental Microbiology Reports **6**(5): 490-500.

Thamdrup, B. (2000). "Bacterial manganese and iron reduction in aquatic sediments." Advances in Microbial Ecology **16**: 41 - 84.

Tilak, A. S. O., S.; Williford, C. W.; Fox, G. A.; Sobecki, T. M.; Larson, S. L. (2013). "Formation of Manganese Oxide Coatings onto Sand for Adsorption of Trace Metals from Groundwater." JOURNAL OF ENVIRONMENTAL QUALITY **42**(6): 1743-1751.

Tobiason, J. E. I., A.A.; W..R. Knocke; J. Goodwill; P. Hargette; R. Bouchard; and L. Zuravnsky (2008). "Characterization and Performance of Filter Media for Manganese Control." Water Research Foundation.

Venkateswaran, K. M., Duane; Dollhopf, Michael; Lies, Douglas; Saffarini, Daad; MacGregor, Barbara; Ringelberg, David; White, David; Nishijima, Miyuki; Sano, Hiroshi; Burghardt, Jutta; Stackebrandt, Erko; Nealson, Kenneth (1999). "Polyphasic taxonomy of the genus Shewanella and description of Shewanella oneidensis sp. ." International Journal of Systematic Bacteriology **49**: 705-724.

Womba, P. P., David; Bellamy, Bill; Kjartanson, Kelly (2000). "Biological Filtration for Ozone and Chlorine DBP Removal." Ozone: Science & Engineering: The Journal of the International Ozone Association **22**(4): 393-413.

Yang, W. Z., Zhen; Zhang, Zhongming; Chen, Hong; Liu, Jin; Ali, Muhammad; Liu, Fan; Li, Lin (2013). "Population Structure of Manganese-Oxidizing Bacteria in Stratified Soils and Properties of Manganese Oxide Aggregates under Manganese-Complex Medium Enrichment." PLoS One **8**(9).

Yapsakli, K. C., Ferhan (2010). "Effect of type of granular activated carbon on DOC biodegradation in biological activated carbon filters." Process Biochemistry **45**(3): 355-362.

8.0 APPENDIX A

Figure 46. Alignment Sequences for the *mtrB* gene qPCR primers

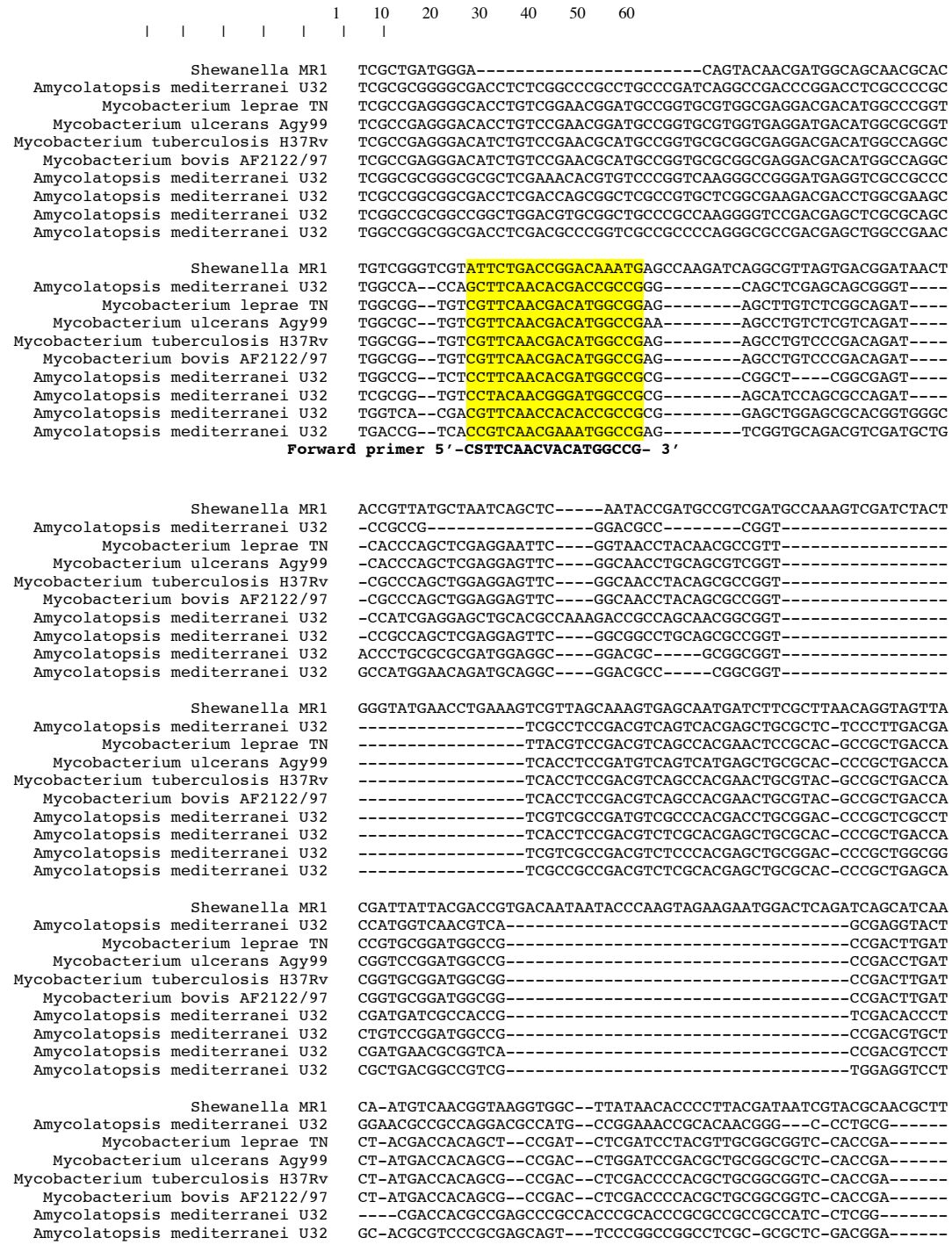

```
  Amycolatopsis mediterranei U32   CG-ACGAGGACGCCGAGCAGC---TGCCGCCGGACACCGCGGTCGCGGCGCG--------
  Amycolatopsis mediterranei U32   GG--CGACCACGGCGGACGGGA--TGGAGGCCGACGCC-CGGGAATC-CGCGCA------

                 Shewanella MR1   TAAAGTTGCCGCAGATTATCGCATTACCCGCGATATCAAACTCGATGGTGGTTATGACTT
  Amycolatopsis mediterranei U32   -------GCTGCTGCGGTCGG----------------AACTGCGGCGGTTCCAGCGGAT-
        Mycobacterium leprae TN    -------ACTGATGGTCAGCG----------------AACTCGATCGATTCGAGACACT-
    Mycobacterium ulcerans Agy99   -------GTTGATGGTCAACG----------------AACTGGACCGGTTCGAGTCCTT-
Mycobacterium tuberculosis H37Rv   -------GTTGATGGTTAGCG----------------AGCTGGACCGATTCGAGACGTT-
   Mycobacterium bovis AF2122/97   -------GTTGATGGTTAGCG----------------AGCTGGACCGATTCGAGACGTT-
  Amycolatopsis mediterranei U32   ----------------CACCC----------------AGGCCCGCCGGCTGGCCAAGCT-
  Amycolatopsis mediterranei U32   -------ACTGCTGGTCGACG----------------AGCTCGACCGGTTCGAGGCGCT-
  Amycolatopsis mediterranei U32   -------GCTGGTGTCGGCCG----------------AGACGCGGCGGCTGACCCGGCT-
  Amycolatopsis mediterranei U32   -------GCTGGCGATCGTCG----------------AGACGCACCGGCTGGTCCGGCT-


                 Shewanella MR1   CAAACGTGACCAACGTGATTATCAAGACCGTGAAACCACGGATGAAAATACCGTTTGGGC
  Amycolatopsis mediterranei U32   ----GGTCGTCGACCTGCTGGAGATCTCGAGAGCCGACCAGGACGAGGG-----------
        Mycobacterium leprae TN    ----GCTCAACGACCTGCTCGAGATCTCGCGGCACGACGCCGGCGTGGC-----------
    Mycobacterium ulcerans Agy99   ----GCTCAACGACCTCCTCGAGATCTCGCGCCACGACGCCGGTGTGGC-----------
Mycobacterium tuberculosis H37Rv   ----GCTCAACGACCTGCTGGAGATCTCGCGGCATGACGCCGGGGTGGC-----------
   Mycobacterium bovis AF2122/97   ----GCTCAACGACCTGCTGGAGATCTCGCGGCATGACGCCGGGGTGGC-----------
  Amycolatopsis mediterranei U32   ----CGTGGAGGACCTCCTCGAAATCGCCCGGTTCGACGCCGGCAAGGC-----------
  Amycolatopsis mediterranei U32   ----GCTCGGCGACCTGCTGGAGATCAGCAGGCTCGACGCCGGTGTGGA-----------
  Amycolatopsis mediterranei U32   ----GGTGCAGGACCTGATCGAGATCTCCCGGTTCGACGCCGGGCGGGC-----------
  Amycolatopsis mediterranei U32   ----CGTCGAGGACCTGATGGAGGTGGCCCGCTTGGACGCCGGCACCGC-----------
                      Reverse primer 5'-   SGAGATCTCSAGCAGGTC  – 3'

                 Shewanella MR1   CCGTTTACGTGTAAACAGCTTCGATACTTGGGACATGTGGGTAAAAGGCAGTTACGGTAA
  Amycolatopsis mediterranei U32   C-------------------------------ACCGGCTCGGT-CGAGCTGGTCGACCTCG
        Mycobacterium leprae TN    C-------------------------------GAACTCTCTGT-CGAGGCGGTTGATTTGC
    Mycobacterium ulcerans Agy99   C-------------------------------GAGCTGTCGGT-TGAGGCGGTCGACCTGC
Mycobacterium tuberculosis H37Rv   C-------------------------------GAGTTGTCGGT-TGAGGCGGTCGACTTGC
   Mycobacterium bovis AF2122/97   C-------------------------------GAGTTGTCGGT-TGAGGCGGTCGACTTGC
  Amycolatopsis mediterranei U32   C-------------------------------GACCTGAGGGT-GGCGCCCGTCGACCTCG
  Amycolatopsis mediterranei U32   G-------------------------------GAGCTGTCCGC-GGAGTACATCGACGTCC
  Amycolatopsis mediterranei U32   G-------------------------------GAGCTGCGCCG-GGAGGAGCTGGACGTCG
  Amycolatopsis mediterranei U32   G-------------------------------CAGCTGCGGGT-GGAGGAGGTCGACGTGG
```